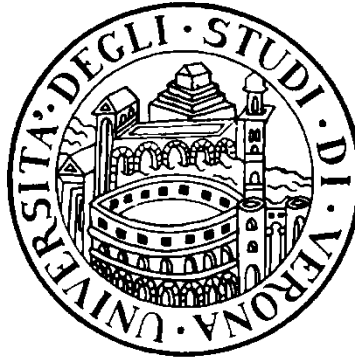


University of Verona



Department of Medicine

Graduated School For Life, Health and Sciences

Doctoral Program in Biomolecular Medicine

Curriculum in Clinical Genomics and Proteomics

Cycle XXXI

***Functional Characterization of Nrf2 in erythroid cells:
from erythropoiesis to mature red cells***

Coordinator: Prof.ssa Lucia De Franceschi

Tutor: Prof.ssa Lucia De Franceschi

Doctoral student: Serge Cedrick Mbiandjeu Toya

INDEX

1. ABSTRACT	3
2. ABBREVIATIONS	4
3. INTRODUCTION	7
4. AIM	19
5. MATERIALS AND METHODS	20
6. CRITICAL RESULTS	26
7. DISCUSSION	42
8. REFERENCES	45
9. PAPERS AND ABSTRACTS	54

1. ABSTRACT

Erythropoiesis is a dynamic and multistep process where early erythroid progenitors undergo differentiation into matured red cells. Nrf2 is a transcription factor that participates in acute response to oxidative stress and controls the expression of anti-oxidant and cytoprotective systems. Mice genetically lacking Nrf2 show a mild chronic hemolytic anemia due to erythrophagocytosis. Here, we show that Nrf2^{-/-} mice display an age-dependent anemia characterized by accelerated senescence of circulating erythrocytes and reduced reticulocyte count, suggesting a perturbation of erythroid maturation process. Indeed, we found ineffective erythropoiesis in 12 months-old Nrf2^{-/-} mice as supported by extramedullar erythropoiesis, increased ROS levels and cell apoptosis. In agreement, Nrf2^{-/-} mice showed a blunted response to stress erythropoiesis induced by either PHZ or Doxo, suggesting an impairment of cellular back up mechanisms against oxidative stress such anti-oxidants and cytoprotective systems. The persistent oxidation promoted activation of UPR system and autophagy, which are unable to fully counteract oxidation re-directing cells towards apoptosis as supported by the increased caspase 3 activity. As a proof of concept, we used Astaxanthin as powerful anti-oxidant administrated in PLGA loaded nanoparticles (ATS-NP). In Nrf2^{-/-} mice, ATS-NP ameliorated the age-dependent anemia and improved ineffective erythropoiesis with inactivation of UPR system and autophagy. In conclusion, we propose Nrf2 as key transcriptional factor against aged related oxidation to ensure erythroid maturation and growth. Future studies should be designed to evaluate the impact of Nrf2 activators as well as of ATS-NP administration in models of pathologic erythropoiesis.

2. ABBREVIATIONS

ARE: antioxidant responsive element

ATF6: activating transcription factor 6

Atg 3: autophagy related protein 3

Atg4: autophagy related protein 4

Atg5: autophagy related protein 5

Atg 7: autophagy related protein 7

Atg 13: autophagy related protein 13

ATS: astaxanthin

ATS-NP: astaxanthin Loaded PLGA nanoparticles

Bcl-X_L: B-cell lymphoma extra large

Bcl-X_s: B-cell lymphoma extra short

Bcl2l1: Bcl2-Like 1

BFU-E: burst forming unit-erythroid

Cdc37: Cell division cycle protein 37

CHOP : CCAAT-enhancer-binding protein homologous protein

Cish: Cytokine-inducible SH2 containing protein

CFU-E: colony forming unit erythroid

Doxo: doxorubicin

EPO: erythropoietin

EPO-R: erythropoietin receptor

FOXO3: Forkhead box O3

Gadd34: growth arrest and DNA damage gene 34

GATA-1: GATA-binding factor 1

Gpx-1: Glutathione peroxidase-1

Gst: Glutathione-S-transferase

Gclc: Glutamate-cysteine ligase catalytic subunit

Gclm: Glutamate-cysteine ligase modifier subunit

HSCs: Hematopoietic stem cells

ho-1: Hemeoxygenase-1

HSP70: Heat-shock protein 70

HSP90: Heat-shock protein 90

IRE: inositol-requiring enzyme

Jak2: Janus-kinase 2

KIR: Keap-1 interacting region

Lamp1: Lysosomal-associated membrane protein 1

LC3(MAP1LC3B): Microtubule-associated proteins 1A/1B light chain 3B

Maf F: Musculoaponeurotic fibrosarcoma protein F

Maf G: Musculoaponeurotic fibrosarcoma protein G

Maf K: Musculoaponeurotic fibrosarcoma protein K

mTOR: Mammalian target of Rapamycin

MCV: mean corpuscular volume

NF-kB: nuclear factor kappa-light-chain-enhancer of activated B cells

Nqo-1: NADPH-quinine oxidoreductase-1

Nrf2: Nuclear factor (Erythroid derived 2) Like 2

PERK: protein kinase R-like endoplasmic reticulum kinase

PHZ: phenylhydrazine

PI3: Phosphatidylinositol-3

PLGA: poly -lactic-co-glycolic acid

Prx2: Peroxiredoxin-2

PrxSO₃: Peroxiredoxin SO₃

Rab 5: Ras-related protein Rab-5

RBCs: Red blood cells

ROS: Reactive oxygen species

RXR α : Retinoid X receptor α

SH2: Src homology 2 domains

Socs3: Suppressor of cytokines signaling 3

SOD2: Superoxide dismutase 2

Srxn: sulfiredoxin

STAT5: Signal transducer and activator of transcription 5

Txn: Thioredoxin

Txnr: Thioredoxin reductase

ULK1: UNC 51 Like kinase-1

UPR: unfolded protein response

3. INTRODUCTION

3.1 Erythropoiesis: a dynamic process

Erythropoiesis is a dynamic, complex and multistep process where early erythroid progenitors undergo differentiation into matured red cells, necessary for O₂/CO₂ exchange.¹⁻² Erythrocytes represent the most common cell type in adult blood and their average life span in human blood is of 120 days. New red cells are constantly produced (2×10^{11} daily)³ to ensure the renewal of aged erythrocytes that are efficiently removed by macrophages mainly present in the spleen. Thus, erythropoiesis plays an important role in maintaining the erythroid lineage.⁴

During embryonic development, early production of erythroid lineage (*primitive erythropoiesis*) occurs within the extraembryonic mesoderm of the yolk sac.⁵

Later in the developing fetal liver, *primitive erythropoiesis* is then replaced by *definitive erythropoiesis*, where enucleated mature erythrocytes are produced from hematopoietic stem cells (HSCs).⁴ This committed differentiation process constantly occurs in the bone marrow, which provides a *niche* composed of macrophages, osteoblasts, endothelial cells, hematopoietic cells, stromal cells, and extracellular matrix. The known function of the *niche* is to favor direct cell-cell contact and exposure of developing erythroid progenitors to growth factors and cytokines.³

The maturation of erythroid precursors occurs into the erythroblastic islands, which are defined structural units in the bone marrow. In spleen, as site of extramedullary erythropoiesis, erythroblastic islands have been described in murine models of anemia. Each erythroblastic island is organized with a central macrophage surrounded by differentiating and enucleating erythroblasts (Fig. 1).⁶⁻⁷ In normal erythropoiesis, the enucleation occurs in the erythroblastic island and expelled nuclei are rapidly phagocytized by the central macrophage. Released nuclei contain very low levels of ATP and a higher exposure of phosphatidylserine on their surface. This serves as an “eat me” signal for apoptotic cells that is used by macrophages to ensure the engulfment of the nuclei.⁸

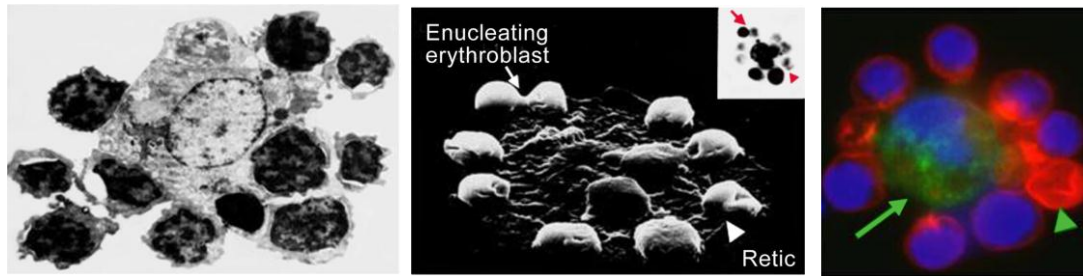


Fig. 1. Micrographs of erythroblastic islands. From left to right are respectively: Transmission electron and scanning electron micrographs and confocal immunofluorescence image. The green arrows indicate macrophage surrounded by maturing erythroblasts. Modified from Mohandas N. et al. Erythroblastic islands: niches for erythropoiesis. *Blood* 2008; 112(3): 470-478

3.1.1 Erythropoiesis is a dynamic process

The production of matured red cells involves proliferation, differentiation and commitment of progenitor cells, which acquire progressively functional and morphological characteristics of erythroid cells. This complex process is divided in two main phases: *early* erythropoiesis and *late* erythropoiesis. During the *early* phase, multi-potential hematopoietic stem cells proliferate and differentiate into committed erythroid progenitors (Fig. 2).² The burst forming unit-erythroid (BFU-E) are large or broken colonies, which expand and develop into colony forming units-erythroid (CFU-Es). These are tightly packed small colonies, which are more abundant than BFU-Es in the bone marrow.⁹ BFU-Es and CFU-Es are typical primitive hematopoietic blast expressing EPO receptors, cell surface markers, signaling intermediates and transcription factors required for differentiation into mature erythroblasts.

The *terminal* or *late* phase of erythropoiesis is a stage starting from pro-erythroblasts to reticulocytes that are later dismissed in the peripheral circulation. In this phase, erythroid precursors undergo several morphological changes characterized by a gradual reduction of cell size, nuclear condensation, cytoplasmic acidification and a marked increase in hemoglobin concentration.¹⁰ These events are associated with changes in membrane protein organization and clearance of organelles towards the generation of mature reticulocyte ready for being transfer from bone marrow to the peripheral circulation.

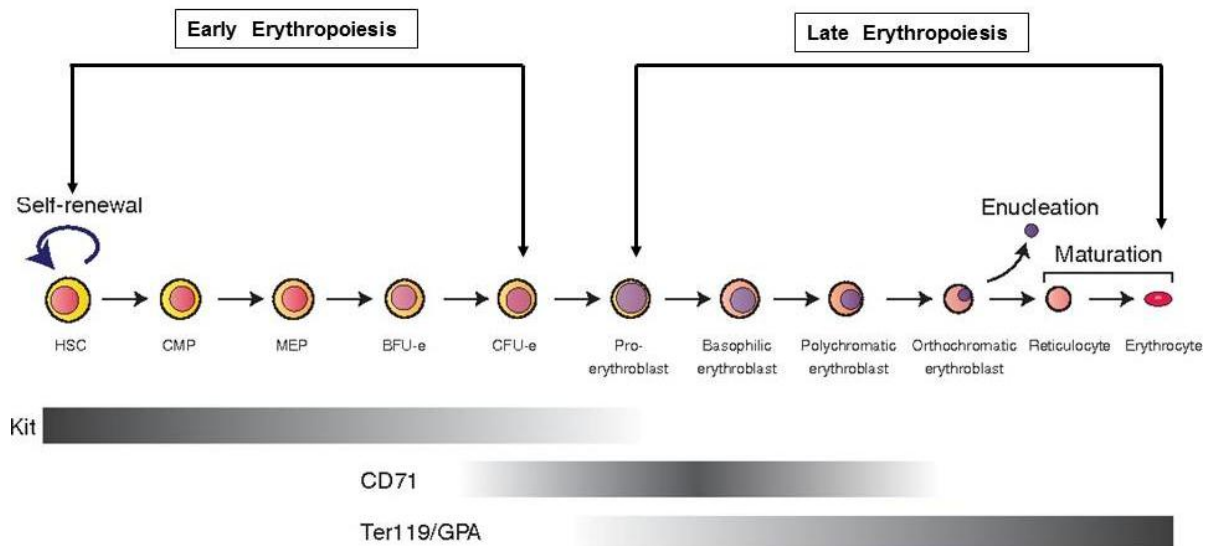


Fig. 2. Schematic diagram of erythroid differentiation. Modified from Dzierzak E. et al. Erythropoiesis: Development and Differentiation. CSHPM 2013; 3(4): a011601

3.1.2 Erythropoietin cascade signaling and oxidation

Erythropoietin (EPO) is the primary regulator of erythropoiesis and it has been demonstrated that erythroid maturation is strictly dependent to EPO signaling cascade.¹¹⁻¹² EPO stimulates erythroid cells proliferation and differentiation through a specific high affinity binding to its receptor (EPO-R), which forms homo-dimers.^{11,13-14} This receptor is expressed on all erythroid cells (from the BFU-E stage to orthochromatic erythroblasts). EPO cascade promotes the production of reactive oxygen species (ROS), which are also generated during heme biosynthesis through iron import in erythroid cells.¹⁵ Upon EPO binding, EPO-R undergoes conformational change that activates a primary tyrosine kinase, Janus-kinase-2 (Jak2).¹⁶ Subsequently, Jak2 phosphorylates eight tyrosine residues in the cytoplasmic tail of EPO-R, generating docking sites for proteins with (SH2) domains, capable of promoting the activation of multiple signaling pathways. Jak2 targets the transcriptional factors STAT5, a master regulator of erythroid maturation events. Recent studies provide evidence that additional Tyr-kinase participates to the EPO signaling cascade beside Jak2. We and others have shown the importance of additional Tyr-kinase in EPO cascade: Lyn and Fyn, two Tyr-kinases of the Src family.¹⁷⁻¹⁸ Noteworthy, both Lyn and Fyn also modulate STAT5 function, resulting in

STAT5 activation.¹⁹⁻²² STAT5 controls the transcription of several genes involved in the terminal erythroid maturation such as *Socs3*, *Cish*, and *Bcl2l1*, which are responsible for the down regulation of EPO-R signaling, chromatin compaction and production of pro-survival factor Bcl-X_s and anti-apoptotic factor Bcl-X_L.²²

Jak2 as well as Lyn and Fyn intersect other signaling pathways important in cell growth and differentiation during erythropoiesis. Indeed, Jak2 activates PI-3 and Akt kinases.

The activation of PI-3 Kinase participates to phospholipids signaling and Ca²⁺ mobilization.²³ Whereas, Akt is involved in cellular response against oxidative stress through (i) the activation of transcription factors such as Forkhead box-O3 (FOXO3) and Nrf2; or (ii) the modulation of mTOR, the gatekeeper of autophagy.²⁴⁻²⁵ In response to oxidation, active FOXO3 translocates into the nucleus with up-regulation of genes involved in redox response such as catalase, superoxide dismutase 2 (SOD2) and glutathione peroxidase 1 (Gpx-1).²⁶ The importance of FOXO3 in erythropoiesis is further supported by evidence in mice genetically lacking FOXO3, which show ineffective erythropoiesis and increased Akt activity. This results in activation of Jak2/Akt/mTOR pathway with repression of autophagy, which contributes to amplified ineffective erythropoiesis of FOXO3^{-/-} mice.²⁴ It is of note that Akt intersects the transcription factor GATA-1, a key regulator of erythroid differentiation.²⁷

Nrf2 is another redox-sensitive transcription factor, which is tightly regulated. In erythropoiesis, Nrf2 is activated in response to oxidation, resulting in up-regulation of genes encoding for anti-oxidant and cytoprotective systems. We have recently shown that the persistent activation of Nrf2 in mice genetically lacking Fyn, that switch-off active Nrf2. This results in accumulation of non-functional/damaged proteins and impaired autophagy with severe oxidative stress and abnormalities in erythropoiesis (Fig. 3).¹⁷

In erythropoiesis, anti-oxidant and cytoprotective systems are crucial. Indeed, previous studies have shown the importance of anti-oxidant and cytoprotective systems in erythropoiesis from engineered knockout mice for anti-oxidant systems.^{15, 28-29} Among them, mice genetically lacking Prx2 show oxidation and ineffective erythropoiesis associated with intense activation of Nrf2 transcription factor as compensatory mechanism against oxidative stress during erythropoiesis.²⁹

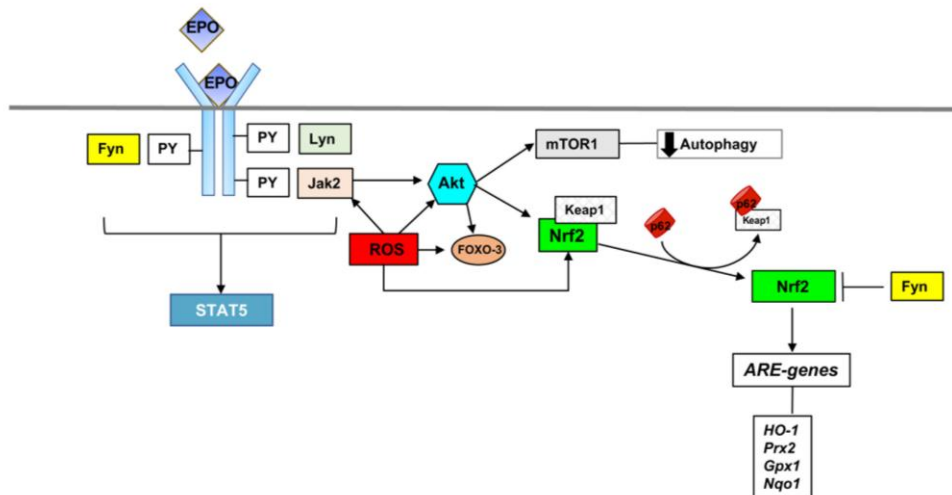


Fig. 3. Schematic diagram of erythropoietin (EPO) cascade. Modified from Beneduce E. et al. Fyn kinase a novel modulator of erythropoietin signaling and stress erythropoiesis. *Am J Hematol.*2019;94:10-20.

3.2. Nrf2 : Structure and function

Nuclear-factor erythroid-derived 2 (Nrf2, also called Nfe2l2) is a cap'n'collar (CNC) basic-region leucine zipper (*bZIP*) transcription factor that participates in acute phase response to oxidative stress and controls the expression of adaptive systems to environmental stressors. This transcriptional factor was firstly described in the laboratory of Yuet Wai Kan.³⁰ Nrf2 is characterized by seven domains known as *Nrf2-ECH* homology (*Neh*) domains (Fig. 4).³¹⁻³³ Each one fulfills specific functions:

- **Neh1** domain comprises the CNC-bZIP region that both dimerizes with small musculoaponeurotic fibrosarcoma (Maf) proteins and binds with DNA.
- **Neh2** and **Neh6** domains negatively controls Nrf2

- **Neh3, Neh4** and **Neh5** domains are transactivation regions important in the recruitment of various proteins.
- **Neh 7** domain mediate the repression of Nrf2 by the retinoid X receptor (RXR) α .

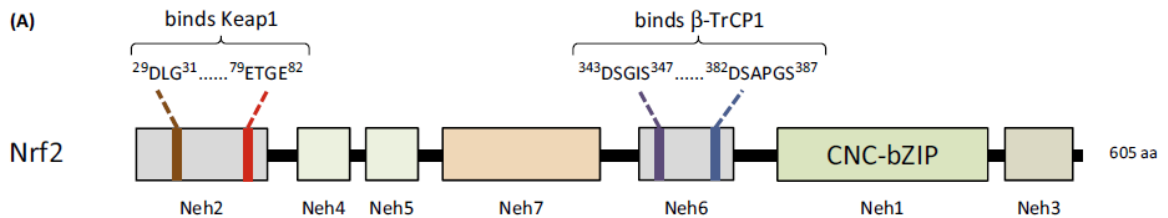


Fig. 4. Nrf2 protein structure and Neh domains indicated. modified from Hayes JD, et al. Trends Biochem Sci, 2014

Nrf2 transcription factor is ubiquitously expressed in human and mouse tissues. Nrf2 binds DNA as heterodimer with small (Maf) proteins such as MafF, MafG and MafK.³⁴ To characterize the function role of Nrf2, different knockout mouse strains have been generated, but the absence of Nrf2 did not produce a clear phenotype. However, *in vivo* animal based studies show that Nrf2 plays a key role in acute phase response to different stresses such as oxidation through its ability to modulate the expression of (i) antioxidant responsive element (ARE-) related genes encoding for enzymes such as Hemeoxygenase-1 (HO-1) or Glutathione peroxidase (Gpx); (ii) drug-metabolizing systems, such as glutathione S-transferase (Gst), NAD(P)H: quinine oxidoreductase-1 (Nqo-1) or phase III drug-detoxifying enzymes involved in cellular efflux and (iii) metabolic pathways.³⁵

In addition, Nrf2 has been showed to control the expression of xCT subunit of system X_c⁻, which import cystine into cells³⁶ along with glutamate-cysteine ligase catalytic(GCLC) and modifier(GCLM) subunits that together catalyze the rate-limiting step in glutathione synthesis.³⁷ Nrf2 also participates to the expression of thioredoxin1 (*txn*),³⁸ thioredoxin reductase (*txnr*)³⁹⁻⁴² and sulfiredoxin(*srxn*)⁴³⁻⁴⁴ that are important systems involved in Prx2 reduction through NADPH system.

3.3 The Interplay between Prx2 and Nrf2

Prx2 is a typical 2-cysteine peroxiredoxin that is involved in the defense against oxidative stress through its ability to reduce and detoxify a vast range of oxidative

elements. It is the third most abundant cytoplasmic protein in red blood cells (RBCs) and it is efficiently able to scavenge low concentration of hydrogen peroxide (H₂O₂) without inactivation due to over-oxidation.⁴⁵⁻⁴⁶ Studies have suggested a potential role of Prx2 in stress-response cytoprotective system in pathological erythropoiesis given its upregulated expression in both murine and human β -thalassemic erythropoiesis.⁴⁵⁻⁴⁶ β -thalassemia is characterized by increased oxidative stress and ROS production related to the imbalance between alpha-beta globin chain synthesis.⁴⁷ Our group has recently showed a functional interplay between Nrf2 and Prx2 to face oxidation in β -thalassemia.²⁹ Our data suggest that in stress erythropoiesis Prx2 is a key cytoprotective system in conjunction with Nrf2 to limit oxidative damage in β -thalassemic mouse erythropoiesis. Nrf2 might function as back-up mechanism in the absence of Prx2, supporting pathologic erythropoiesis to ensure terminal differentiation.

Evidence from Prx2^{-/-} mice exposed to an iron overload diet indicates that Prx2 is a new regulator of iron homeostasis and proposed the modulation of Prx2 activity as a novel clinical strategy to face iron overload clinical problems.⁴⁸

3.4 Studies in mouse models: Nrf2^{-/-} mice or Nrf2^{up/up} mice

In the last decade, different Nrf2^{-/-} mouse strains have been generated to study the *in vivo* role of Nrf2 in response to stresses such as oxidation or acute inflammation. We carried out a revision of the literature and the results of the main studies on Nrf2^{-/-} mice or Nrf2^{up/up} mice are reported in Table 1.

Table 1. Summary of the main studies in Nrf2^{-/-} and Nrf2^{up/up} mice

Mouse strain	Phenotype	Ref.
	<ul style="list-style-type: none"> - Extramedullar erythropoiesis (splenomegaly) - Age-dependent hemolytic anemia - Anisopoikilocytosis and presence of Howell-jolly body, marker of Hb oxidation - Severe anemia in response to <i>in vivo</i> hydrogen peroxide (H₂O₂) treatment - Increased erythrophagocytosis 	Lee J M 2004 ⁴⁹

Nrf2^{-/-} mice	<ul style="list-style-type: none"> - Down-regulation of Nrf2-related antioxidant systems such as GSH 	
	<ul style="list-style-type: none"> - Splenomegaly and age-related weight loss in female mice - Autoantibody production and immune complex deposition (C3, IgG and IgM) in multiple organs such as kidney, liver and heart - Amplified inflammatory response (mononuclear cell infiltration) in kidney, liver and heart - Increased apoptosis and cell oxidation in kidney and liver - Down-regulation of Nrf2 related detoxification genes (ALDH, GSTs and FMO) in liver 	Jiang Li 2004 ⁵⁰
	<ul style="list-style-type: none"> - Significant delay in regeneration of ischemic induced liver injury - Increased cell apoptosis and oxidation cell in hepatectomized liver - Reduced expression of Nrf2 target genes such as Gst and Nqo1 in liver - Reduced cell survival and proliferation in ischemic induced liver injury, most likely related reduction in activation of PI3 kinase/Akt signaling 	Beyer T 2008 ⁵¹
	<ul style="list-style-type: none"> - Down-regulation of iron transporters: <i>Fpn1</i> and <i>Nramp1</i> in macrophages - Reduced mRNA expression of <i>Hepcidin</i> and TfR1 macrophages 	Harada N 2011 ³⁵
	<ul style="list-style-type: none"> - Up-regulation of G6Pase in liver during fasting - Increased lipid peroxidation (oxidative stress) in liver - Reduced hepatic expression of detoxification enzymes (Nqo1 and Gsta1) and redox proteins (Txn) 	Zhang Y J 2013 ⁵²
	<ul style="list-style-type: none"> - High sensibility of Nrf2^{-/-} hepatocytes to iron overload - Necrotic and apoptotic areas in iron-induced liver - Increased inflammatory cell infiltrates in iron-induced liver cytotoxicity - Increased markers of oxidation in iron-induced liver cytotoxicity 	Silva-Gomes 2014 ⁵³
	<ul style="list-style-type: none"> - Increased sensitivity risk to develop lung tumors - Reduction in pulmonary T cells populations 	Zhang D 2017 ⁵⁴

	<ul style="list-style-type: none"> - Increased T cell suppressors in spleen - Increased cytokines 	
	<ul style="list-style-type: none"> - Reduction in Nrf1 expression - Down-regulation of detoxifying and antioxidant enzymes in female mice - Delayed rate of bone acquisition in female mice - High rate of bone acquisition in male mice 	Pellegrini GC 2017 ⁵⁵
	<ul style="list-style-type: none"> - Increased eNOS expression in aorta and heart - Increased cardioprotection against I/R 	Erkens R 2018 ⁵⁶
	<ul style="list-style-type: none"> - Reduced sensitivity to induce Snat3 expression during metabolic acidosis - Up-regulation of oxidative stress markers during metabolic acidosis 	Lister A 2018 ⁵⁷
Nrf2^{up/up} mice	<ul style="list-style-type: none"> - Delay red cell maturation - Aberrant retention of mitochondria within the phenotypically mature cells - Defect in ribophagy (high retention of ribosomes) in mature cells - Abnormal expression of autophagy genes (<i>NIX</i> and <i>ULK1</i>) 	Gothwal M 2016 ⁵⁸
	<ul style="list-style-type: none"> - Down-regulation of pro-inflammatory genes (<i>C4</i>) - Reduced loss of optic tract 	Sigfridsson E 2018 ⁵⁹

3.5 Autophagy and Erythropoiesis

Autophagy, literally meaning “Self-eating” is an organized process where cellular components and organelles are sequestered into a double membrane vesicle called “autophagosome”, and targeted for lysosomal degradation.⁶⁰ In cell homeostasis, autophagy plays an important role in maintaining a quality control of essential cellular component on protein degradation/clearance. In presence of severe oxidation, autophagy levels can be dramatically increased to ensure cell survival.⁶⁰

Erythropoiesis is a dynamic process requiring reduction of cell volume, clearance of unfolded/damaged proteins and organelles to gain at the end the generation of reticulocytes. Previous studies have shown that autophagy-related genes such as Ulk1 and Atg13, interacts with the HSP90-Cdc37 complex, promoting mitochondrial clearance (mitophagy) during erythroid differentiation.⁶¹ In addition, Ulk1 and Atg7 have also been described to be involved in mitophagy during erythroid maturation. Studies in Atg7^{-/-} mouse erythroid cells show an impairment of autophagosome elongation with mitochondrial engulfment, resulting in delayed mitochondrial clearance.⁶²⁻⁶³ Similar data have been also reported in Ulk1^{-/-} mice model in which reticulocytes display a defect in degradation of mitochondria and RNA-bound ribosomes during *in vitro* maturation process.⁶⁴ In addition, Ulk1 also mediates an alternative Atg5/Atg7 independent macroautophagy, a dominant process during mitochondrial clearance in maturing reticulocytes.⁶⁵ Noteworthy, Ulk1^{-/-} mice is also characterized by the presence of red cell populations retaining mitochondria, suggesting an increased hemoglobin content in both reticulocytes and matured red cells.

Recently we have documented the role of Ulk1, Atg13 and Atg7 in autophagic flux during erythroid maturation in “*in vitro*” model of human erythropoiesis derived from CD34+ cells of patients with chorea-acanthocytosis, a neurodegenerative disorder involving basal ganglia and erythroid cells.⁶⁶

The importance of autophagy in erythroid maturation is further supported by evidence provided by pharmacologic inhibitors of mTOR, the gatekeeper of autophagy. In β -thalassemic mice, a model of stress erythropoiesis, rapamycin blocks mTOR and activates autophagy, inducing proliferation of immature erythroblasts with increased red cells production.²³ Similar data have been also reported in mouse model for sickle cell disease, supporting the critical role of autophagy in assisting erythroid maturation and quality control processes.

3.6 Autophagy/apoptosis: Role of caspase

Oxidative stress promotes the activation of autophagy as a strategy of the cell to adapt and cope with a stressful environment. Whenever the stress is severe or prolonged, apoptotic programs are activated and autophagy is blocked. Thus, the

balance between autophagy and apoptosis is crucial in cell fate. The activation of autophagy generally precedes cell apoptosis which is the terminal event for cells.⁶⁷

In presence of severe or prolonged stress, autophagy might be blocked by the action of protease such as caspases, which cleave key autophagy related proteins, resulting in acceleration of cellular death. Among autophagy related proteins, Atg3 and Beclin1 have been reported to be directly targeted by caspases.⁶⁸⁻⁶⁹ In erythropoiesis, caspase-1, -2, -3, -5, -6, -7, -8 and -9 have been described to play a relevant role in cell maturation and growth.⁷⁰⁻⁷¹ Indeed, caspases-3 and 7 have been suggested to cleave transcription factors such as GATA-1, promoting the arrest of cell growth and maturation.⁷²⁻⁷³ Furthermore, caspase-3 has been also involved in chromatin condensation and loss of nucleus during the terminal phase of erythropoiesis, supporting the multitarget action of caspase in erythroid maturation events.⁷⁴

3.7 The functional link between Nrf2 and autophagy

The transcription factor Nrf2 is activated in response to oxidative stress, modulating the expression of anti-oxidant or cytoprotective systems such as Prx2. Previous studies have shown a functional interplay between Nrf2 and Prx2 against severe or prolonged oxidation in erythropoiesis.²⁹ Once activated Nrf2 is translocated to the nucleus, up-regulating the ARE genes such as Heme-oxygenase-1 (HO-1), which is important for the breakdown of heme, or Nqo-1 and GCLM (glutamate-cysteine ligase modifier subunit) as anti-oxidant systems. When Nrf2 is switched off, Keap-1 complexes with Nrf2 and promotes its ubiquitylation through autophagy. The autophagy adaptor protein p62 facilitates the selective degradation of protein cargo. p62 contains a KIR motif that binds with Keap-1 during the transport of cargo protein into “autophagosome” (Fig. 5).⁷⁵ Recent studies in cells genetically lacking Atg5 or Atg7 have documented a prolonged activation of Nrf2, as result of the accumulation of p62-Keap-1 aggregates in the cytosol.⁷⁶⁻⁷⁷ These findings support the functional crosstalk between autophagy and Nrf2 and indicate the importance of preservation of regulatory pathways modulating Nrf2 activation/inhibition.

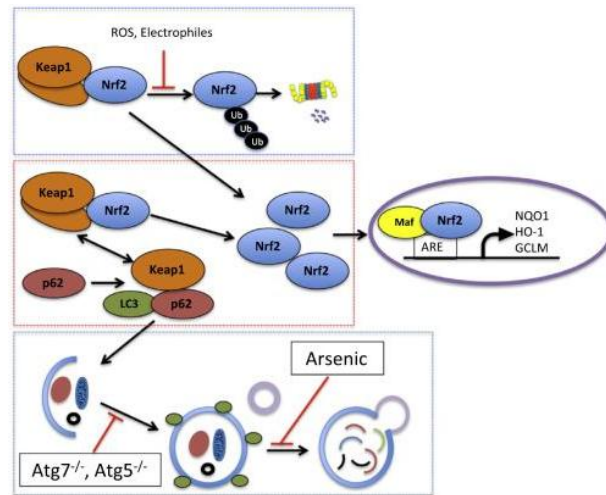


Fig. 5. Regulatory pathways of Nrf2 Signaling. Modified from Zhang DD. et al. p62 links autophagy and Nrf2 Signaling. *FRBM*.2015;88:199-204.

4. AIM OF STUDY

Understanding the role of Nrf2 in erythroid maturation

5. MATERIALS AND METHODS

5.1 Drugs and chemicals

NaCl, Na₃VO₄, TRIS, Tween 20, EDTA, choline, MgCl₂, MOPS, Na₂HPO₄, KH₂PO₄, NaF, bicine, β-mercaptoethanol, benzamidine, glycine, glycerol, potassium cyanide, bromphenol blue, sodium dodecil sulphate (SDS), hydrocortisone, albumin from bovine serum (BSA), May-Grunwald-Giemsa's Azur-Eosin-Methylene Blue solution, Astaxanthin, Poly(D,L-lactide-co-glycolide) (PLGA) were obtained from Sigma/Aldrich (St Louis, MO, USA); dithiotreitol (DTT), was from Fluka (Buchs, Switzerland); protease inhibitor cocktail tablets were from Roche (Basel, Switzerland); Prestained protein ladder, Triton X-100 and Temed were purchased from GE Healthcare Life Biosciences (Little Chalfont, UK); 40% Acrylamide/Bis Solution, 37.5:1 was from BIO-RAD (California, USA); Luminata Forte and Luminata classico Western Hrp solutions were from Mercks Group (Armstad, Germany); Annexin V Binding Buffer was from eBioscience (San Diego, USA); Dulbecco's Phosphate Buffered Saline (DPBS) was from Lonza (Belgium). Alpha-MEM, L-glutamine and Fetal Cow Serum (FCS) were from ThermoFisher (Massachusetts, USA); Penicillin-Streptomycin and Amphotericin were from Euroclone (Milan, Italy); MethoCult™ M3234 was from StemCell Technologies (Milan, Italy).

5.2 Mouse strains and design of the study

We studied the following mouse strains: C57BL/6J as normal control (wild-type; WT), and Nrf2^{-/-} mice.⁴⁹ Based on our preliminary experiments, we used female mice aging from 4 to 12 months old for both C57BL/6J and Nrf2^{-/-} strains. Mouse blood was collected by retro-orbital venipuncture in anesthetized mice using heparinized capillares according to the general guidelines of local animal facility, University of Verona. Whenever indicated, severe anemia induction was done by intraperitoneal injection of PHZ (40 mg/Kg body weight)⁷⁸ or Doxorubicin (0.25 mg/Kg body weight).⁷⁹ Blood was collected at day 2, 4, 8, 11 and 14 from PHZ injection and at day

3, 6 and 9 after Doxorubicin injection. Spleen and bone marrow were collected at day 4 from PHZ injection and at day 9 after Doxorubicin injection. Whenever indicated, mice were treated through intraperitoneal injection with Astaxanthin Loaded PLGA nanoparticles (ATS-NP) at the dosage of 2mg/kg or vehicle every two days for four weeks.

Hematological parameters, red cell indices and reticulocyte count were evaluated on ADVIA 120 Hematology System (Siemens Healthcare GmbH, Germany) as previously described.⁸⁰ Hematocrit and hemoglobin were manually determined.⁸¹⁻⁸²

5.3 Treatment of red cells with oxidative agents

Red Blood cells (RBCs) from WT and Nrf2^{-/-} mice were treated *in vitro* with three different oxidative agents: Hydrogen peroxide (H₂O₂; 50 μM), Diamide (2 mM) and PHZ(20 μM) based on data previously reported in mouse erythrocytes.⁴⁶ Whenever indicated, RBCs were pretreated with sodium azide (NaN₃; 100mM) to inhibit catalase before exposure to oxidative agents.⁸³⁻⁸⁴ Treated and untreated red cells were either analyzed to measure ROS levels and Annexin V⁺ cells or lysed for membrane ghost and cytosolic fraction preparation.⁸⁰

5.4 Immunoblot analysis of mouse red cell membrane ghost and cytosol fraction

Red cell membrane ghost and cytosol fraction were prepared as previously described.⁸⁰ Whenever Prx2 was evaluated through western blot, 100mM of NEM was added in the lysis buffer to avoid possible artifacts related to Prx2 oxidation during cell preparation.⁴⁶ Proteins from ghosts and the cytosol fraction were solubilized in reducing or non-reducing sample buffer (50 mM Tris, pH 6.8, 2% SDS, 10% glycerol, few grains of bromphenol blue added of 5% β-mercaptoethanol for reducing conditions) and analyzed by one-dimensional SDS–polyacrylamide gel electrophoresis. Gels were either stained with colloidal Coomassie or transferred to nitrocellulose membranes for immunoblot analysis with specific antibodies: anti-phospho-Syk (Tyr 525/526) (Cell signaling Technology, Leiden, NL); anti-Syk (Cell

signaling Technology, Leiden, NL); anti-Prx2 (Clone1E8, Abcam, Cambridge, UK); anti-peroxiredoxin-SO3 antibody (clone LF-PA0004; LabFrontier); anti-band 3 antibody (clone IVF12, DSHB, IA, USA); anti-catalase (Abcam, Cambridge, UK); anti-HSP70, anti-G6PD, anti-TrxR-1 and anti-NQO1 (Santa Cruz Biotechnology, Texas, USA); anti-HSP90 (Cell signaling Technology, Leiden, NL); anti-Actin (clone BIII-136; Sigma–Aldrich) and anti-carbonic anhydrase (Chemicon, Temecula, USA) as loading controls. Anti Phospho-Tyrosine immunoprecipitation (IP) experiments were carried out as previously reported;⁶⁶ anti IgG rabbit (GE Healthcare Life Sciences, Little Chalfont, UK) was used as loading control. Blots were developed using the Luminata Forte or Luminata Classico Western chemiluminescence reagents. Images were acquired using Image Quant Las Mini 4000 Digital Imaging System (GE Healthcare Life Sciences, Little Chalfont, UK) and densitometric analysis of band intensities was carried out using the ImageQuant TL software (GE Healthcare Life Sciences).

5.5 Flow cytometric analysis of mouse bone marrow and spleen erythroid precursors

Flow cytometric analysis of erythroid precursors from bone marrow and spleen of mice was carried out using CD44-Ter119 gating strategy as previously described.⁸⁵ Briefly cells were centrifuged at 1,500 rpm for 5 min at 4°C and resuspended in the proper volume of BEPS (PBS 1X, BSA 1%, EDTA 2 mM, NaCl 25 mM). Cells were incubated first with CD16/32 to block Fc receptor for 15 min at 4°C in the dark, then later incubated with CD45-APC-Cy7, CD44-FITC, CD71-PE and Ter119-APC (eBioscience, San Diego, USA) antibodies for 45 min at 4°C in the dark. Cells were washed and centrifuged at 1,500 rpm for 5 min at 4°C, resuspended in BEPS, and 7AAD for cell viability was added immediately before the analysis. (Fig. 6)

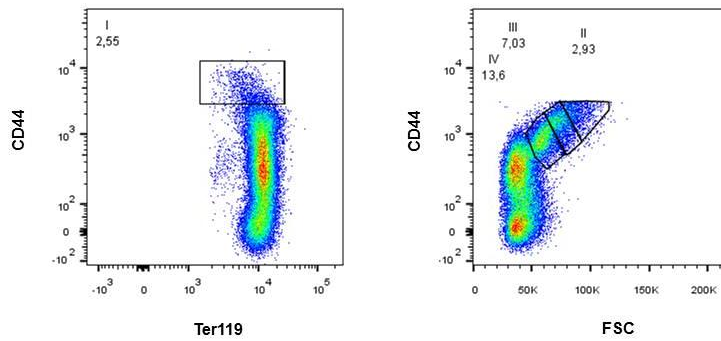


Fig. 6. Example of cytofluorimetric scatter for erythroid precursors from WT mice. **Left panel:** analysis of CD44^{low}-Ter119⁺ Pop I corresponding to pro-erythroblasts. **Right panel:** analysis of CD44⁺ Pop II, III, IV corresponding to basophilic, polychromatic and orthochromatic erythroblasts respectively.

ROS levels of the erythroid precursors were determined using the General Oxidative Stress Indicator, CM-H2DCFDA (LifeTechnologies, Carlsbad, CA) on CD44-Ter119 gated populations as previously described.^{16,29}

Apoptotic erythroblasts were analyzed on CD44-Ter119 gated populations using the Annexin-V PE Apoptosis detection kit (eBioscience, San Diego, CA), following the manufacturer's instructions.²⁷

Oxidative DNA damage was determined by 8OHdG flow cytometric analysis as previously described with some modifications.⁸⁶ Briefly erythroid precursors from mouse bone marrow were stained with CD44-FITC, CD71-PE and Ter119-BV450 (eBiosciences, CA, USA); fixed and permeabilized with BD Cytofix/Cytoperm and the BD Cytoperm Plus permeabilization reagent (BD Biosciences, CA, USA) respectively. Cells were then stained with primary anti-8OHdG (Santa Cruz Biotechnology, CA, USA) and secondary anti-mouse eFluor647 (Santa Cruz Biotechnology, CA, USA).

All the analysis were performed with the FACSCanto-II™ flow cytometer (Becton Dickinson, San Jose, CA, USA) and data were analyzed with the FlowJo software (Tree Star, Ashland, OR, USA).

5.6 Cell sorting of murine bone marrow erythroblasts

Total erythroblasts (CD44⁺Ter119⁺FSC^{high}) were sorted from WT and Nrf2^{-/-} mouse bone marrow using a FACS Aria-IIITM cell sorter (Becton Dickinson, San Jose, CA, USA) as previously reported.⁸⁵ Sorted cells were used for (i) immunofluorescence assay;²⁹ (ii) immunoblot analysis;²⁹ (iii) molecular analysis through QRT-PCR;⁴⁸ and (iv) CPP32/Caspase-3 Fluorometric protease assay (BioVision, Milpitas, CA, USA; following the manufacturer's instructions); and (v) nuclear protein isolation, using the Q-proteome Nuclear Protein Kit (Qiagen, Hilden, Germany; following the manufacturer's instructions).

The Immunofluorescence analysis of sorted erythroblasts was carried out using the following antibodies: anti-Nrf2 and anti-Lamp-1 (Abcam, Cambridge, UK); anti-Prx2(EPR51554, Abcam, Cambridge, UK); anti-APG7 (Atg7) (ProSci, Poway, CA, USA).

For Immunoblot analysis the following specific antibodies were used: anti-NFkB-phospho-S536 (Cell Signaling Technology, Leiden, NL); anti-NFkB p65 and anti-Atg5 (Cell Signaling Technology, Leiden, NL); anti-Nrf2-phospho-S40 (Clone EP1809Y, Abcam, Cambridge, UK); anti-Nrf2 (Abcam, Cambridge, UK); anti-Gadd34, anti-Lamp-1, anti-SQSTM1/P62, anti-Rab5 and anti-LC3A/B (Abcam, Cambridge, UK); anti-Atg4 (Santa Cruz Biotechnology, Heidelberg, Germany); anti-APG7 (Atg7) (ProSci, Poway, CA, USA); anti-ATF6 (Novus Biologicals, Centennial, CO, USA); anti-CHOP (Thermo Fisher Scientific, Massachusetts, USA); anti-Actin (clone BIII-136; Sigma-Aldrich, Saint Louis, MO, USA) and anti-GAPDH (Sigma-Aldrich, Saint Louis, MO, USA) as loading controls.

5.7 Preparation of Astaxanthin Loaded PLGA nanoparticles (ATS-NP)

A single emulsion solvent evaporation method was used for the synthesis of the Astaxanthin Loaded PLGA nanoparticles (ATS-NP) .⁸⁷ Briefly, 20 mg of PLGA (7–17 kDa PLGA 50:50 with uncapped end-groups; Sigma-Aldrich, St. Louis, MO) were dissolved in 2 mL of a mixture of 85% acetone and 15% ethanol. The organic phase was added dropwise to 20 mL of 0.5% aqueous polyvinyl alcohol surfactant under

stirring. The obtained emulsion was maintained under stirring overnight to let the organic solvents evaporate. Produced nanoparticles were collected by centrifugation at 13,000 g for 20 min at 10 °C and washed several times with 0.01M phosphate-buffered saline, pH 7.4 (PBS) to remove residues. Finally, 5% mannitol was added as a cryoprotectant and the NPs were divided into proper aliquots and lyophilized for storage.

5.8 Statistical analysis

Data were analyzed using either the t-test or the 2-way analysis of variance (ANOVA) for repeated measures between mice of various genotypes. A difference with a $P < 0.05$ was considered significant.

6. CRITICAL RESULTS

6.1 Nrf2^{-/-} mouse red cells show low expression of Nrf2 dependent anti-oxidant systems and increased susceptibility to oxidation

Nrf2^{-/-} mice showed anisopoikilocytosis and Howell-Jolly body in red cells (arrows in Fig. 7a).⁴⁹ Increased ROS levels was documented in Nrf2^{-/-} mouse red cells when compared to wild-type erythrocytes (Fig. 7b). This was mainly related to the reduction in the expression of Nrf2 related anti-oxidant systems such as NAD(P)H: quinine oxidoreductase-1 (Nqo1), Prx2 and catalase (Fig. 7c). The high pro-oxidant environment of Nrf2^{-/-} mouse red cells was also supported by increased membrane translocation of HSP70 and 90 compared to wild-type erythrocytes. Noteworthy, we observed a reduction in the amount of Prx2 associated to the membrane similarly to that reported in β -thalassemic red cells (Fig. 7d). This may be related to either low expression of Prx2 or occupancy of the integral membrane protein band 3, which is a known docking site for Prx2.⁴⁶ In Nrf2^{-/-} mouse red cells, increased amount of phosphatidyl-serine (PS) positive erythrocytes indicate the presence of membrane lipid-peroxidation, contributing to reduce Nrf2^{-/-} mouse red cell membrane mechanical stability (Fig. 7e). Taken together, our data indicate that the absence of Nrf2 results in reduction of red cell anti-oxidant and cytoprotective systems, promoting oxidation and accelerated senescence of erythrocytes from Nrf2^{-/-} mice.

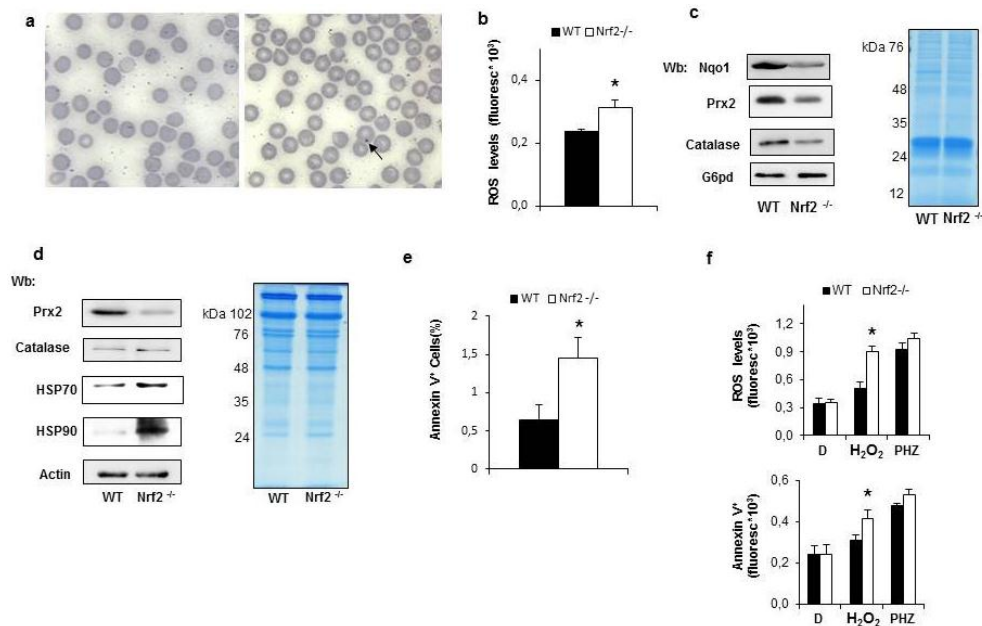


Fig. 7. (a) Morphology of red cells from Nrf2^{-/-} and WT mice. **(b)** ROS in red cells from Nrf2^{-/-} and WT mice. Data are presented as means±SD (n=6) *P<0.05 compared to WT. **(c)** and **(d)** Western blot analysis of cytosolic fraction and membrane fraction of red cells from Nrf2^{-/-} and WT mice. One experiment of other six with similar result is shown. **(e)** Annexin V⁺ red cells in Nrf2^{-/-} and WT mice. Data are presented as means±SD (n=6) *P<0.05 compared to WT. **(f)** ROS and annexin V⁺ cells in red cells from Nrf2^{-/-} and WT mice exposed respectively to D: diamide, H₂O₂: Hydrogen peroxide; PHZ: Phenylhydrazine. Data are presented as means±SD (n=6) *P<0.05 compared to WT.

We then used exogenous oxidants such as diamide, H₂O₂ or phenylhydrazine (PHZ) to test the response of Nrf2^{-/-} erythrocytes to *in vitro* oxidative stress. Nrf2^{-/-} mouse erythrocytes showed a higher sensitivity to H₂O₂ compared to wild-type erythrocytes (Fig. 7f). Whereas, no major difference between Nrf2^{-/-} and WT mouse red cells was observed in presence of either diamide or PHZ (Fig. 7f). Since in red cells Prx2 is one the main cytoprotective systems against H₂O₂, we evaluated Prx2 dimerization and the amount of PrxSO₃ in red cells from both mouse strains exposed to H₂O₂ and PHZ. As shown in Fig. 8a, Prx2 dimerization was higher in PHZ wild-type red cells compared to Nrf2^{-/-} mouse red cells. Whereas the amount of PrxSO₃, corresponding to over-oxidized Prx2,⁸⁸ was higher in Nrf2^{-/-} mouse red cells exposed to both H₂O₂ or PHZ compared to wild-type erythrocytes (Fig. 8b). These data indicate that Nrf2^{-/-} erythrocytes are more susceptible to H₂O₂ and PHZ mediated oxidative stress than wild-type erythrocytes. Indeed, when catalase was blocked by sodium-azide, Prx2 dimerization was higher in Nrf2^{-/-} red cells exposed to H₂O₂ than in wild type

erythrocytes, supporting the increased susceptibility of *Nrf2*^{-/-} erythrocytes to H₂O₂ and PHZ oxidation.

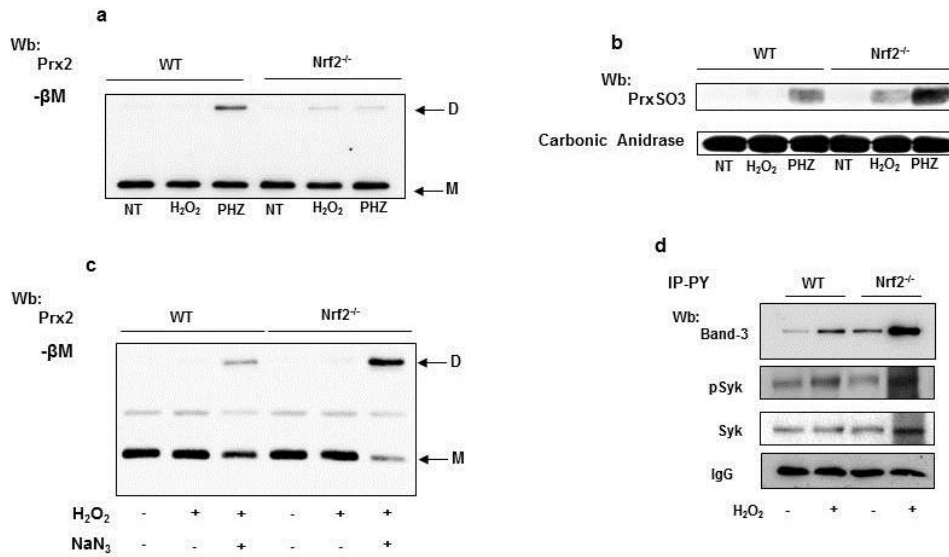


Fig. 8. (a) Western blot analysis of cytosolic fraction of treated RBCs for Prx2 dimers. (D) is for Dimers while (M) for monomers. Exogenous oxidants are: H₂O₂ = Hydrogen peroxide; PHZ = Phenylhydrazine. (b) PrxSO₃ expression in the cytosolic fraction of treated RBCs. Carbonic anhydrase was used as protein loading control. (c) Western blot analysis of cytosolic fraction of treated RBCs for Prx2 dimers. The Exogenous oxidants is H₂O₂ and NaN₃ = sodium azide (Potent catalase inhibitor). (d) Tyr-phosphorylation state of band 3 in *Nrf2*^{-/-} erythrocytes associated with the activation of Syk pathway in response to H₂O₂ treatment. Data are presented as means±SD (n=6) *P<0.05 compared to WT.

Previous studies have shown that oxidation modulates intracellular signaling targeting band 3 throughout the activation of Src kinase or Syk related kinase.⁸⁹ *Nrf2*^{-/-} erythrocytes displayed increased Tyr-phosphorylation of band 3 on steady state and in response to H₂O₂ when compared to wild-type mouse erythrocytes. This was associated with the activation of the canonical Syk pathway in red cells from both mouse strains, but again to a higher extent in *Nrf2*^{-/-} erythrocytes as compared to treated wild-type red cells (Fig. 8d). Collectively, our data indicate that *Nrf2*^{-/-} erythrocytes have lower anti-oxidant capacity than wild-type red cells, requiring an intense activation of intracellular signaling to ensure *Nrf2*^{-/-} red cell survival against oxidation.

6.2 Age-dependent ineffective erythropoiesis characterized Nrf2^{-/-} mice

Since aging is a process characterized by oxidative stress, we reasoned that Nrf2 might be important in erythroid maturation events during mouse aging.

Table 2. Hematological Parameters and Red Cell Indices in Aging			
Wild-Type and Nrf2^{-/-} Mice			
	Wild-type animals		
	4 months-old mice (n=6)	8 months-old mice (n=6)	12 months-old mice (n=6)
Hct (%)	46.1 ± 1.4	45.9 ± 0.7	44.8±0.2
Hb (g/dl)	14.8 ± 0.5	15 ± 0.1	14.3±0.4
MCV (fl)	51.3 ± 0.2	51.0 ± 0.1	52.2±0.3
MCH (g/dl)	15.9 ± 0.7	16.5 ± 0.3	15.6±0.2
RDW (%)	12.4±0.08	13.5 ± 0.1	12.7±0.3
Retics (10³ cells/uL)	450 ± 22	431 ± 51	248±24°
MCVr(fl)	54.9± 2	56.7 ± 3	59.9±1.8°
	Nrf2^{-/-} animals		
	4 months-old mice (n=6)	8 months-old mice (n=6)	12 months-old mice (n=6)
Hct (%)	44.3 ± 0.8	41.8 ± 1.1 ^{o*}	33.6±3 ^{o*}
Hb (g/dl)	13.2 ± 0.5	12 ± 0.2 ^{o*}	11±0.5 ^{o*}
MCV (fl)	51.8 ± 1.5	50.0 ± 2.0	57.2±1.3 ^{o*}
MCH (g/dl)	16.7 ± 1.1	16 ± 0.3	16.1±0.4
RDW (%)	13.9 ± 0.55	13.2 ± 0.4	14.1±0.4 ^{o*}
Retics (10³ cells/uL)	380± 20*	190 ± 59 ^{o*}	180±12 ^{o*}
MCVr(fl)	61.2± 1.3*	61 ± 1.4*	65±0.2 ^{o*}

Hct: hematocrit; Hb: hemoglobin; MCV: mean corpuscular volume; MCH: mean corpuscular hemoglobin; RDW: red cell distribution width; Retics: reticulocytes; *p< 0.05 compared to wild-type mice; °p<0.05 compared to 4 months-old mice.

As shown in table 2, Nrf2^{-/-} mice developed an age-dependent macrocytic anemia associated with increased RDW as index of anisopiklytosis and a marked reduction in reticulocytes, which displayed increased cell volume (MVCr). This finding suggests the

presence of ineffective erythropoiesis in *Nrf2*^{-/-} mice when compared to aging wild-type animals.

To study erythropoiesis in *Nrf2*^{-/-} mice, we used a recently developed flow cytometry strategy.²⁹ *Nrf2*^{-/-} mice displayed an aged dependent splenomegaly associated with the appearance of extramedullary erythropoiesis as supported by the increased amount of splenic CD44⁺ Ter119⁺ cells (Fig. 9a-b) without significant change in erythroid maturation profile (data not shown). Increased ROS levels was evident in erythroblasts in the early phase of erythropoiesis without major difference in orthochromatic erythroblasts when compared to wild-type animals. The increased amount of 8-Hydroxydeoxyguanosine (8-OHdG) supports the presence of oxidative DNA damage in *Nrf2*^{-/-} mouse erythroblasts compared to wild-type cells (Fig. 9c-d). We also observed increase apoptotic (Annexin V⁺ Cells) *Nrf2*^{-/-} erythroblasts from the early phase of erythropoiesis compared to wild-type cells (Fig. 9e). These data suggest an increased pro-oxidant environment in *Nrf2*^{-/-} erythroblasts, which might be possibly related to down-regulation of Nrf2 dependent ARE genes. Indeed, we found down-regulation of *Catalase*, *Srxn2*, *Ho-1*, *Trx* and *Prx2* (Fig. 9f). As back-up mechanism to support stress erythropoiesis, we found increased activation of NF-κB, another redox sensitive transcriptional factor, in sorted erythroblasts from *Nrf2*^{-/-} mice compared to wild-type animals (data not shown). All together, these findings suggest that the absence of Nrf2 increases the susceptibility of erythroblasts to oxidative stress with the development of an age dependent ineffective erythropoiesis.

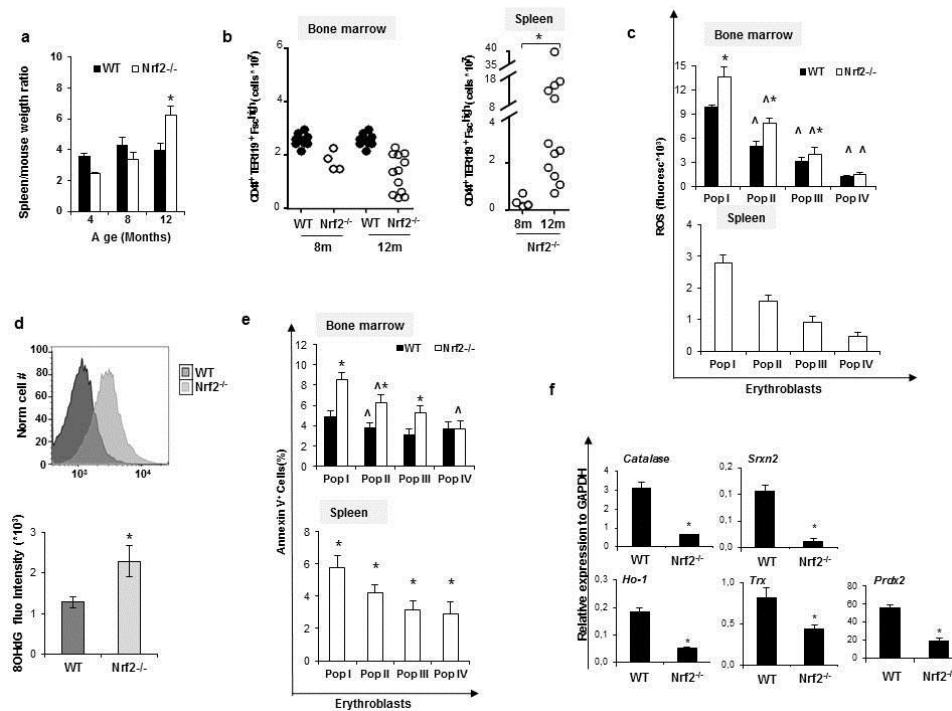


Fig. 9. (a) Spleen weight/mouse weight ratio of WT and Nrf2^{-/-} mice. **(b)** Cytofluorimetric analysis of maturation pattern of erythroid precursors from bone marrow and spleen using the following surface markers: CD44 and Ter119. **(c)** ROS levels in erythroid precursors from bone marrow and spleen of Nrf2^{-/-} mice and WT control. **(d)** DNA oxidative damage of erythroblast populations from Nrf2^{-/-} mice and WT control. **(e)** Amount of Annexin V⁺ cells in erythroid precursors from bone marrow and spleen of Nrf2^{-/-} mice and WT control. **(f)** RT-PCR expression of Catalase, Srxn2, Ho-1, Trx and Prx2 on sorted mouse erythroblast populations from Nrf2^{-/-} mice and WT control. Data are presented as means±SD (n=6) *P<0.05 compared to WT.

6.3 Age dependent activation of Nrf2 sustains erythropoiesis in wild-type mice

To understand whether Nrf2 might be important during mouse aging in normal erythropoiesis, we evaluated Nrf2 localization and activity in sorted erythroblasts from wild-type at 4 and 12 months of age. As shown in Fig. 10a, Nrf2 was activated in sorted erythroid precursors from 12 months-old wild-type mice compared to younger animals (Nrf2 nuclear translocation in Fig. 10a; phospho-Nrf2 as active Nrf2 in Fig. 10b). Whereas, no major change in activation of NF-κB was evident in erythroid precursors from aging wild-type mice (Fig. 10b). This suggest an age dependent activation of Nrf2 in wild-type mice as confirmed by the up-regulation of two ARE-related genes such as *Ho-1* and *Prx2* (Fig. 10c). Previously, we described a functional link between Nrf2 and Prx2 in models of stress erythropoiesis.²⁹ Since aging is characterized by increased oxidative stress, we asked whether Prx2 might translocate to the nucleus acting as local cytoprotector. As shown in Fig. 10d, we observed a

nuclear localization of Prx2 in 12 months-old wild-type sorted erythroid precursors by immunofluorescent microscopy. This was further validated by immunoblot analysis of nuclear fraction from sorted polychromatic (population III) and orthochromatic (population IV) erythroblasts of wild-type animals, confirming the nuclear localization of Prx2 in erythroblasts (Fig. 10e). We used sorted erythroblasts from Prx2^{-/-} mice as control. All together, these data indicate the importance of Nrf2 to limit oxidation in aging by up-regulation of ARE-genes and nuclear translocation of Prx2 to assist cell growth and maturation.

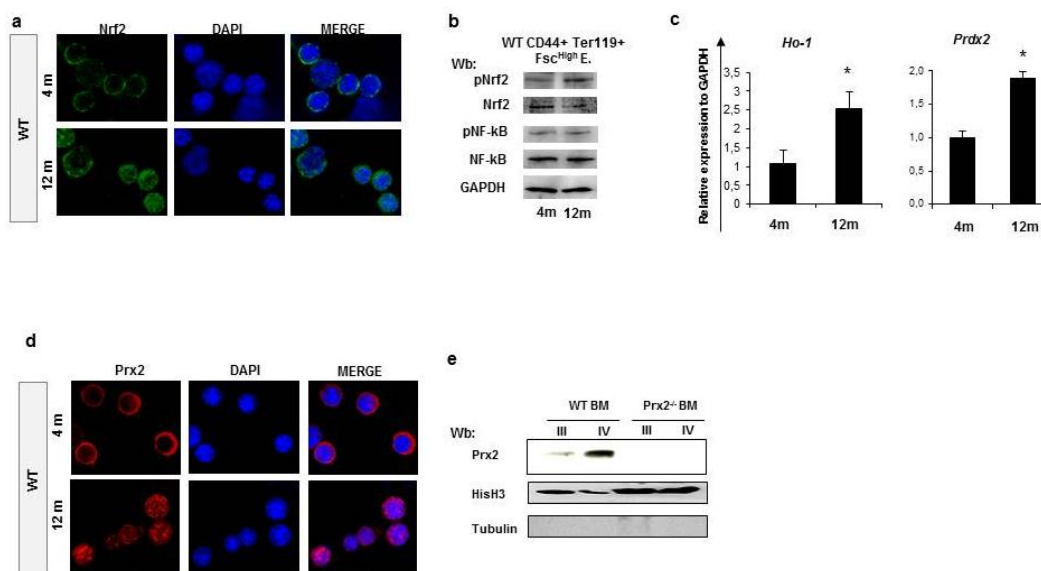


Fig. 10. (a) Nrf2 immunostaining of sorted erythroid precursors from bone marrow of 4 and 12-months old wild-type (WT) mice. **(b)** Western blot analysis of phosphor-Nrf2(p-Nrf2), Nrf2, phosphor-NFkB(p-NFkB) and NFkB in sorted erythroid precursors from bone marrow of 4 and 12-months old WT mice. GAPDH was used as protein loading control. **(c)** RT-PCR expression of Ho-1 and Prx2 on sorted mouse erythroblast populations from bone marrow of 4 and 12-months old WT mice. Data are presented as means±SD (n=6) *P<0.05 compared to WT. **(d)** Prx2 immunostaining of sorted erythroid precursors from bone marrow of 4 and 12-months old WT mice. **(e)** Western blot analysis of Prx2 in sorted erythroid precursors (nuclear fraction) from bone marrow of 4 and 12-months old WT mice. HisH3 was used as protein loading control.

6.4 Nrf2^{-/-} mice showed a delay response to stress erythropoiesis

We then explored the response of Nrf2^{-/-} mice to stress erythropoiesis induced respectively by PHZ or doxorubicin (Doxo). PHZ treatment induced acute hemolytic anemia in both mouse strains; however, the drop in hematocrit level was more pronounced in Nrf2^{-/-} mice when compared to wild-type animals (Fig. 11a, upper

panel). This was associated with a marked reduction in reticulocyte count in *Nrf2*^{-/-} mice at day 4 after PHZ treatment compared to wild-type animals (Fig. 11a, lower panel). In agreement we found no change in extramedullar erythropoiesis in *Nrf2*^{-/-} mice when compared to wild-type animals, which displayed a marked increase in erythropoietic spleen activity as expected in response to PHZ treatment (Fig. 11b).¹⁶ We also found an accumulation of both polychromatic and orthochromatic erythroblasts in bone marrow and spleen from both mouse strains, which was associated with increased amount of apoptotic polychromatic and orthochromatic erythroblasts in bone marrow and spleen from both mouse strains. Noteworthy, the amount of apoptotic orthochromatic erythroblasts was higher in *Nrf2*^{-/-} mice when compared to wild-type animals (Fig. 11c-d).

We then evaluated the effect of Doxo treatment on erythropoiesis of both mouse strains. As shown in Fig. 11e (upper panel), we found a significant reduction of Hct in *Nrf2*^{-/-} mice after 9 days of Doxo administration compared to wild-type. This was associated with a marked decrease in reticulocyte count in *Nrf2*^{-/-} mice at day 9 after Doxo administration (Fig. 11e, lower panel). This agreed with the reduction in total erythroblasts in both bone marrow and spleen site (Fig. 11f-g). In addition, the amount Annexin V⁺ cells was significantly increased in polychromatic and orthochromatic erythroblasts of *Nrf2*^{-/-} mice as compared to wild-type animals (Fig. 11h). Collectively, these findings indicate a blunted response to stress erythropoiesis in mice genetically lacking *Nrf2*.

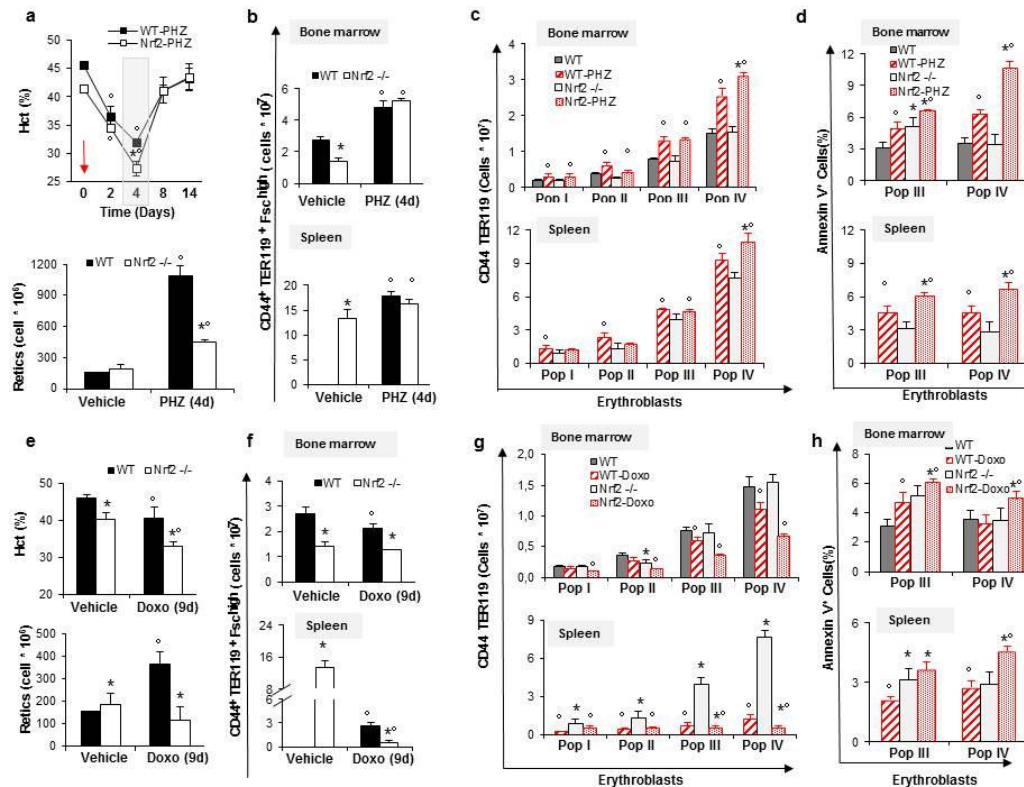


Fig. 11. (a) Hematocrit (%) and Reticulocyte count in WT and Nrf2^{-/-} mice exposed to PHZ injection. (b) Cytofluorimetric analysis of total erythroid precursors from bone marrow and spleen of WT and Nrf2^{-/-} mice using the following surface markers: CD44 and Ter119. (c) Cytofluorimetric analysis of maturation pattern of erythroid precursors from bone marrow and spleen of WT and Nrf2^{-/-} mice using the following surface markers: CD44 and Ter119. (d) Amount of annexin V⁺ cells in populations III corresponding to polychromatic erythroblasts (Pop III) and population IV corresponding to orthochromatic erythroblasts (Pop IV) from either spleen or bone marrow of WT and Nrf2^{-/-} mice respectively ad day 4 after PHZ administration. (e) Hematocrit (%) and Reticulocyte count in WT and Nrf2^{-/-} mice exposed to Doxo injection. (f) Cytofluorimetric analysis of total erythroid precursors from bone marrow and spleen of WT and Nrf2^{-/-} mice using the following surface markers: CD44 and Ter119. (g) Cytofluorimetric analysis of maturation pattern of erythroid precursors from bone marrow and spleen of WT and Nrf2^{-/-} mice using the following surface markers: CD44 and Ter119. (h) Amount of annexin V⁺ cells in populations III corresponding to polychromatic erythroblasts (Pop III) and population IV corresponding to orthochromatic erythroblasts (Pop IV) from either spleen or bone marrow of WT and Nrf2^{-/-} mice respectively ad day 9 after Doxo administration. Data are presented as means \pm SD (n=6) *P<0.05 compared to WT.

6.5 Nrf2^{-/-} erythroblasts showed activation of UPR system and impaired autophagy

To better understand the impact of chronic oxidation in Nrf2^{-/-} mouse erythropoiesis, we explored the back-up mechanisms involved in proteostasis network against oxidation such as the unfolded protein response system (UPR) and the autophagy-lysosomal pathway. UPR system has a cytoprotective role in restoring endoplasmic reticulum homeostasis in presence of cellular stress.⁹⁰ The activation of UPR facilitates proteins degradation and/or processing of unfolded/damaged proteins to

ensure cell survival. UPR system is organized in three arms: (i) ATF6, (ii) IRE and (iii) PERK, which included CHOP and Gadd34.⁹¹

Previous reports have shown that abnormalities in UPR system deeply affect hematopoiesis as reported in a mouse model defective of UFBPI, which is characterized by severe endoplasmic reticulum (ER)-stress and pancytopenia.⁹⁰ Nrf2^{-/-} erythroid precursors displayed a blockage of UPR system activity as supported by the increased expression of ATF6 and Gadd34 associated with reduction of CHOP (Fig. 12a).⁹¹ These data suggest that chronic oxidation in Nrf2^{-/-} erythroid cells overcomes the ability of UPR system to maintain cell homeostasis.

To support cell homeostasis in presence of severe or prolonged stress, UPR system is able to induce autophagy and in turn autophagy might alleviate UPR system, counterbalancing ERS.⁹²⁻⁹³ Given that efficient autophagy is required for erythroid maturation, we therefore evaluated the expression of some key proteins of autophagy in sorted erythroid precursors from bone marrow of both mouse strains. We focused our analysis on (i) LC3 as initiator of autophagy; (ii) Atg4, involved in fusion of autophagosomes with lysosomes; (iii) Atg7, involved in autophagosome structure; (iv) Atg5 involved in maturation of autophagosome together with Rab 5 which contributes to recycling endosomes; and (v) specific markers of different trafficking compartments such as Lamp1 for multivesicular bodies/late endosomes, or p62 as protein cargo.⁷⁶ As shown in Fig. 12b, we found activation of LC3, associated with reduction in Atg4, Atg5 and Atg7, suggesting an activation of autophagy. However, we observed an accumulation of Rab5, indicating a possible impairment of the autophagic flux (Fig. 12b). The amount of Lamp1 was slightly reduced in Nrf2^{-/-} erythroblasts, whereas p62 was significantly decreased compared to wild-type erythroblasts. Since p62 expression depends on Nrf2 function, we evaluated p62 mRNA level in erythroblasts from both mouse strains. p62 mRNA level was down-regulated in Nrf2^{-/-} erythroblasts compared to wild-type cells (data not shown), possibly contributing to the lower expression of p62 observed in Nrf2^{-/-} erythroblasts. To better understand whether the impaired autophagy involved autophagosome and endosome recycling, we used immunofluorescent microscopy with specific antibodies. As shown in Fig. 12c, Nrf2^{-/-} erythroblasts displayed punctae of Atg7

organized in large clusters more abundant than in wild-type erythroblasts. Whereas, the amounts of Lamp-1 punctae in *Nrf2*^{-/-} erythroblasts were higher than in wild-type erythroblasts, suggesting a cell engulfment of LAMP-1 positive autophagosome (Fig. 12c). Our data indicate the attempt of *Nrf2*^{-/-} erythroblasts to face oxidation by activation of UPR system and autophagy. However, the persistent oxidative stress re-directs cells towards apoptosis as supported by the increase of caspase-3 activity observed in *Nrf2*^{-/-} erythroblasts when compared to wild-type cells (Fig. 12d).

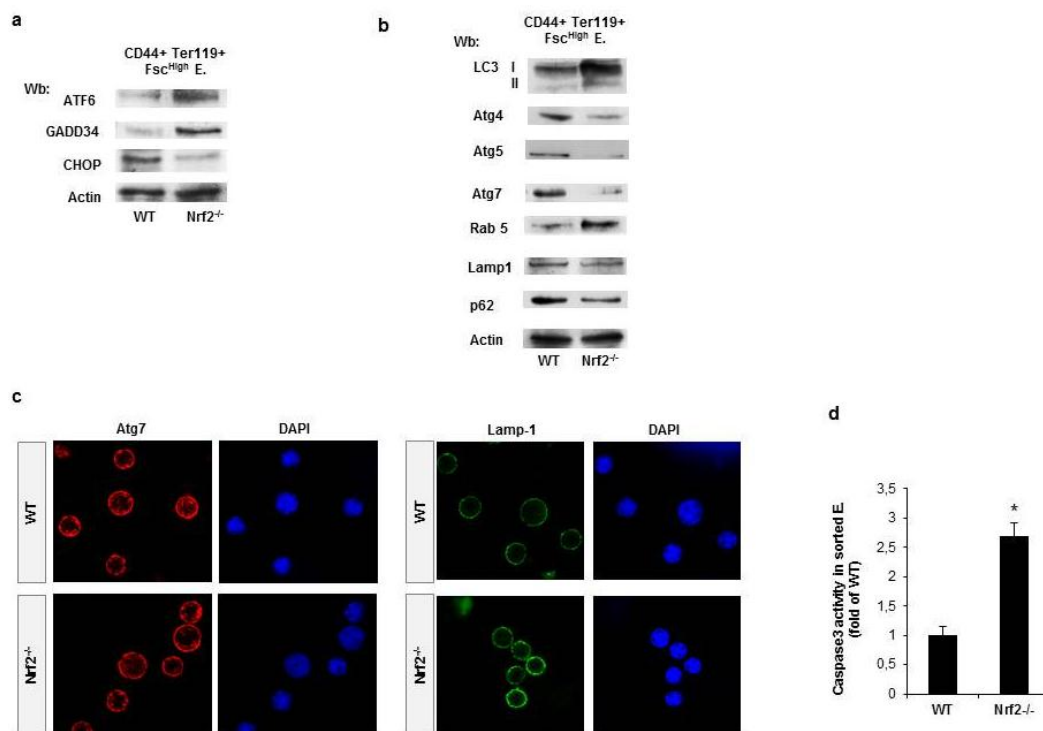


Fig. 12. (a) Western blot (Wb) analysis of ATF6, CHOP and Gadd34 in sorted erythroid precursors from bone marrow of 12-months old WT and *Nrf2*^{-/-} mice. Actin was used as protein loading control. (b) Western blot (Wb) analysis of Atg4, Atg5, Atg7, Lamp-1, p62, Rab5 and LC3 in sorted erythroid precursors from bone marrow of 12-months old WT and *Nrf2*^{-/-} mice. Actin was used as protein loading control. (c) Atg7 and Lamp-1 immunostaining of sorted erythroid precursors from bone marrow of 12-months old WT and *Nrf2*^{-/-} mice. (d) Detection of caspase 3 activation by its cleavage of a fluorescent substrate in sorted erythroid precursors from bone marrow of WT and *Nrf2*^{-/-} mice. Data are presented as means±SD (n=6) *P<0.05 compared to WT.

6.6 Astaxanthin treatment ameliorates stress erythropoiesis in *Nrf2*^{-/-} mice

To understand whether the reduction of oxidative stress might beneficially impact *Nrf2*^{-/-} mouse erythropoiesis, we treated *Nrf2*^{-/-} mice with Astaxanthin, a powerful antioxidant, loaded in lyophilized PLGA nanoparticles (ATS-NP; Fig. 13a).

Astaxanthin (3,3'-dihydroxy- β -carotene-4,4'-dione) is nontoxic and organic carotenoid, mostly present in aquatic organisms. Astaxanthin displays a wide variety of biological effects including: anti-inflammatory, antiapoptotic, neuroprotective and cardioprotective effects (Table 3).⁹⁴⁻⁹⁵

Table 3. Effects of Astaxanthin in cell-based and animal-based systems

Models	Effects of Astaxanthin	Ref.
In vitro Studies	<p><i>ARPE-19 cells, pretreated 24h with ATS (20μM) and exposed to Hydrogen peroxide (200μM) for 24h</i></p> <ul style="list-style-type: none"> - Inhibition of intracellular ROS production - Activation of antioxidant systems (HO-1, Nqo1, Gclc and Gclm). 	Zhongrui Li 2013 ⁹⁶
	<p><i>BV2 Cells pretreated 4h with ATS (10μM) and exposed to LPS-induced inflammation for 4h</i></p> <ul style="list-style-type: none"> - Inhibition of LPS-induced microglia activation - Regulation of M2 microglia polarization 	Xiaojun W. 2017 ⁹⁷
	<p><i>Breast cancer cell lines (MCF and MDA-MB-231), treated for 24h with ATS (25 μM or 50 μM)</i></p> <ul style="list-style-type: none"> - Inhibition of breast cancer cell migration - Activation of cancer cell apoptosis (High concentration) 	Buckley Mc. 2018 ⁹⁸
In vivo Studies	Animal models	
	<p><i>Cyclophosphamide-induced oxidative stress in rats pretreated orally 3 days and 10 days after cyclophosphamide injection with ATS (25 mg/kg daily)</i></p> <ul style="list-style-type: none"> - Protection from DNA damage (DNA fragmentation) - Down regulation of Pro-apoptotic protein(p38 and p53) 	Tripathi DN 2009 ⁹⁹
	<p><i>Streptozotocin-induced diabetes mellitus (DM) rats, treated through intraperitoneal injection with ATS (10, 20 and 40 mg/kg) for 5 days</i></p> <ul style="list-style-type: none"> - Reduction of blood glucose levels - Reduced activity of caspase 3 and 9 in cerebral cortex of DM rats 	Xu Lianbao 2015 ¹⁰⁰
<p><i>MPTP-induced Parkinson mouse model, treated through ATS-enriched diet to achieve the dose of 30 mg/kg daily for 5 weeks</i></p>	Grimmig B 2017 ¹⁰¹	

	<ul style="list-style-type: none"> - Protection from oxidative induced neurodegeneration - Reduction of Microglia migration in SNpc 	
	<p><i>Streptozotocin-induced diabetic rats, treated through intraperitoneal injection with ATS (25 mg/kg daily) for 12 weeks</i></p> <ul style="list-style-type: none"> - Protection from oxidative damage in the kidney - Reduced accumulation of ECM components 	Xiaoyu Zhu 2018 ¹⁰²
	Human clinical studies	
	<p><i>Non obese subjects with high levels of serum triglyceride, treated with ATS (6, 12, 18 mg/day) for 12 weeks</i></p> <ul style="list-style-type: none"> - Reduced serum triglyceride levels - Increased HDL-cholesterol 	Yoshida H 2010 ¹⁰³
	<p><i>Young and adult healthy females, treated with ATS (8 mg/day) for 8 weeks</i></p> <ul style="list-style-type: none"> - Reduced DNA damage - Increased immune response in young healthy females 	Park Soon J 2010 ¹⁰⁴
	<p><i>Obese adults, treated with ATS (5 and 8 mg/day) for 3 weeks</i></p> <ul style="list-style-type: none"> - Suppression of lipid peroxidation - Activation of antioxidant systems 	Choi Duck H 2011 ¹⁰⁵

Astaxanthin is a carotenoid with strong anti-oxidative and without any pro-oxidative properties.¹⁰⁶ Astaxanthin has unique molecular structure, quenching single oxygen and scavenging free radicals, preventing lipid peroxidation.¹⁰⁷⁻¹⁰⁸ The impact of astaxanthin has been evaluated in previous *in vitro* and *in vivo* animal based models as well as in human subjects (dosage ranging from 4 to 100 mg/day) (Table 3).

Although Astaxanthin is a lipophilic molecule characterized by a low oral bioavailability. The bioavailability of Astaxanthin might be enhanced by lipid-based formulations or by using nanotechnologic approaches such as nanostructured lipids carriers, nanoemulsions or nanodispersion systems.¹⁰⁹⁻¹¹²

Food and Drug Administration as well as EMEA have approved the use of different therapeutic molecules encapsulated in PLGA nanoparticles, which are poly -lactic-co-glycolic acid (PLGA) based biodegradable and biocompatible polymers.¹¹³ This strategy allows the optimization of drug delivery and the reduction of drug toxicity. PLGA nanoparticles are generally cleared by (i) phagocytic uptake in spleen and liver; (ii) hepatic filtration; (iii) kidney extraction.¹¹⁴

In our study, mice were treated with Astaxanthin-NP at the dosage of 2 mg/Kg every two days for four weeks. Organ distribution of ATS was determined by mass spectrometric analysis at 24 hours after ATS administration (Fig. 13a). ATS was identified in spleen, liver and kidney from both mouse strains (Fig. 13a). However, ATS concentration was higher in *Nrf2*^{-/-} mouse organs when compared to wild-type animals. This might be related to different clearance-time between wild-type and *Nrf2*^{-/-} mice, possibly determined by activated macrophages in spleen and liver as well as to the presence of extramedullary erythropoiesis in *Nrf2*^{-/-} mice.

ATS-NP ameliorates anemia of *Nrf2*^{-/-} mice, with normalization of red cell volume, reduction in RDW, indicating a decrease in red cell anisopoikilocytosis and increase of reticulocyte count compared to vehicle treated animals (Table 4).

	Vehicle Wild-type mice (12 months-old) (n=6)	ATS-NP Wild-type mice (12 months-old) (n=6)	Vehicle <i>Nrf2</i>^{-/-} mice (12 months-old) (n=6)	ATS-NP <i>Nrf2</i>^{-/-} mice (12 months-old) (n=5)
Hct (%)	44.8±0.2	45.9 ± 0.7	33.6±3*	43.5±0.9*^
Hb (g/dl)	14.3±0.4	15 ± 0.1	11±0.5*	14.0±0.4^
MCV (fl)	52.2±0.3	51.0 ± 0.1	57.2±1.3*	53.5±1.1^
MCH (g/dl)	15.6±0.2	16.5 ± 0.3	16.1±0.4	16.3±0.2
RDW (%)	12.7±0.3	13.5 ± 0.1	14.1±0.4*	12.6±0.4^
Retics (10³ cells/uL)	248±24	431 ± 51^	180±12*	355±65^
MCVr(fl)	59.9±1.8	56.1±2	65±0.2*°	62±1.6^

Hct: hematocrit; Hb: hemoglobin; MCV: mean corpuscular volume; MCH: mean corpuscular hemoglobin; RDW: red cell distribution width; Retics: reticulocytes; *p< 0.05 compared to wild-type mice; ^p<0.05 compared to vehicle treated animals.

ATS-NP improved Nrf2^{-/-} erythropoiesis as indicated by (i) the marked reduction of (i) splenic erythropoiesis (stress erythropoiesis) and (ii) the amount of apoptotic Nrf2^{-/-} erythroblasts compared to vehicle treated animals (Fig. 13b-c). In agreement we found lower caspase-3 activity in sorted Nrf2^{-/-} erythroblasts than in vehicle treated Nrf2^{-/-} cells (Fig. 13d). The beneficial effects of ATS-NP on Nrf2^{-/-} erythropoiesis was associated with the reduction of UPR system, suggesting a restoring function of ER; and (ii) the increase autophagy related proteins, indicating an inactivation of autophagy (Fig. 13e). These findings indicate that ATS-NP efficiently reduced oxidative stress in erythropoiesis from Nrf2^{-/-} mice, ensuring cell survival with reduction of pro-apoptotic events and amelioration of quality control processes in generation of mature red cells. Indeed, ATS-NP Nrf2^{-/-} mice showed a significant reduction in red cell ROS levels and in the amount of annexin V⁺ erythrocytes compared to vehicle treated Nrf2^{-/-} animals (Fig. 13f).

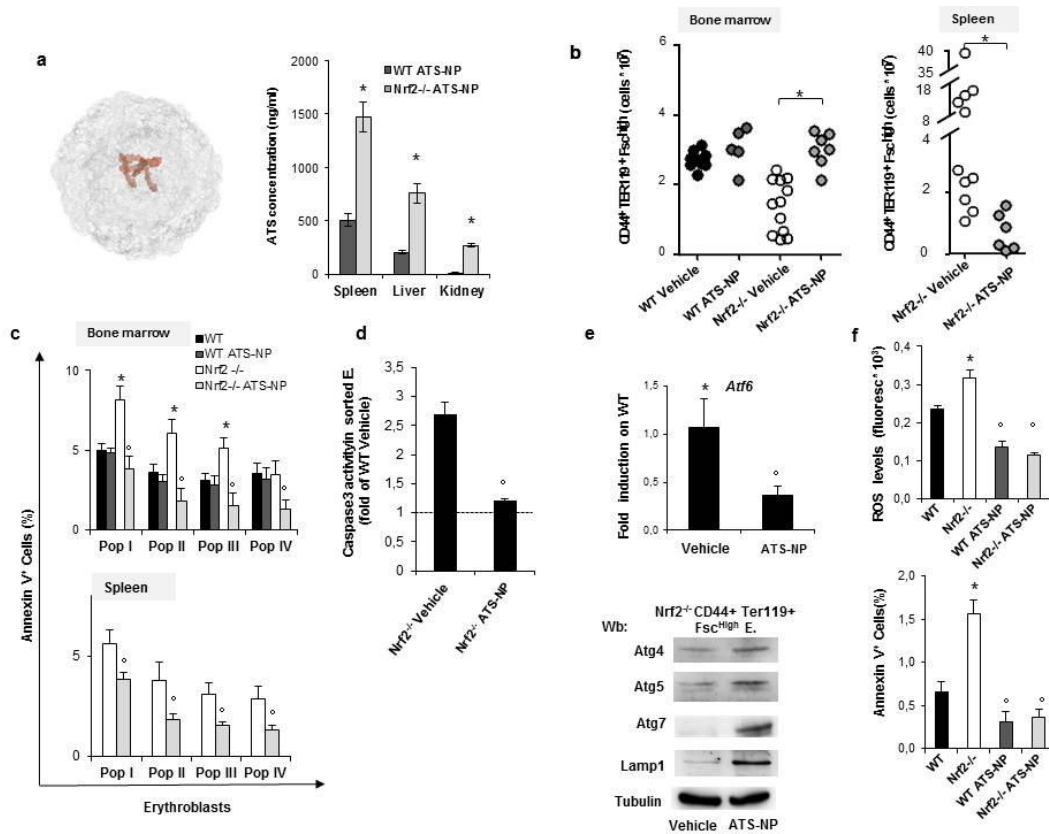


Fig. 13. (a) Schematic representation of an Astaxanthin Loaded PLGA nanoparticle and organ distribution of Astaxanthin molecules in both mice strains during treatment. In red, the Astaxanthin molecule encapsulated in the PLGA nanoparticle structure (b) Cytofluorimetric analysis of maturation pattern of erythroid precursors from bone marrow and spleen of vehicle and treated WT and *Nrf2*^{-/-} mice using the following surface markers: CD44 and Ter119. (c) Amount of Annexin V⁺ cells in erythroid precursors from bone marrow and spleen of vehicle and treated WT and *Nrf2*^{-/-} mice. (d) Detection of caspase 3 activation by its cleavage of a fluorescent substrate in sorted erythroid precursors from bone marrow of vehicle and treated *Nrf2*^{-/-} mice. (e) RT-PCR expression of *Atf6* on sorted mouse erythroblast populations from bone marrow of vehicle and treated *Nrf2*^{-/-} mice (upper panel). Western blot (Wb) analysis of Atg4, Atg5, Atg7 and LAMP1 in sorted erythroid precursors from bone marrow of vehicle and treated *Nrf2*^{-/-} mice (lower panel). Tubulin was used as protein loading control. (f) Annexin V⁺ red cells in vehicle and treated *Nrf2*^{-/-} and WT mice (upper panel). ROS in red cells from vehicle and treated *Nrf2*^{-/-} and WT mice (lower panel). Data are presented as means ± SD (n=6) *P<0.05 compared to WT.

7. DISCUSSION

In the present study, we show for the first time the key role of Nrf2 in stress erythropoiesis and in quality control process involved in erythroid maturation. In agreement with a previous study, we found increased membrane protein and lipid oxidation in Nrf2^{-/-} mouse red cells when compared to wild-type erythrocytes.⁴⁹ This was associated with red cell membrane translocation of classical chaperone proteins (HSP70 and 90) and activation of canonical signaling pathway mediated by Syk kinase, targeting the integral membrane protein band 3. The reduction of red cell anti-oxidant machinery, related to the absence of Nrf2, increases the susceptibility of Nrf2^{-/-} mouse red cells to *in vitro* H₂O₂ stress. This also sustains an accelerated *in vivo* red cell senescence, resulting in a slight but significant reduction of Nrf2^{-/-} red cell survival compared to wild-type erythrocytes (data not shown). A previous study has shown increased erythrophagocytosis of Nrf2^{-/-} mouse erythrocytes mediated by both PS exposure and naturally occurring anti-band 3 antibody.⁴⁹ Here, we confirmed the presence of natural occurring anti-band 3 antibody; however, in Nrf2^{-/-} mice, we documented an age-dependent anemia associated with reduced reticulocyte count in presence of constant levels of natural occurring anti-band 3 antibody, suggesting a perturbation of erythropoiesis as additional factor to the accelerated red cell senescence in generating anemia of Nrf2^{-/-} mice. Indeed, ineffective erythropoiesis was found in 12 months-old Nrf2^{-/-} mice as supported by (i) extramedullary erythropoiesis; (ii) increased ROS levels throughout maturing erythroblasts; (iii) erythroblasts oxidative DNA damage; and (iv) increased cell apoptosis in all erythroblast subpopulations. Our data indicate that the down-regulation of Nrf2 dependent ARE-genes encoding for anti-oxidant systems promotes a highly pro-oxidant environment with detrimental effects on Nrf2^{-/-} erythropoiesis. The increased susceptibility of Nrf2^{-/-} mice to oxidative stress is also supported by the blunted response to stress erythropoiesis induced by either PHZ or Doxo. Thus, the activation of Nrf2 is required against exogenous oxidative stress or endogenous oxidation as observed in aging process. Indeed, we found activation of Nrf2 in erythroblasts from 12 months-old wild-type mice associated with a slight reduction in Hb and a

significant decrease in reticulocyte count compared to younger wild-type animals. The up-regulation of Prx2 and its nuclear translocation further support the cooperation between Nrf2 and Prx2 to limit cell oxidation and to assist cell growth and maturation.

Perturbation of cellular back up mechanisms against oxidation such as UPR system and autophagy might also contribute to ineffective erythropoiesis of aging Nrf2^{-/-} mice. Nrf2 is generally activated by UPR system and is involved in the synthesis of autophagy related proteins. Thus, the blockage in the UPR system and the inactivation of autophagy observed in Nrf2^{-/-} mice might be related to the persistent oxidation due to the defective cellular anti-oxidant machinery, re-directing cells towards apoptosis. The beneficial effects of Astaxanthin-NP treatment further support this working model. In fact, in Nrf2^{-/-} mice ATS-NP ameliorates age-dependent macrocytic anemia and improves ineffective erythropoiesis with inactivation of cellular adaptive mechanisms such as UPR system and autophagy.

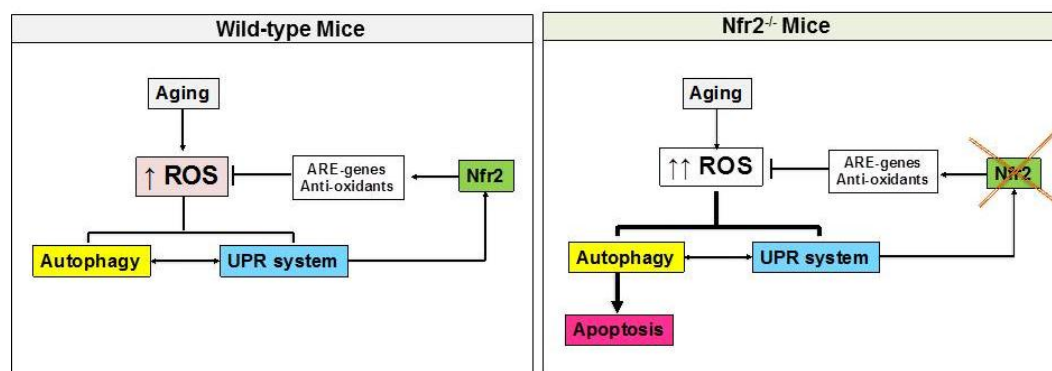


Fig. 14. Schematic diagram of the working model proposed for Nrf2 transcription factor to limit oxidative stress induced by aging during erythropoiesis. In wild-type mice, the physiological generation of ROS during aging is controlled by antioxidant systems related to the activation of Nrf2. In Nrf2^{-/-} mice, the absence of Nrf2 promotes perturbation of cellular back up mechanism against oxidation such as UPR system and autophagy, leading to cells apoptosis.

In conclusion, we propose Nrf2 as key transcriptional factor in erythropoiesis against oxidation induced by aging or by exogenous oxidants (e.g. PHZ or Doxo). The beneficial effects of ATS-NP on anemia of Nrf2^{-/-} mice further support the importance of Nrf2 to ensure a powerful anti-oxidant machinery during erythroid maturation events.

Future perspective

Since Nrf2 is important to limit aging induced oxidation in erythropoiesis, we plan to evaluate Nrf2 function in other models of pathologic erythropoiesis such as sickle cell disease or Pyruvate kinase deficiency. In addition, we will evaluate the impact of Nrf2 activating agents such as dimethyl-fumarate in pathologic erythropoiesis (β -thalassemia) or in stress erythropoiesis (i.e. PHZ treatment).

Since Astaxanthin-NP treatment showed beneficial effects in Nrf2^{-/-} mouse erythropoiesis, we plan to test ATS-NP in a mouse model for β -thalassemia, which is characterized by severe oxidative stress and block in erythroid maturation. We will compare the effects of ATS-NP with other anti-oxidant such as N-acetylcysteine or resveratrol that we and others previously reported to improve anemia of β -thalassemia.²⁷⁻²⁸

8. REFERENCES

1. **Weissman I. L, et al.** Stem cells: units of development, units of regeneration, and units in evolution. *Cell* 100: 157–168, 2000.
2. **Orkin S. H, et al.** Hematopoiesis: an evolving paradigm for stem cell biology. *Cell* 132: 631–644, 2008.
3. **Dzierzak E, et al.** Erythropoiesis: Development and Differentiation. *Cold Spring Harb Perspect Med* 3:a011601, 2013.
4. **Palis J, Robertson S et al.** Development of erythroid and myeloid progenitors in the yolk sac and embryo proper of the mouse. *Development*. 126:5073-5084, 1999.
5. **Lawson K.A, et al.** Clonal analysis of epiblast fate during germ layer formation in the mouse embryo. *Development*. 113:891-911, 1991.
6. **Bernard J.** The erythroblastic island: past and future. *Blood cells* 17:5-10, 1991.
7. **Sadahira Y, et al.** Role of the macrophage in erythropoiesis. *Pathol. Int.*49:841-848, 1999.
8. **Yoshida H, et al.** Phosphatidylserine-dependent engulfment by macrophage of nuclei from erythroid precursors cells. *Nature* 437:754–758, 2005.
9. **Migliaccio A.R, et al.** Standardization of progenitor cell assay for cord blood banking. *Ann. Ist Super sanità.*37:595-600, 2001.
10. **Alter B.P.** Biology of erythropoiesis. *Ann. NY Acad. Sci.* 731:36–47, 1994.
11. **Constantinescu S.N, et al.** The erythropoietin receptor: structure, activation and intracellular signal transduction. *Trends Endocrin Met.* 10:18–23, 1999.
12. **Fang J, et al.** EPO modulation of cell-cycle regulatory genes, and cell division in primary bone marrow erythroblasts. *Blood* 110:2361-2370, 2007.
13. **Rane S. G, et al.** JAKs, STATs and Src kinases in hematopoiesis. *Oncogene* 21:3334–3358, 2002.
14. **D’andrea A. D, et al.** Expression cloning of the murine erythropoietin receptor. *Cell* 57:277–285, 1989.
15. **Franco SS, et al.** Resveratrol accelerates erythroid maturation by activation of FoxO3 and ameliorates anemia in beta-thalassemic mice. *Haematologica* 99: 267–275, 2014.

16. **Witthuhn B. A, et al.** JAK2 associates with the erythropoietin receptor and tyrosine phosphorylated and activated following stimulation with erythropoietin. *Cell* 74: 227–236, 1993.
17. **Beneduce E, et al.** Fyn kinase is a novel modulator of erythropoietin signaling and stress erythropoiesis. *Am J Hematol.* 94 :10-20, 2019.
18. **Thomas S. M, Brugge J.S.** Cellular functions regulated by Src family kinase. *Ann. Rev. Cell. Dev. Biol.* 13:513-609, 1997.
19. **Socolovsky M, et al.** Stat5 signaling specifies basal versus stress erythropoietic response through distinct binary and graded dynamic modalities. *Plos Biol.* 10:e1001383, 2012.
20. **Lodish H. F, et al.** Ineffective erythropoiesis in Stat5a (-/-)5b(-/-) mice due to decreased survival of early erythroblasts. *Blood* 98:3261-3273, 2001.
21. **Socolovsky M, et al.** Suppression of Fas-FasL coexpression by erythropoietin mediates erythroblasts expansion during the erythropoietic stress response in vivo. *Blood* 108:123-133, 2006.
22. **Perkins A. C, et al.** Direct targets of pSTAT5 signaling in erythropoiesis. *PLos One* 12:e0180922, 2017.
23. **Bouscary C, et al.** Critical role for PI 3-kinase in the control of erythropoietin-induced erythroid progenitor proliferation. *Blood* 101:3436-3443, 2003.
24. **Ghaffari S, et al.** FOXO3-mTOR metabolic cooperation in the regulation of erythroid cell maturation and homeostasis. *Am J Hematol.* 89:954-963, 2014.
25. **Knight Z. A, et al.** A critical role for mTORC1 in erythropoiesis and anemia. *Elife* 3:e01913, 2014.
26. **Ghaffari S, et al.** Foxo3 is essential for the regulation of Ataxia telangiectasia mutated and oxidative stress-mediated homeostasis of hematopoietic stem cells. *J. Biol. Chem.* 283:25692-25705, 2008.
27. **Gregory T, et al.** GATA-1 and erythropoietin cooperate to promote erythroid cell survival by regulating *bcl-xL* expression. *Blood* 94:87-96, 1999.
28. **Ghaffari S, et al.** Foxo3 is required for the regulation of oxidative stress in erythropoiesis. *J. Clin. Invest.* 117:2133-2144, 2007.

29. **Mattè A, et al.** The Interplay Between Peroxiredoxin-2 and Nuclear Factor-Erythroid 2 Is Important in Limiting Oxidative Mediated Dysfunction in β -Thalassemic Erythropoiesis. *Antioxid Redox Signal.* 23:1284-97, 2015.
30. **Moi P, et al.** Isolation of NF-E2-related factor2 (Nrf2), a NF-E2-like basic leucine zipper transcriptional activator that binds to the tandem NFE2/AP1 repeat of the beta-globin locus control region. *Proc. Natl. Acad. Sci. U.S.A.* 91: 9926-9930, 1994.
31. **Hayes J.D, et al.** Cancer chemoprevention mechanisms mediated through the Keap1-Nrf2 pathway. *Antioxid Redox Signal* 13:1713-1748, 2010.
32. **Wang H, et al.** RXR α inhibits NRF2-ARE signaling pathway through direct interaction with the Neh7 domain of Nrf2. *Cancer Res.* 73:3097-3108, 2013.
33. **Baird L, et al.** The cytoprotective role of Keap1-Nrf2 pathway. *Arch. Toxicol.* 85:241-272, 2011.
34. **Motohashi H, et al.** Small Nrf proteins serve as transcriptional cofactors for keratinocyte differentiation in the Keap1-Nrf2 regulatory pathway. *Proc. Natl. Acad. Sci.* 101:6379-6384, 2004.
35. **Harada N, et al.** Nrf2 regulates ferroportin 1-mediated iron efflux and counteracts lipopolysaccharide-induced ferroportin 1 mRNA suppression in macrophages. *Biochim. And Biophys.* 508:101-109, 2011.
36. **Lewerenz J, et al.** The cystine/glutamate antiporter system x_c⁻ in health and disease: from molecular mechanisms to novel therapeutic opportunities. *Antioxid. Redox. Signal.* 18:522-555, 2013.
37. **Higgins L. G, et al.** Transcription factor Nrf2 mediates an adaptive response to sulforaphane that protects fibroblasts in vitro against the cytotoxic effects of electrophiles peroxides and redoxcycling agents. *Toxicol. Appl. Pharmacol.* 237:267-280, 2009.
38. **Hawkes H. J, et al.** Regulation of the human thioredoxin gene promoter and its key substrates: A study of functional and putative regulatory elements. *Biochim. And Biophys.* 1840:303-314, 2013.
39. **MacLeod A. K, et al.** Characterization of the cancer chemopreventive Nrf2-dependent gene battery in human keratinocytes: demonstrating that the KEAP1-NRF2 pathway, and not the BACH1-NRF2 pathway, controls cytoprotection against

- electrophiles as well as redox-cycling compounds . *Carcinogenesis* 30:1571-1580, 2009.
40. **Malhotra D, et al.** Global mapping of binding sites for Nrf2 identifies novel targets in cell survival response through ChIP-Seq profiling and network analysis. *Nucleic Acids Res.* 38:5718-5734, 2010.
 41. **Agyeman A. S, et al.** Transcriptomic and proteomic profiling of KEAP1 disrupted and sulforaphane-treated human breast epithelial cells reveals common expression profiles. *Breast Cancer Res . Treat.* 132:175-187, 2012.
 42. **Chorley B. N, et al.** Identification of novel NRF2-regulated genes by ChIP-Seq: influence on retinoid X receptor alpha. *Nucleic Acids Res.* 40:7416-7429, 2012.
 43. **Abbas K, et al.** Nitric oxide activates on Nrf2/sulfiredoxin antioxidant pathway in macrophages. *Free Radic. Biol. Med.* 51:107-114, 2011.
 44. **Jeong W, et al.** Role of sulfiredoxin as a regulator peroxiredoxin function and regulation of its expression. *Free Radic. Biol. Med.* 66:75-87, 2011.
 45. **Johnson R.M, et al.** The effects of disruption of genes for peroxiredoxin-2, glutathione peroxidase-1, and catalase on erythrocyte oxidative metabolism. *Free Radic. Biol. Med.* 48:519-525, 2010.
 46. **Mattè A, et al.** Peroxiredoxin-2 expression is increased in beta-thalassemic mouse red cells but is displaced from the membrane as a marker of oxidative stress. *Free Radic. Biol. Med.* 49:457-466, 2010
 47. **Rund D, et al.** Beta-thalassemia mouse red cells but is displaced from the membrane as a marker of oxidative stress. *N. Engl. J. Med.* 353:1135-1146, 2005.
 48. **Mattè A, et al.** Peroxiredoxin-2: a novel regulator of iron homeostasis in ineffective erythropoiesis. *Antioxid. Redox. Signal.* 28:1-14, 2018.
 49. **Lee J. M, et al.** Targeted disruption of Nrf2 causes regenerative immune-mediated hemolytic anemia. *PNAS.* 101:9751-9756, 2004.
 50. **Jiang li. M, et al.** Genetic dissection of systemic autoimmune disease in Nrf2-deficient mice. *Physiol Genomics.* 18:261-272, 2004.
 51. **Beyer T. A, et al.** Impaired liver regeneration in Nrf2 Knockout mice: role of ROS-mediated insulin/IGF1 resistance. *EMBO Journal.* 27:212-223, 2008.

52. **Zhang Y. J, et al.** Genetic activation of Nrf2 protects against fasting-induced oxidative stress in livers of mice. *PlosOne*. 8:e59122, 2013.
53. **Sandro Silva-Gomes, et al.** Transcription factor NRF2 protects mice against dietary iron-induced liver by preventing hepatocytic cell death. *Journal of Hepatology* 60:354-361, 2014.
54. **Zhang D, et al.** Identification of unfavorable immune signature in advanced lung tumors from Nrf2-Deficient mice. *Antioxid. Redox. Signal*. 29:1535-1552, 2018.
55. **Pellegrini G. G, et al.** Nrf2 regulates mass accrual and the antioxidant endogenous response in bone differently depending on sex and age. *Plos One*. 12:e0171161, 2017.
56. **Erkens R, et al.** Nrf2 deficiency unmasks the significance of Nitric oxide synthase activity for cardioprotection. *Oxid. Med. Cell. Longev*. 2018:8309698, 2018.
57. **Lister A, et al.** Nrf2 regulates the glutamine transporter Slc38a3 (SNAT3) in kidney in response to metabolic acidosis. *Sci. Rep*. 4:5629, 2018.
58. **Gothwal M, et al.** A novel role for Nuclear Factor erythroid 2 in erythroid maturation by modulation of mitochondrial autophagy. *Haematologica* 101: 1054-1064, 2016.
59. **Sigfridsson E, et al.** Astrocyte-specific overexpression of Nrf2 protects against optic tract damage and behavioural alterations in mouse model of cerebral hypoperfusion. *Sci. Rep*. 8:12552, 2018.
60. **Yang Zhifen, et al.** Mammalian autophagy: core molecular machinery and signaling regulation . *Curr Opin Cell Biol*. 22: 124-131, 2016.
61. **Joo J. H, et al.** HSP90-Cdc37 chaperone complex regulates Ulk1- and Atg13-mediated mitophagy. *Mol. Cell* 43: 572-585, 2011.
62. **Mortensen M, et al.** The autophagy protein Atg7 is essential for hematopoietic stem cell maintenance. *J. Exp. Med*. 208: 455-467, 2011.
63. **Zhang J, et al.** Mitochondrial clearance is regulated by Atg7-dependent and – independent mechanisms during reticulocyte maturation. *Blood* 114: 157-164, 2009.
64. **Kundu M, et al.** Ulk1 plays a critical role in the autophagic clearance of mitochondria and ribosomes during reticulocyte maturation. *Blood* 112: 1493-1502, 2008.

65. **Honda S, et al.** Ulk1-mediated Atg5-independent macroautophagy mediates elimination of mitochondria from embryonic reticulocytes. *Nat. Commun.* 5: 4004, 2014.
66. **Lupo F, et al.** A new molecular link between defective autophagy and erythroid abnormalities in chorea-acanthocytosis. *Blood* 128: 2976-2987, 2016.
67. **Maiuri M. C, et al.** Self-eating and self-killing: crosstalk between autophagy and apoptosis. *Nat. Rev. Mol. Cell. Biol.* 8:741-752, 2007.
68. **Wirawan C, et al.** Caspase-mediated cleavage of Beclin-1 inactivates Beclin-1-induced autophagy and enhances apoptosis by promoting the release of proapoptotic factors from mitochondria. *Cell Death Dis.* 1:e18, 2010.
69. **Luo S, et al.** Apoptosis blocks Beclin-1-dependent autophagosomes synthesis: an effect rescued by Bcl-X_L. *Cell Death Differ* 17:268-277, 2010.
70. **Gregoli P. A, et al.** Function of caspases in regulating apoptosis caused by erythropoietin deprivation in erythroid progenitors. *J. Cell Physiol.* 178:133-143, 1999.
71. **Zermati A, et al.** Caspase activation is required for terminal erythroid differentiation. *J. Exp. Med.* 193:247-254, 2001.
72. **De Maria R, et al.** Negative regulation of erythropoiesis by caspase-mediated cleavage of GATA-1. *Nature.* 401:489-493, 1999.
73. **Zeuner A, et al.** Control of erythroid cell production via caspase-mediated cleavage of transcription factor SCL/Tal-1. *Cell Death Diff.* 10:905-913, 2003.
74. **Zhao B, et al.** Chromatin condensation during terminal erythropoiesis. *Nucleus* 7:425-429, 2016.
75. **Jiang Tao, et al.** p62 links autophagy and Nrf2 signaling. *Free Radical Biol. Med.* 88: 199-204, 2015.
76. **Inami Y, et al.** Persistent activation of Nrf2 through p62 in hepatocellular carcinoma cells. *J. Cell Biol.* 193: 275-284, 2011.
77. **Lam H. C, et al.** Histone deacetylase 6-mediated selective autophagy regulates COPD-associated cilia dysfunction. *J. Clin. Invest.* 123: 5212-5230, 2013.
78. **De Franceschi, et al.** Oxidative stress and β -thalassemic erythroid cells behind the molecular defect. *Oxid Med Cell Longev.* 2013:985210, 2013.

79. **Bartnikas TB, et al.** Transferrin is a major determinant of hepcidin expression in hypotransferrinemic mice. *Blood*. 117:630-637, 2011.
80. **Mattè A, et al.** The novel role of peroxiredoxin-2 in red cell membrane protein homeostasis and senescence. *Free Radic Biol Med*. 76:80-88, 2014.
81. **De Franceschi L, et al.** In vivo reduction of erythrocyte oxidant stress in a murine model of beta-thalassemia. *Haematologica*. 89:1287-1298, 2004.
82. **De Franceschi L, et al.** Combination therapy of erythropoietin, hydroxyurea, and clotrimazole in a beta thalassemic mouse: a model for human therapy. *Blood*. 87:1188-1195, 1996.
83. **Low FM, et al.** Peroxiredoxin 2 and peroxide metabolism in the erythrocyte. *Antioxid. Redox Signal*. 10:1621–1630, 2008.
84. **Manta B, et al.** The peroxidase and peroxynitrite reductase activity of human erythrocyte peroxiredoxin 2. *Arch. Biochem. Biophys*. 484:146–154, 2009.
85. **Liu J, et al.** Quantitative analysis of murine terminal erythroid differentiation in vivo: novel method to study normal and disordered erythropoiesis. *Blood* 121: e43–e49, 2013.
86. **Cambi M, et al.** Development of a specific method to evaluate 8-hydroxy, 2-deoxyguanosine in sperm nuclei: relationship with semen quality in a cohort of 94 subjects. *Reproduction* 145: 227–235, 2013.
87. **Arshady, R et al.** Preparation of biodegradable microspheres and microcapsules: 2. Polyactides and related polyesters. *J. Control. Release* 17: 1–21, 1991.
88. **Olivieri O, et al.** Oxidative damage and erythrocyte membrane transport abnormalities in thalassemias. *Blood*. 84:315-320, 1994.
89. **Turrini F, et al.** Binding of Naturally occurring antibodies to oxidatively and nonoxidatively modified erythrocyte Band 3. *Biochim. And Biophys*. 1190:297-303, 1994.
90. **Cai Y, et al.** UFBP1, a key component of the Ufm1 conjugation system, is essential for Ufm1-mediated regulation of erythroid development. *PLoS Genet*. 11:e1005643, 2015.


91. **Federti E, et al** . Peroxiredoxin-2 plays a pivotal role as multimodal cytoprotector in the early phase of pulmonary hypertension. *Free Radical Biol. Med.* 112: 376-386, 2017.
92. **Fernandez A, et al** . Melatonin and endoplasmic reticulum stress: relation to autophagy and apoptosis. *J. Pineal Res.* 59: 292-307, 2015.
93. **Yan M. M, et al** . Interplay between Unfolded protein response and autophagy promotes tumor drug resistance. *Oncology Letters.* 10: 1959-1969, 2015.
94. **Wu H, et al** . Astaxanthin as a potential neuroprotective agent for neurological diseases. *Mar. Drugs* 13: 5750-5766, 2015.
95. **Chew W, et al** . Astaxanthin decreases inflammatory biomarkers associated with cardiovascular disease in human umbilical vein endothelial cells. *Am. J. Adv. Food Sci. Technol.* 1: 1-17, 2013.
96. **Zhongrui L, et al** . Astaxanthin protects ARPE-19 cells from oxidative stress via upregulation of Nrf2-regulated phase II enzymes through activation of PI3K/Akt. *Molecular Vision* 19: 1656-1666, 2013.
97. **Xiaojun W, et al** . Astaxanthin acts via LRP-1 to inhibit inflammation and reverse lipopolysaccharide-induced M1/M2 polarization of microglial cells. *Oncotarget* 8: 69370-69385, 2017.
98. **Buckley Mc, et al** . Effects of astaxanthin on the proliferation and migration of breast cancer cells in vitro. *Antioxidants* 7: E135, 2018.
99. **Tripathi D. N, et al** . Astaxanthin intervention ameliorates cyclophosphamide-induced oxidative stress, DNA damage and early hepatocarcinogenesis in rat: Role of Nrf2, p53, p38 and phase-II enzymes. *Mutation Research* 696: 69-80, 2010.
100. **Lianbao Xu, et al** . Astaxanthin improves cognitive deficits from oxidative stress, nitric oxide synthase and inflammation through upregulation of PI3K/Akt in diabetic rats. *Int. J. Clin. Exp. Pathol.* 8: 6083-6094, 2015.
101. **Grimmig B, et al** . Astaxanthin is neuroprotective in aged mouse model of Parkinson's disease. *Oncotarget* 9: 10388-10401, 2018.
102. **Xiaoyu Z, et al** . Astaxanthin promotes Nrf2/ARE signaling to alleviate renal fibronectin and collagen IV accumulation in diabetic rats. *J. Diabetes Res.* 2018: 6730315, 2018.

103. **Yoshida H, et al** . Administration of natural astaxanthin increases serum HDL-cholesterol and adiponectin in subjects with mild hyperlipidemia. *Atherosclerosis* 209: 520-523, 2010.
104. **Park J. S, et al** . Astaxanthin decreases oxidative stress and inflammation and enhance immune response in humans. *Nutrition & Metabolism* 7: 18, 2010.
105. **Choi H. D, et al** . Effects of astaxanthin on oxidative stress in overweight and obese adults. *Phytother. Res.* 25: 1813-1818, 2011.
106. **Martin H. D, et al** . Chemistry of carotenoid oxidation and free radical reactions. *Pure Appl. Chem.* 71: 2253-2262, 1999.
107. **Hama S, et al** . Scavenging of hydroxyl radicals in aqueous solution by astaxanthin encapsulated in liposomes. *Biol. Pharm. Bull.* 35: 2238-2242, 2012.
108. **Kushimoto Y, et al** . Potential anti-atherosclerotic properties of astaxanthin. *Mar. Drugs* 14: 35, 2016.
109. **Ruiz V. R, et al** . Astaxanthin-loaded nanostructured lipid carriers for preservation of antioxidant activity. *Molecules* 23: 2601, 2018.
110. **Shu G, et al** . Formulation and characterization of astaxanthin enriched nanoemulsions stabilized using gisens saponins as natural emulsifiers . *Food Chemistry* 255: 67- 74, 2018.
111. **Arnajan N, et al** . Effects of homogenization process parameters on physicochemical properties of astaxanthin nanodispersions prepared using a solvent-diffusion technique. *Inter. J. Nanomedicine* 10: 1109- 1118, 2015.
112. **Odeberg J. M, et al** . Oral bioavailability of antioxidant astaxanthin in humans is enhance by incorporation of lipid based formulations. *Eur. J. Pharm. Sci.* 19: 299- 304, 2003.
113. **Rinku B, et al** . Ursolic acid loaded PLGA nanoparticles: in vitro and in vivo evaluation to explore tumor targeting ability of B16F10 melanoma cell lines. *Pharm. Res.* 33: 2691- 2703, 2016.
114. **Nabar G. M, et al** . Micelle-templated, poly(lactic-co-glycolic acid) nanoparticles for hydrophobic drug delivery. *Inter. J. Nanomedicine* 13: 351-366, 2018.

9. PAPERS AND ABSTRACTS

RESEARCH ARTICLE

Fyn kinase is a novel modulator of erythropoietin signaling and stress erythropoiesis

Elisabetta Beneduce¹ | Alessandro Matte¹ | Luigia De Falco² | Serge Mbiandjeu¹ | Deborah Chiabrando³ | Emanuela Tolosano³ | Enrica Federti¹ | Sara Petrillo³ | Narla Mohandas⁴ | Angela Siciliano¹ | Wilson Babu¹ | Vijay Menon⁵ | Saghi Ghaffari⁵ | Achille Iolascon² | Lucia De Franceschi¹ 

¹Department of Medicine, University of Verona, AOUI Verona, Verona, Italy

²Department of Biochemistry, Federico II University, Naples, Italy

³Department of Molecular Biotechnology and Health Sciences, University of Torino, Torino, Italy

⁴New York Blood Center, New York, New York

⁵Department of Cell, Development and Regenerative Biology, Icahn School of Medicine at Mount Sinai, New York, New York

Correspondence

Lucia De Franceschi, Department of Medicine, University of Verona, Policlinico GB Rossi; P. Le L. Scuro, 10; 37134 Verona, Italy.
Email: lucia.defranceschi@univr.it

Abstract

The signaling cascade induced by the interaction of erythropoietin (EPO) with its receptor (EPO-R) is a key event of erythropoiesis. We present here data indicating that Fyn, a Src-family-kinase, participates in the EPO signaling-pathway, since Fyn^{-/-} mice exhibit reduced Tyr-phosphorylation of EPO-R and decreased STAT5-activity. The importance of Fyn in erythropoiesis is also supported by the blunted responsiveness of Fyn^{-/-} mice to stress erythropoiesis. Fyn^{-/-} mouse erythroblasts adapt to reactive oxygen species (ROS) by activating the redox-related-transcription-factor Nrf2. However, since Fyn is a physiologic repressor of Nrf2, absence of Fyn resulted in persistent-activation of Nrf2 and accumulation of nonfunctional proteins. ROS-induced over-activation of Jak2-Akt-mTOR-pathway and repression of autophagy with perturbation of lysosomal-clearance were also noted. Treatment with Rapamycin, a mTOR-inhibitor and autophagy activator, ameliorates Fyn^{-/-} mouse baseline erythropoiesis and erythropoietic response to oxidative-stress. These findings identify a novel multimodal action of Fyn in the regulation of normal and stress erythropoiesis.

1 | INTRODUCTION

Erythropoiesis is a complex multistep process during which committed erythroid progenitors undergo terminal differentiation to produce circulating mature red cells. Erythroid differentiation is characterized by the production of reactive oxygen species (ROS) in response to erythropoietin (EPO) and by the large amount of iron imported into the cells for heme biosynthesis.¹ During erythropoiesis, ROS could function as second messenger by modulating intracellular signaling pathways. EPO activates a signaling cascade, involving Jak2, as the primary kinase, and Lyn, a Tyr-kinase of the Src family (SFK), as secondary kinase.²⁻⁴ These two kinases target STAT5 transcription factor, one of the key master transcription regulators involved in erythroid maturation events.²⁻⁵

Previous studies have shown that the mice genetically lacking Lyn (Lyn^{-/-}) display reduced STAT5 activation and defective response to

phenylhydrazine- (PHZ) induced stress erythropoiesis.²⁻⁴ Fyn, is another member of the SFKs that is also expressed in hematopoietic cells.⁶⁻¹⁰ Fyn has been invoked as an additional regulatory kinase for the canonical thrombopoietin/Jak2 pathway in megakaryopoiesis.¹¹ In addition, Fyn has been shown to target STAT5 and to participate to STAT5 activation in mast-cells in response to FCRI engagement.⁸ Furthermore, Fyn intersects different intracellular signaling pathways such as Toll like receptor in macrophages or in T cells^{12,13} and participates to the regulation of the redox sensitive transcriptional factor Nrf2.¹⁴⁻¹⁶ Following acute phase response, Fyn switches-off active Nrf2, triggering its exit from the nucleus and degradation.¹⁴⁻¹⁷ In erythroid maturation events, the activation of Nrf2 is crucial to support stress erythropoiesis induced by the oxidant, PHZ, and in modulating ineffective erythropoiesis in β -thalassemic mice.^{18,19} In other cellular models, it has been shown that impairment of Nrf2 post-induction regulation results in perturbation of cell homeostasis and in accumulation of poly-ubiquitylated protein aggregates due to deregulated autophagy.¹⁶ Autophagy is activated in response to different cellular

Elisabetta Beneduce and Alessandro Matte have equally contributed to this study.

stresses to ensure cell survival and ensure the clearance of the damaged proteins.^{18,19} We recently showed that in chorea-acanthocytosis the impairment of autophagy promotes accumulation of proteins, resulting in engulfment of the cells and in perturbation of erythropoiesis combined with increased oxidative stress.²⁰

In present study, we explored the role of Fyn in regulating normal and stress erythropoiesis. We show that in addition to Jak2 and Lyn, Fyn is an additional kinase involved in EPO signaling cascade by targeting STAT5 activation. The absence of Fyn reduces the efficiency of the EPO signal and promotes the generation of ROS and the over-activation of Jak2-Akt-mTOR pathway, with repression of autophagy. The absence of Fyn also results in persistent activation of Nrf2 and accumulation of damaged proteins. This is further amplified by the blockage of autophagy mediated by mTOR activation, which markedly perturbs the response to stress erythropoiesis induced by either phenylhydrazine (PHZ) or Doxorubicin. In Fyn^{-/-} mice, the rescue experiments with Rapamycin, an mTOR inhibitor and autophagy activator, co-administrated to PHZ further validated the importance of autophagy as adaptive mechanism to stress erythropoiesis in presence of perturbation of EPO cascade.

2 | METHODS

2.1 | Mouse strains and design of the study

The Institutional Animal Experimental Committee of University of Verona (CIRSAL) and the Italian Ministry of Health approved the experimental protocols. Two-month old female wild-type (WT) and Fyn^{-/-} mice were studied. Where indicated, WT and Fyn^{-/-} mice were treated with EPO (10 U/mouse/day for 5 days by intraperitoneal injection),³ or Phenylhydrazine (PHZ: 40 mg/kg on day 0 by intraperitoneal injection)¹⁹ or Doxorubicin (DOXO: 0.25 mg/kg on day 0 by intraperitoneal injection)²¹ to study stress erythropoiesis. Rapamycin was administrated at the dosage of 10 mg/kg/d by intraperitoneal injection for 1 week, then mice were analyzed. In experiments with PHZ co-administration, Rapamycin was given at the dosage of 10 mg/kg/d by intraperitoneal injection 1 day before PHZ administration (40 mg/kg body; single dose at day 0) and then Rapamycin was maintained for additional 14 days. N-Acetylcysteine (NAC, 100 mg/kg body; intraperitoneally injected) was administrated for 3 weeks as antioxidant treatment.^{18,19} In mouse strains, hematological parameters, red cell indices and reticulocyte count were evaluated at baseline and at different time points (6, 8, and 11 days after EPO injection; at 2, 4, 8, and 14 days after PHZ injection; at 3, 6, and 9 days after DOXO injection; at 2, 4, 8, 14 days after Rapamycin plus PHZ injection) as previously reported.^{22,23} Blood was collected with retro-orbital venipuncture in anesthetized mice using heparinized microcapillary tubes. Hematological parameters were evaluated on a Siemens Hematology Analyzer (ADVIA 2120). Hematocrit and hemoglobin were manually determined.^{24,25}

2.2 | Flow cytometric analysis of mouse erythroid precursors and molecular analysis of sorted erythroid cells

Flow cytometric analysis of erythroid precursors from bone marrow and spleen from WT and Fyn^{-/-} was carried out as previously described using the CD44-Ter119 or CD71-Ter119 strategies.^{18,26,27} Analysis of apoptotic basophilic, polychromatic and orthochromatic erythroblasts was carried out on the CD44-Ter119 gated cells using the Annexin-V PE Apoptosis detection kit (eBioscience, San Diego, CA) following the manufacturer's instructions. Erythroblasts ROS levels were measured as previously reported by Matte et al.¹⁸ Sorted cells were used for (i) morphological analysis of erythroid precursors on cytospin preparations stained with May Grunwald-Giemsa; (ii) immuno-blot analysis with specific antibodies against anti-P-Ser473-Akt, anti-Akt, anti-P-Ser2448-mTOR, anti-mTOR, anti-Jak2 (Cell Signaling, Massachusetts); anti-P-Ser40-Nrf2, anti-Nrf2, anti-p62, anti-Rab5 (Abcam, Cambridge, UK); anti-Keap1 (Proteintech, Manchester, UK); anti-EPO-R (Sigma-Aldrich, Missouri); anti-STAT5, anti-Lyn (Santa Cruz Biotechnology, Texas); anti-GAPDH (Santa Cruz Biotechnology, Texas) and anti-catalase (Abcam, Cambridge, UK) were used as loading control; (iii) immunoprecipitation assay; and (iv) RT-PCR analysis. Details of immunoprecipitation, RT-PCR and immuno-blot protocols used for the analysis of sorted erythroblasts are described in Supplementary materials and methods.

2.3 | CFU-E, BFU-E assay

CFU-E and BFU-E assay was carried out using MethoCult as previously reported.²⁸ Details are present in Supplementary Methods.

2.4 | Immunofluorescence assay for p62 and FOXO3 in sorted erythroblasts

Immunofluorescence assay for p62 and FOXO3 in sorted erythroblasts was carried out as previously described.^{20,25,29} Details are reported in Supplementary materials and methods.

2.5 | LysoTracker and MitoTracker analysis in maturing reticulocytes

To obtain reticulocyte enriched RBC fraction, WT and Fyn^{-/-} mice were intraperitoneally injected with PHZ (40 mg/kg) at day 0, 1, 3 to induce reticulocytosis, and blood was collected in heparinized tubes at day 7, as previously described.³⁰ RBCs were washed three times with the maturation medium (60% IMDM, 2 mM L-glutamine, 100 U Penicillin-Streptomycin, 30% FBS, 1% BSA and 0.5 µg/mL Amphotericin), diluted 1/500 in maturation medium and cultured in a cell culture incubator at 37°C, 5% of CO₂ for 3 days. Clearance of Lysosome and Mitochondria, on the CD71/Ter119 gated RBC populations, were analyzed at day 0 and 3 of culture using the LysoTracker Green DND-26 (ThermoFisher Scientific) and the MitoTracker Deep Red (ThermoFisher Scientific) probes, respectively, following the manufacturer's instructions. Samples were acquired using the FACSCantoll flow cytometer (Becton Dickinson, San Jose, CA) and data were

processed with the FlowJo software (Tree Star, Ashland, OR) as previously described.^{18,25}

2.6 | Pearl's analysis of liver and spleen

Immediately following dissection, spleen and liver were formalin-fixed and paraffin-embedded for Pearl's staining and blinded analyzed.

2.7 | Molecular analysis of liver

Protocols used for RNA isolation, cDNA preparation and quantitative qRT-PCR have been previously described.³¹ Detailed primer sequences are available on request and shown in Supporting Information Table 1S. Liver immuno-blot analysis was performed as previously described.^{18,32}

2.8 | Measurement of heme and heme-oxygenase-1 activity

Liver heme content was measured using a fluorescence assay, as previously reported.³³ Details are reported in Supporting Information. HO-1 activity was evaluated in tissue microsomal fractions by spectrophotometric determination of bilirubin produced from hemin added as the substrate, as previously reported.³⁴

2.9 | Statistical analysis

Data were analyzed using either *t*-test or the 2-way analysis of variance (ANOVA) for repeated measures between the mice of various genotypes. A difference with a $P < .05$ was considered significant.

3 | RESULTS

3.1 | The absence of Fyn results in decreased efficiency of EPO-signaling pathway

Fyn^{-/-} mice displayed a slight microcytic anemia characterized by a small but significant reduction in hemoglobin, microcytosis and increased reticulocyte counts compared to WT animals (Table 1). To understand whether iron deficiency might account for the observed microcytosis, we evaluated iron accumulation in the liver and spleen.

TABLE 1 Hematological parameters and red cell indices in wild-type and Fyn^{-/-} mice

	Wildtype mice (n = 15)	Fyn ^{-/-} mice (n = 15)
Hct (%)	48.2 ± 1.3	46.1 ± 0.8*
Hb (g/dL)	15.9 ± 0.6	14.3 ± 0.5*
MCV (fL)	50.3 ± 0.4	46.5 ± 1.3*
MCH (g/dL)	15.3 ± 0.3	14.8 ± 1.1
RDW (%)	11.6 ± 0.3	13.2 ± 0.4*
Retics (103 cells/ μ L)	451 ± 40.7	559 ± 45*

Abbreviations: Hb, hemoglobin; Hct, hematocrit; MCH, mean corpuscular hemoglobin; MCV, mean corpuscular volume; RDW, red cell distribution width; Retics, reticulocytes.

* $p < 0.05$ compared to wild-type mice.

No differences in Pearl's staining for iron in either liver or spleen of Fyn^{-/-} compared to wild type mice was observed (Supporting Information Figure 1Sa). In agreement, expression levels of H-Ferritin in liver were similar in both mouse strains, whereas expression of L-Ferritin was slightly, but significantly lower in Fyn^{-/-} mice compared to WT mice (Supporting Information Figure 1Sb). Haptoglobin levels were measured to determine the possible contribution of hemolysis to microcytic anemia in Fyn^{-/-} mouse. Up-regulation of haptoglobin mRNA levels was noted in liver from Fyn^{-/-} mice, while plasma haptoglobin levels were similar in both mouse strains (Supporting Information Figure 1Sc, d). These findings suggest that in mice genetically lacking Fyn, the noted mildly compensated anemia is not related to either iron deficiency or chronic hemolysis.

To better define the Fyn^{-/-} mouse hematologic phenotype, we carried out the morphologic analysis of erythroblasts at distinct stages of terminal erythroid differentiation. As shown in Figure 1A, decreased chromatin condensation and larger cellular size was a characteristic feature of different populations of sorted Fyn^{-/-} mouse erythroblasts (pop II: basophilic erythroblasts; pop III: polychromatic erythroblasts and pop IV: orthochromatic erythroblasts; Figure 1A). Furthermore, an increase in number of total erythroblasts in bone marrow was noted (Figure 1B), without evidence of extramedullary erythropoiesis (data not shown). The maturation profile of erythroblasts revealed an accumulation of orthochromatic erythroblasts (Supporting Information Figure 2Sa). When CD44/Ter119 approach was used to characterize erythropoiesis, no major differences in either total erythroblasts or in erythroblasts subpopulations between WT and Fyn^{-/-} mice were observed (Supporting Information Figure 2Sb, c). Up-regulation of EPO gene expression in kidney was found in Fyn^{-/-} mice compared to that of WT animals (Supporting Information Figure 2Sd). In addition, we found increased ROS levels throughout Fyn^{-/-} erythroid maturation from basophilic erythroblasts (pop II) to polychromatic (pop III) and orthochromatic erythroblasts (pop IV) compared to WT cells (Figure 1C, upper panel). This was associated with higher amounts of Annexin V⁺ cells in the different subpopulation of erythroblasts compared to WT cells (Figure 1C, lower panel). Collectively, these findings indicate a decreased efficiency of EPO signaling pathway in the absence of Fyn. To understand the impact of Fyn on EPO cascade, we evaluated the EPO-Jak2-STAT5 signaling pathway in sorted Fyn^{-/-} erythroblasts. As shown in Figure 1D, reduced activation of EPO-receptor (EPO-R) as reflected by decreased EPO-R Tyrosine phosphorylation, was noted in erythroblasts genetically lacking Fyn (Figure 1D). This was associated with increased activation of Jak2 kinase without any change in Lyn activity compared to WT cells (Figure 1D). Total expression of EPO-R was similar in sorted erythroblasts from both mouse strains; whereas Jak2 expression was higher in Fyn^{-/-} erythroblasts compared to healthy cells (Supporting Information Figure 2Se). In agreement with the reduction in EPO-R activation, we observed a significant decrease in STAT5 activity with concomitant down-regulation of *Cish* expression, a well-documented gene target of STAT5 in sorted Fyn^{-/-} erythroblasts (Figure 1D; Supporting Information Figure 2Sf). Following treatment with recombinant EPO (10 U/day for 5 days), Fyn^{-/-} mice showed blunted increases in Hct and reticulocyte counts compared to WT animals (Figure 1E).

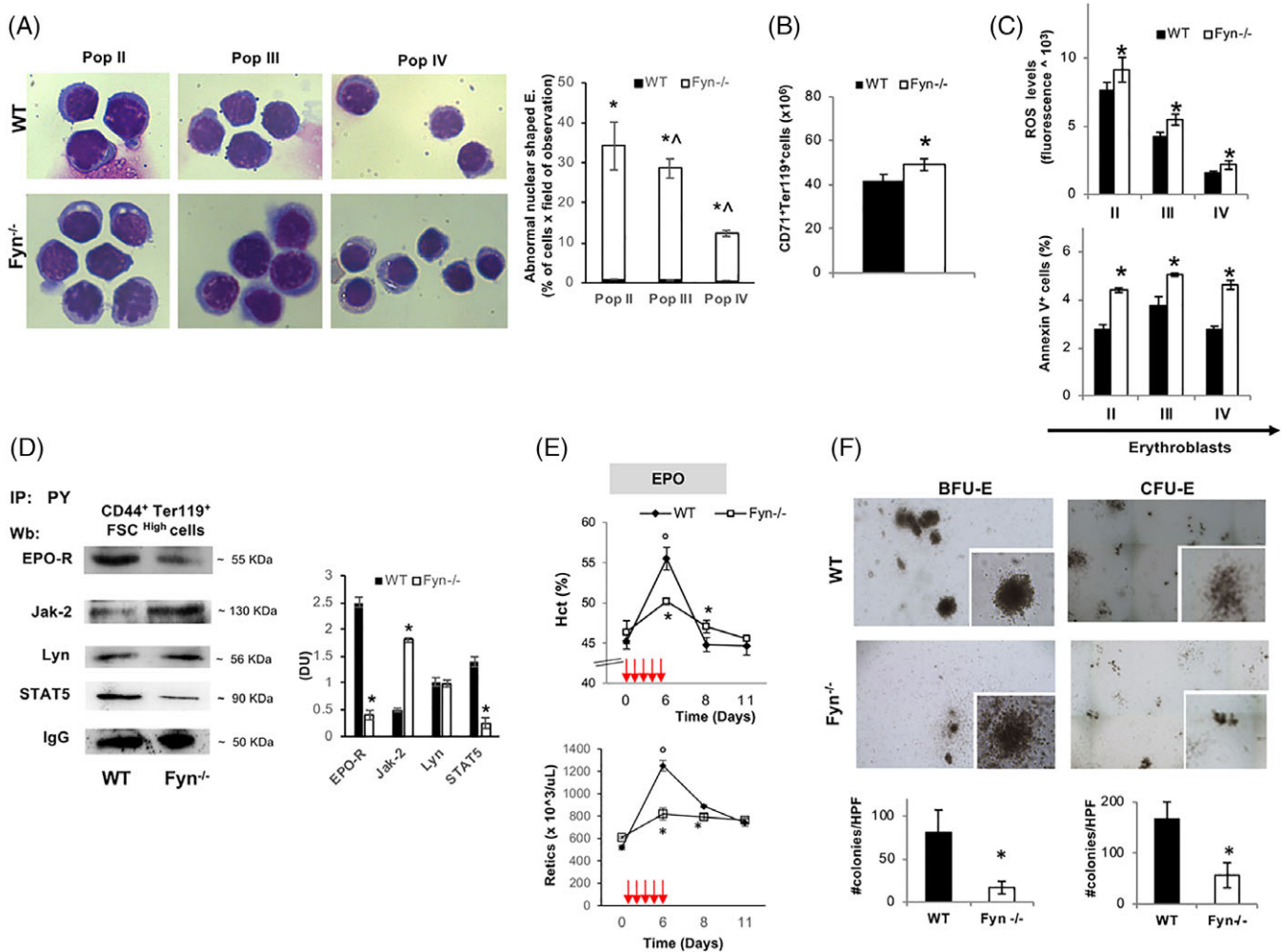


FIGURE 1 The absence of Fyn results in perturbation of EPO signaling cascade. A, Left panel. Morphology of sorted erythroid precursors: population II (pop II), corresponding to basophilic erythroblasts; population III (pop III), corresponding to polychromatic erythroblasts and population IV (pop IV), corresponding to orthochromatic erythroblasts, from bone marrow of wild-type (WT) and Fyn^{-/-} mice. Cytospins were stained with may-Grunwald-Giemsa. One representative image from a total of 10 for each mouse strains. Right panel. Abnormal nuclear shaped erythroblasts and binuclear erythroblasts from WT and Fyn^{-/-} mice evaluated on cytopsin stained with may-Grunwald-Giemsa. Data are presented as means \pm SD ($n = 8$ from each strain); * $P < .05$ compared to WT; $\Delta P < .05$ compared to pop II⁻. B, Cyto-fluorimetric analysis of total erythroid precursors from the bone marrow of WT and Fyn^{-/-} mice using the following surface markers: CD71 and Ter119 (see also the Supporting Information Materials and Methods and Figure 2Sa for maturation profile). Data are presented as means \pm SD ($n = 8$); * $P < .05$ compared to WT. C, Upper panel: ROS levels in erythroid precursors from bone marrow of wild-type (WT) and Fyn^{-/-} mice. Data are presented as means \pm SD ($n = 10$ from each strain); * $P < .05$ compared to WT. Lower panel: Amount of Annexin V⁺ cells in pop II, III, and IV from bone marrow of WT and Fyn^{-/-} mice. Data are presented as means \pm SD ($n = 8$ from each strain); * $P < .05$ compared to WT. D, Total Tyrosin-(Tyr) phosphorylated proteins were immunoprecipitated from 2.5×10^5 bone marrow sorted erythroblasts of WT and Fyn^{-/-} mice and detected with antibody to EPO- receptor (EPO-R), Janus kinase-2 (Jak-2), Lyn kinase (Lyn), signal transducer and activator of transcription 5 (STAT5). The experiment shown is representative of six such experiments. IgG was used as loading control. Right panel: Densitometric analyses of the immunoblot bands similar to those shown are presented at right (DU: Densitometric unit). Data are shown as means \pm SD ($n = 6$; * $P < .01$ compared to WT). E, Hematocrit (%) and reticulocyte count in ($n = 6$) and Fyn^{-/-} ($n = 6$) mice exposed to recombinant erythropoietin injection (EPO 50 U/kg/die, red arrows). Data are presented as means \pm SD; * $P < .05$ compared to WT mice; $\Delta P < .05$ compared to baseline values. F, The CFU-E and BFU-E from WT and Fyn^{-/-} mice were quantified (#CFU-E or BFU-E/dish; lower panel); data are shown as means \pm SD ($n = 6$; $P < .05$ compared to WT) [Color figure can be viewed at wileyonlinelibrary.com]

To explore whether the reduced efficiency of EPO cascade might also involve erythroid progenitors, we carried out the in vitro erythroid cell colony forming assay. A lower number of CFU-E and BFU-E colony forming cells were found in Fyn^{-/-} bone marrow (Figure 1F). This was associated again with lower activation of EPO-R mediated signaling cascade with a reduced activation of STAT5 but hyper-activation of Jak2 in Fyn^{-/-} CFU-E (Supporting Information Figure 2Sg).

Our data indicate that Fyn is involved in EPO signaling cascade and that absence of Fyn lead to increased ROS generation, which may contribute to the hyper-activation of Jak2 in presence of reduced efficiency of EPO signaling pathway.³⁵ Thus, the very mild microcytic anemia phenotype of Fyn^{-/-} mice is likely to be related more to reduced STAT5 activation, as observed in mice genetically lacking STAT5 than to perturbation of iron metabolism.³⁶

3.2 | *Fyn*^{-/-} mice display increased sensitivity to PHZ or doxorubicin induced stress erythropoiesis

Since EPO is the primary signal in stress erythropoiesis, we treated *Fyn*^{-/-} mice with either PHZ to induce acute hemolytic anemia due to severe oxidative stress or Doxorubicin that temporarily represses erythropoiesis with generation of ROS.^{19,21} PHZ treatment induced a similar drop in Hct levels in both mouse strains at day 2 following PHZ administration (Figure 2A, upper panel). However, the Hct and reticulocyte recovery were blunted in *Fyn*^{-/-} mice compared to control animals (Figure 2A, upper and lower panel). Extramedullary erythropoiesis as assessed by increased splenic erythropoiesis showed a

blunted response in *Fyn*^{-/-} mice at day 4 following PHZ treatment with a compensatory increase by day 14 (Figure 2B, upper panel, see also Supporting Information Figure 3Sa for absolute values of number of erythroblasts at day 4 after PHZ). In bone marrow, we observed a mild increase in total erythroblasts in both mouse strains at day 2 and 4 after PHZ injection (Figure 2B, lower panel). It is of interest to note that in *Fyn*^{-/-} mice at day 8 following PHZ treatment, we observed a significant increase in the total number of bone marrow erythroblasts as possible compensatory mechanism due to the failure in efficient activation of splenic extramedullary erythropoiesis (Figure 2B, lower panel). The amount of Annexin V⁺ cells following PHZ treatment was

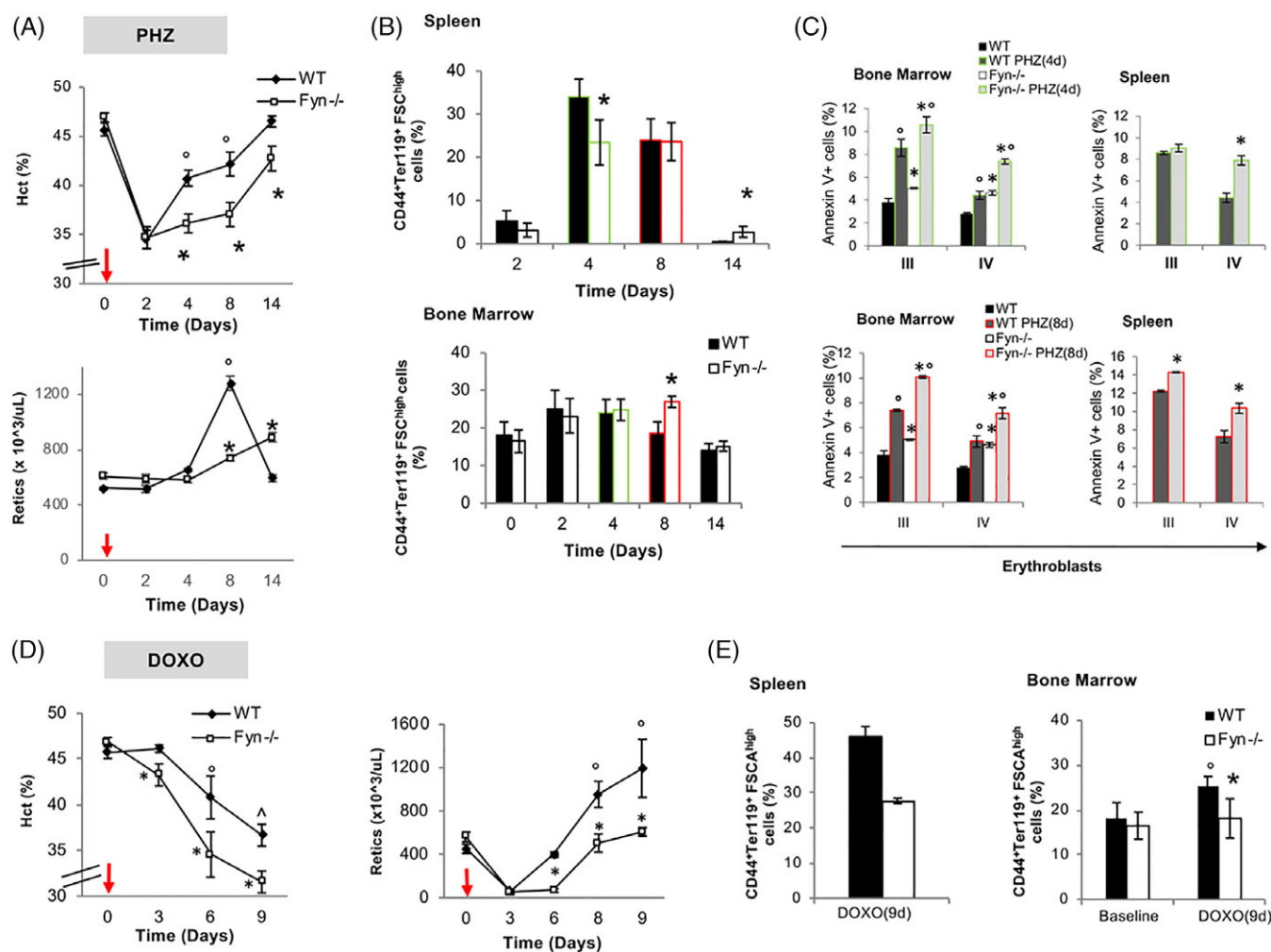


FIGURE 2 A blunted response to stress erythropoiesis characterizes *Fyn*^{-/-} mice. A, Hematocrit (%) and reticulocyte count in WT (*n* = 6) and *Fyn*^{-/-} (*n* = 6) mice exposed to phenylhydrazine injection (PHZ/kg/die, red arrows). Data are presented as means ±SD; **P* < .05 compared to WT mice; °*P* < .05 compared to baseline values. B, Cyto-fluorimetric analysis of total erythroid precursors from the bone marrow and the spleen of WT and *Fyn*^{-/-} mice using the following surface markers: CD44 and Ter119 (see also the Supporting Information and Methods and Figure 3Sa for absolute values). Data are presented as means ±SD (*n* = 6); **P* < .05 compared to WT. since we focus on day 4 and day 8 after PHZ administration, we highlighted them respectively in green and red. This color code is used also in C. C, Amount of Annexin-V⁺ cells in population III (pop III), corresponding to polychromatic erythroblasts and population IV (pop IV), corresponding to orthochromatic erythroblasts from either spleen or bone marrow of WT and *Fyn*^{-/-} mice respectively at 4 (green) and 8 (red) days after PHZ administration. Data are presented as means ±SD (*n* = 6 from each strain); **P* < .05 compared to WT. D, Hematocrit (%) and reticulocyte count in WT (*n* = 6) and *Fyn*^{-/-} (*n* = 6) mice exposed to doxorubicin injection (DOXO 0,25 mg/kg/die, red arrows). Data are presented as means ±SD; **P* < .05 compared to WT mice; °*P* < .05 compared to baseline values. E, Cyto-fluorimetric analysis of total erythroid precursors from the bone marrow and the spleen of WT and *Fyn*^{-/-} mice using the following surface markers: CD44 and Ter119 (see also the Supporting Information and Methods and Figure 3Sb for absolute values) 9 days after doxorubicin injection. Data are presented as means ±SD (*n* = 6); **P* < .05 compared to WT; °*P* < .05 compared to baseline values [Color figure can be viewed at wileyonlinelibrary.com]

higher in $Fyn^{-/-}$ polychromatic and orthochromatic erythroblasts compared to WT cells (Figure 2C).

Doxorubicin induced a more severe and prolonged anemia in $Fyn^{-/-}$ mice than in WT animals (Figure 2D, left panel). At day 3 and 6 following Doxorubicin treatment, we noted a plateau in reticulocyte count in $Fyn^{-/-}$ mice (Figure 2D), suggesting a substantial impairment in the reticulocyte response compared to Doxorubicin treated WT animals. Enumeration of total number of erythroblasts in spleen and bone marrow at day 9 after Doxorubicin administration, showed a substantial reduction in both bone marrow and splenic erythropoiesis in $Fyn^{-/-}$ mice compared to WT animals (Figure 2E; see also Supporting Information Figure 3Sb for absolute values). Increases in the numbers of Annexin V⁺ polychromatic and orthochromatic erythroblasts were noted in $Fyn^{-/-}$ mice compared to WT animals at 9 days after Doxorubicin administration (Supporting Information Figure 3Sc). The findings of diminished responsiveness of $Fyn^{-/-}$ mice to stress erythropoiesis induced by PHZ or Doxorubicin, further validate the importance of Fyn in EPO signaling cascade.

3.3 | Increased activation of Akt in $Fyn^{-/-}$ mice contributes to the modulation of redox cellular response during erythropoiesis

In normal and disordered erythropoiesis, previous studies have shown that Jak2 and oxidation can activate Akt, which affects multiple targets during erythropoiesis (Supporting Information Figure 4Sa).⁴ Notably, Akt is also important in mediating cellular response to oxidation by the activation of two redox sensitive transcriptional factors, Forkhead box-O3 (FOXO3) and Nrf2, as well as of mTOR, the gatekeeper of autophagy activation.³⁷⁻³⁹ $Fyn^{-/-}$ mouse erythroblasts displayed higher levels of active Akt (Ser 473) compared to WT cells (Supporting Information Figure 4Sb). The activation of FOXO3 was evaluated by both immunomicroscopy and immunoblot analysis, this latter using a specific antibody against inactive phospho-FOXO3. In $Fyn^{-/-}$ mouse erythroblasts, we found a slight but not significant increase in activation of FOXO3 compared to WT erythroblasts (Supporting Information Figure 4Sc).

We then focused on Nrf2 since Fyn is important in post-induction regulation of Nrf2.¹⁶ We found increased activation of Nrf2, as indicated by higher phospho-Nrf2 form in $Fyn^{-/-}$ mouse erythroblasts compared to WT cells (Supporting Information Figure 5Sa). The up-regulation of ARE-genes for anti-oxidant systems such as catalase, Gpx1, HO1, and Prx2 confirmed the increased Nrf2 function in $Fyn^{-/-}$ mouse erythroblasts (Supporting Information Figure 5Sb). Immunoblot analysis with specific antibodies for the corresponding proteins further validated the activation of Nrf2 pathway (Supporting Information Figure 5Sc).

However, the increased expression of anti-oxidant and cytoprotective system related to Nrf2 function does not completely counteract the induced oxidative damage of $Fyn^{-/-}$ mouse erythroblasts. Overall these effects are similar to those observed in both cell and animal models characterized by prolonged Nrf2 activation, which is associated with severe and even lethal phenotype,^{15,40} mainly related to the accumulation of damaged proteins and the perturbation of autophagy.

Among the many Nrf2 related genes up-regulated in $Fyn^{-/-}$ mouse erythroblasts, we focused on HO-1, the main heme-catabolizing enzyme under stress conditions and a major player in the maintenance of cell homeostasis.⁴¹

3.4 | Heme-oxygenase activity and heme levels are similar in $Fyn^{-/-}$ and WT mice

Since systemic heme homeostasis is orchestrated by the liver, we evaluated the impact of Fyn deficiency on hepatic heme catabolism. First, we confirmed the increased activation of Nrf2 in $Fyn^{-/-}$ liver compared to WT counterpart (Supporting Information Figure 6Sa). When we analyzed HO-1 expression and HO-1 activity in this organ, despite similar levels of HO-1 mRNA in the livers of WT and $Fyn^{-/-}$ mice, HO-1 protein level was higher in the $Fyn^{-/-}$ mice. Similar findings were also noted in erythroid cells (Supporting Information Figure 6Sb). Interestingly, in spite of increased protein levels, hepatic HO activity was unchanged in $Fyn^{-/-}$ animals (Supporting Information Figure 6Sc) suggesting no alteration in heme catabolism. This conclusion was supported by the finding that the heme content in the liver was similar in WT and $Fyn^{-/-}$ mice (Supporting Information Figure 6Sd). Thus, in the absence of Fyn, HO-1 protein is increased but its activity is unchanged in $Fyn^{-/-}$ mice, suggesting the accumulation of functionally inactive HO-1.¹⁶ Autophagy is the master control system regulating protein quality and clearance of damaged proteins.^{37,39,42} The lysosomal related cargo p62 protein can be used as indirect marker of autophagy and its accumulation correlates with impairment of autophagy.⁴³ In liver from $Fyn^{-/-}$ mice, we found an accumulation of p62, suggesting a blockage of autophagy in the absence of Fyn (Supporting Information Figure 6Se, f). In agreement, mTOR was more active in liver from $Fyn^{-/-}$ mice compared to WT animals (Supporting Information Figure 6Sg).^{37,44,45} These data imply impaired autophagy in liver from mice genetically lacking Fyn.

3.5 | Impaired autophagy related to mTOR activation characterizes $Fyn^{-/-}$ mouse erythropoiesis

Since autophagy is also important during erythropoiesis,⁴² we explored mTOR signaling during erythroid maturation in $Fyn^{-/-}$ mouse. As shown in Figure 4A, $Fyn^{-/-}$ mouse erythroblasts displayed increased activation of phospho-mTOR compared to WT cells in association with accumulation of p62, similarly to that noted in $Fyn^{-/-}$ mouse liver (Figure 3A) as well as of Rab5, a small GTP protein involved in the late phases of autophagy (Figure 3A).³⁹ Consistent with impaired autophagy during erythropoiesis in $Fyn^{-/-}$ mouse, we noted accumulation of p62 in large clusters in $Fyn^{-/-}$ erythroblasts compared to WT cells (Figure 3B, Supporting Information Figure 7Sa). Since p62 acts as autophagy adaptor, controlling proteins turnover,^{15,16} we evaluated Keap1, a known substrate of p62.^{16,43} In $Fyn^{-/-}$ erythroblasts, we found increased accumulation of Keap1 compared to WT cells (Supporting Information Figure 7Sb). Co-immunoprecipitation with either antibodies to p62 (Figure 3C) or Keap1 (Figure 3D) showed accumulation of p62-Keap1 complex in $Fyn^{-/-}$ mouse erythroblasts. If the perturbation of autophagy in $Fyn^{-/-}$ mice is physiologically relevant to erythroid maturation, it is also likely to affect reticulocyte maturation.^{30,42,46} To test this possibility, we evaluated the in vitro maturation of reticulocytes from PHZ treated mice.³⁰ Decreased maturation of $Fyn^{-/-}$ mouse reticulocyte was detected by decreased lysosomal clearance with LysoTracker analysis (Supporting Information Figure 7Sc, d). Interesting, no difference in mitochondrial clearance using MitoTracker analysis was noted (Supporting Information Figure 7Sd, lower panel).

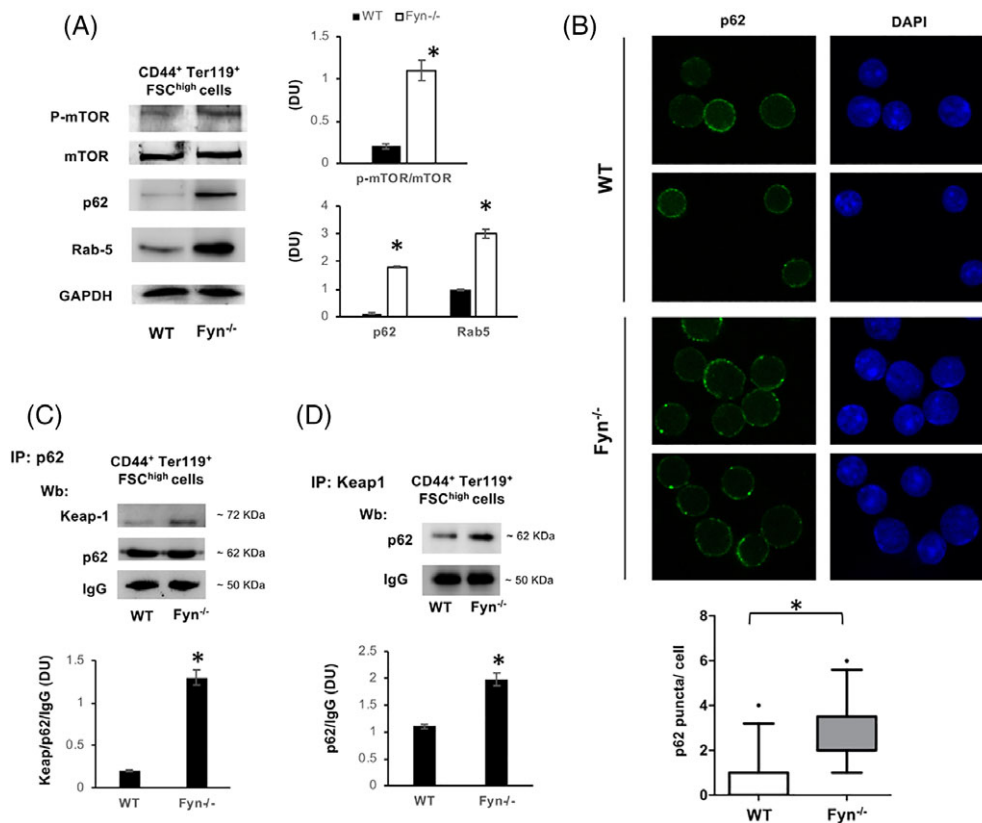


FIGURE 3 Activation of mTOR and impaired autophagy characterize Fyn^{-/-} mouse erythroblasts. A, Western-blot (Wb) analysis of phospho-mTOR (p-mTOR), m-TOR, p62 and Rab 5 in sorted 1.5 × 10⁶ CD44⁺Ter119⁺FSC^{high} bone marrow cells from WT (n = 4) and Fyn^{-/-} mice. GAPDH was used as protein loading control. Densitometric analyses of the immunoblot bands similar to those shown are presented at right (DU: Densitometric unit). Data are shown as means ±SD (n = 4; *P < .01 compared to WT). B, p62 immunostained cytospin preparations of sorted CD44⁺Ter119⁺FSC^{high} bone marrow cells from WT and Fyn^{-/-} mice counterstained with DAPI. Lower panel: The puncta mean fluorescence was measured using image J software. Data are presented as means ±SD (n = 3); *P < .05 compared to WT. C, Immunoprecipitates (IP) containing equal amounts of p62 were obtained from 2.5 × 10⁶ sorted CD44⁺Ter119⁺FSC^{high} bone marrow cells from WT and Fyn^{-/-} mice, then subjected to immunoblot with anti-Keap1 or p62 antibody (Wb: Western-blot). The experimental results shown are representative of four similar separate experiments. IgG was used as loading control. Densitometric analyses of the immunoblot bands similar to those shown are presented at lower panel (DU). Data are shown as means ±SD (n = 4; *P < .01 compared to WT). D, IP of Keap 1 were obtained from sorted 2.5 × 10⁶ CD44⁺Ter119⁺FSC^{high} bone marrow cells from WT and Fyn^{-/-} mice, then subjected to immunoblot with anti- p62 antibody (Wb: Western-blot). The experimental results shown are representative of 4 similar separate experiments. IgG was used as loading control. Densitometric analyses of the immunoblot bands similar to those shown are presented at lower panel (DU). Data are shown as means ±SD (n = 4; *P < .01 compared to WT) [Color figure can be viewed at wileyonlinelibrary.com]

Documentation of increased accumulation of p62 in Fyn^{-/-} reticulo- cyte further supports the impairment of autophagy during erythroid maturation in Fyn^{-/-} mice (Supporting Information Figure 7Se).

3.6 | The mTOR inhibitor Rapamycin unblocks autophagy defect and ameliorates erythropoiesis in Fyn^{-/-} mice

We next tested whether Rapamycin, a known mTOR inhibitor, may modulate Fyn^{-/-} mouse erythropoiesis as reported for other models of pathologic erythropoiesis.^{37,38,42,47} In Fyn^{-/-} mice, Rapamycin administration reduced total erythroblasts, while no significant effects were observed in control animals as previously reported^{37,38,42,47} (Figure 4A). In Fyn^{-/-} mice treated with Rapamycin, this was associated with amelioration of the terminal phase of erythropoiesis (Supporting Information Figure 8Sa). Rapamycin significantly reduced the generation of ROS and the amount of Annexin- V+ positive cells only in erythroid precursors from Fyn^{-/-} mice (Figure 4B, C). In agreement with

Rapamycin induced activation of autophagy, we found a significant reduction in levels of p62 in erythroblasts from Rapamycin treated Fyn^{-/-} mice compared to vehicle treated animals (Figure 4D).

We also evaluated the impact of anti-oxidant treatment with N-acetylcysteine (NAC), which has been shown to indirectly modulate autophagy by reducing intracellular oxidation.^{48,49} In Fyn^{-/-} mice, NAC reduced total number of erythroblasts, increased orthochromatic erythroblasts and reduced the amount of Annexin V+ cells, indicating an amelioration of erythropoiesis in Fyn^{-/-} mice (Supporting Information Figure 8Sb, c, d). The findings indicate that Rapamycin unblocks autophagy, allowing the degradation of accumulated proteins and ameliorating erythropoiesis in Fyn^{-/-} mice.

3.7 | Rapamycin rescues the abnormal response of Fyn^{-/-} erythroblasts to stress erythropoiesis

Next, we investigated whether Rapamycin may alleviate the PHZ-induced stress erythropoiesis in Fyn^{-/-} mice. As shown in Figure 4F,

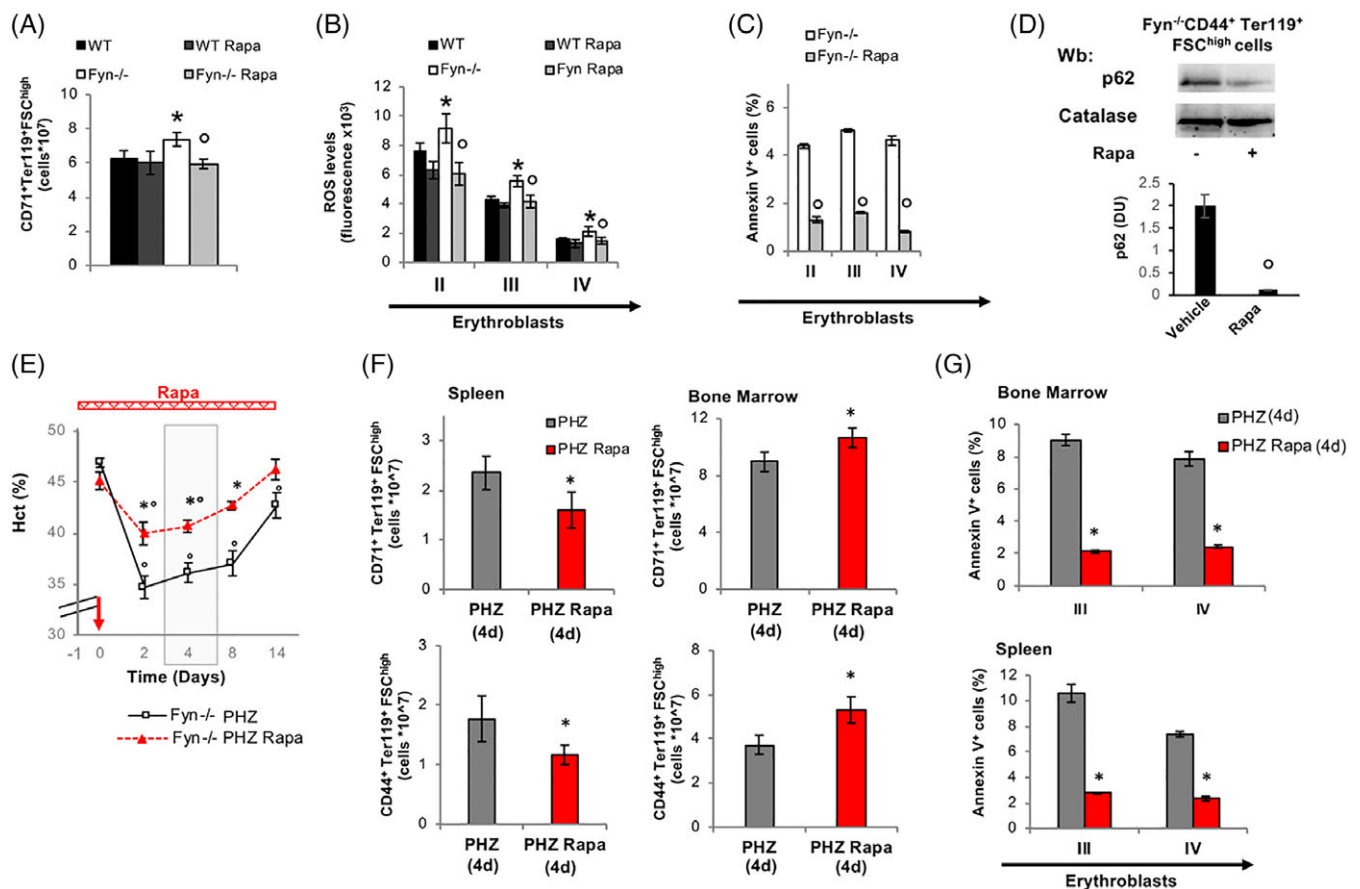


FIGURE 4 The mTOR inhibitor, Rapamycin rescues the abnormal response of $Fyn^{-/-}$ erythroblasts to stress erythropoiesis. A, Effect of treatment with Rapamycin (Rapa) on total erythroid precursors (CD71-Ter119) from the bone marrow of WT and $Fyn^{-/-}$ mice. Data are presented as means \pm SD ($n = 6$); * $P < .05$ compared to WT; $^{\circ}P < .05$ compared to vehicle treated animals. B and C, Effect of Rapamycin treatment (Rapa) on ROS levels and Annexin V⁺ cells in erythroid precursors: Population II (pop II), corresponding to basophilic erythroblasts; population III (pop III), corresponding to polychromatic erythroblasts and population IV (pop IV), corresponding to orthochromatic erythroblasts from bone marrow of WT and $Fyn^{-/-}$ mice. Data are presented as means \pm SD ($n = 6$ from each strain); * $P < .05$ compared to WT; $^{\circ}P < .05$ compared to vehicle treated animals. D, Western-blot (Wb) analysis of p62 in 1.5×10^6 sorted CD44⁺Ter119⁺FSC^{high} bone marrow cells with and without Rapamycin from $Fyn^{-/-}$ mice. Catalase was used as protein loading control. Densitometric analyses of the immunoblot bands similar to those shown are presented at right (DU: Densitometric unit). Data are shown as means \pm SD ($n = 4$); * $P < .01$ compared to WT). E, Hematocrit (%) in $Fyn^{-/-}$ ($n = 6$) mice treated with either phenylhydrazine alone (PHZ) or combined with Rapamycin (Rapa- red bar is the time of treatment with it). The red arrow indicates the injection of PHZ. Data are presented as means \pm SD; * $P < .05$ compared to PHZ treated animals; $^{\circ}P < .05$ compared to baseline values. The gray area identifies the window time for characterization of the stress erythropoiesis in $Fyn^{-/-}$ mice. F, Cyto-fluorimetric analysis of total erythroid precursors from either bone marrow or spleen of $Fyn^{-/-}$ mice treated with either PHZ alone or Rapamycin (Rapa) plus PHZ (4 days after injection). Results from CD44-Ter119 (lower panel) or CD71Ter119 (upper panel) strategies are shown. Data are presented as means \pm SD ($n = 4$); * $P < .05$ compared to PHZ treated animals; $^{\circ}P < .05$ compared to baseline values. (G) Amount of Annexin V⁺ cells in population III (pop III), corresponding to polychromatic erythroblasts and population IV (pop IV), corresponding to orthochromatic erythroblasts from either spleen or bone marrow of $Fyn^{-/-}$ mice. Data are presented as means \pm SD ($n = 4$ from each strain); * $P < .05$ compared to WT [Color figure can be viewed at wileyonlinelibrary.com]

the administration of Rapamycin in PHZ treated $Fyn^{-/-}$ mice resulted in milder anemia and faster recovery compared to PHZ treated $Fyn^{-/-}$ mice. At day 4 following PHZ administration, a plateau in Hct value is evident in both $Fyn^{-/-}$ mouse groups; we focused therefore on this time point to carry out a detailed analysis of. As shown in Figure 4G, we found decreased extramedullary splenic erythropoiesis and increased bone marrow erythropoiesis in PHZ-Rapamycin treated $Fyn^{-/-}$ mice compared to PHZ treated animals.

Annexin-V⁺ cells were also markedly reduced by the co-administration of Rapamycin and PHZ in $Fyn^{-/-}$ mouse erythroblasts from both bone marrow and spleen compared to PHZ alone (Figure 4H). It is interesting to note that, in WT animals the co-administration of Rapamycin worsened the PHZ induced stress

erythropoiesis as previously reported³⁸ (Supporting Information Figure 9Sa-c). Collectively, these data support the idea that by activating autophagy it is possible to rescue the altered response of $Fyn^{-/-}$ mice to stress erythropoiesis.

4 | DISCUSSION

We have identified *Fyn* as a new kinase involved in EPO signaling cascade during normal and stress erythropoiesis. Previous studies have documented a similar role for *Jak2* and *Lyn* kinases in erythropoiesis.^{2-4,50,51} The reduction in EPO induced phosphorylation of STAT5 noted in $Fyn^{-/-}$ mouse erythroid cells implies a role for *Fyn*

downstream of STAT5 and suggests that Fyn is implicated in EPO signaling pathway by modulating the activation of EPO-R through STAT5. Similar findings have been reported for mice genetically lacking Lyn,⁵⁰ supporting the important and nonredundant role of Fyn in the EPO-mediated signaling cascade. Our findings also suggest that multiple kinases may be important in coordinating stress erythropoiesis in health and disease.

In Fyn^{-/-} mice, the reduced effectiveness of EPO signaling is associated with increase ROS generation and cell apoptosis. The attempt of Fyn^{-/-} mouse erythroblasts to adapt to oxidative stress is indicated by the activation of the redox related transcription factor Nrf2.^{35,37} However, the persistent activation of Nrf2 due to the absence of its physiologic repressor Fyn, resulted in accumulation of damaged/nonfunctional proteins that further amplified the intracellular oxidative stress.^{15,16} Indeed, Fyn^{-/-} mice display impaired functioning of several cytoprotective systems, such as HO-1 indicating an impairment of the protein quality control process mediated by autophagy.

Previous studies have shown that perturbation of autophagy is detrimental for erythroid maturation and has been documented in condition with disordered erythropoiesis such as β -thalassemic syndromes or chorea-acanthocytosis or during iron deficiency.^{20,37,46,52,53}

In Fyn^{-/-} mice, the ROS mediated activation of Jak2-Akt-mTOR pathway represses autophagy and thereby contributes to the ineffective erythropoiesis of Fyn^{-/-} mice.^{4,39} Consistent with this hypothesis, in Fyn^{-/-} mouse erythroblasts we found accumulation of the autophagy cargo protein p62, a marker of autophagy inhibition. In addition, p62 was also complexed with Keap1, the Nrf2 shuttle protein,¹⁶ further supporting the dysregulation of Nrf2 and the blockage of autophagy during Fyn^{-/-} erythropoiesis. The accumulation of Rab5, a small GTPase involved in endocytic vesicular transport,⁵⁴ suggested a possible perturbation of the autophagy lysosomal system in Fyn^{-/-} mice. Indeed, we found a reduction in lysosome clearance during Fyn^{-/-} mouse reticulocyte maturation in presence of preserved clearance of mitochondria compartment.

The ability of Rapamycin, a known mTOR inhibitor and autophagy activator, to ameliorate Fyn^{-/-} mouse baseline erythropoiesis and to prevent accumulation of p62 support the notion of impaired autophagy in Fyn^{-/-} mice. This is further corroborated by the observation that Rapamycin co-administrated with PHZ restored the erythropoietic response in Fyn^{-/-} mice. These finding shed a new light on the link between dysregulation of Nrf2 and impairment of autophagy in stress erythropoiesis, demonstrating the multimodal action of Fyn in establishing the developmental program of erythropoiesis.

In conclusion, our data indicate that Fyn kinase is a novel and relevant regulator of erythropoiesis, contributing to activation of the EPO signaling cascade, and further increasing the complexity of this pathway. The absence of Fyn and the reduced efficiency of EPO signal generate a "domino effect" affecting several mechanisms associated with response to an increased oxidative stress (Supporting Information Figure 9Sd). The dysregulation of post-induction regulation of Nrf2 due to the absence of Fyn, results in accumulation of aggregated proteins, which further increase cellular oxidative stress. A concomitant activation of Jak2-Akt-mTOR pathway results in repression of autophagy (Supporting Information Figure 9Sd), which can be rescued with

Rapamycin, further reinforce the importance of autophagy as adaptive mechanism to stressful conditions associated with perturbations of the EPO signaling pathway. Future studies will be required to fully characterize the role Fyn in cellular signaling in pathologic erythropoiesis.

ACKNOWLEDGMENTS

This work was supported by FUR-UNIVR (LDF).

CONFLICT OF INTEREST

The authors have nothing to disclose.

AUTHOR CONTRIBUTIONS

De Franceschi, Iolascon designed the experiments, analyzed the data and wrote the manuscript.

Tolosano, Ghaffari, Mohandas contributed to study design and the writing of the manuscript.

Beneduce, Matte contributed in designing the experiments, carried out the experiments, analyzed the data and contributed in writing the manuscript.

SCMT carried out CFU-E-BFU-E assay.

Chiabrando, Petrillo performed the experiments on heme.

Menon carried out the immunomicroscopy on FOXO3.

De Falco carried out the molecular analysis and contributed to data analysis.

Siciliano, Federti, and *Babu* contributed to immunoblot experiments.

ORCID

Lucia De Franceschi  <http://orcid.org/0000-0001-7093-777X>

REFERENCES

- Chiabrando D, Mercurio S, Tolosano E. Heme and erythropoiesis: more than a structural role. *Haematologica*. 2014;99:973-983.
- Karur VG, Lowell CA, Besmer P, Agosti V, Wojchowski DM. Lyn kinase promotes erythroblast expansion and late-stage development. *Blood*. 2006;108:1524-1532.
- Ingle E, McCarthy DJ, Pore JR, et al. Lyn deficiency reduces GATA-1, EKLF and STAT5, and induces extramedullary stress erythropoiesis. *Oncogene*. 2005;24:336-343.
- Oikonomidou PR, Rivella S. What can we learn from ineffective erythropoiesis in thalassemia? *Blood Rev*. 2017;32(2):130-143.
- Harder KW, Quilici C, Naik E, et al. Perturbed myelo/erythropoiesis in Lyn-deficient mice is similar to that in mice lacking the inhibitory phosphatases SHP-1 and SHIP-1. *Blood*. 2004;104:3901-3910.
- He X, Deng Y, Yue W. Investigating critical genes and gene interaction networks that mediate cyclophosphamide sensitivity in chronic myelogenous leukemia. *Mol Med Rep*. 2017;16:523-532.
- Geahlen RL, Handley MD, Harrison ML. Molecular interdiction of Src-family kinase signaling in hematopoietic cells. *Oncogene*. 2004;23:8024-8032.
- Pullen NA, Barnstein BO, Falanga YT, et al. Novel mechanism for ϵ -IRI-mediated signal transducer and activator of transcription 5 (STAT5) tyrosine phosphorylation and the selective influence of STAT5B over mast cell cytokine production. *J Biol Chem*. 2012;287:2045-2054.
- Tsygankov AY, Spana C, Rowley RB, Penhallow RC, Burkhardt AL, Bolen JB. Activation-dependent tyrosine phosphorylation of Fyn-

- associated proteins in T lymphocytes. *J Biol Chem.* 1994;269:7792-7800.
10. Laurenzana I, Caivano A, Trino S, et al. A Pyrazolo[3,4-d]pyrimidine compound inhibits Fyn phosphorylation and induces apoptosis in natural killer cell leukemia. *Oncotarget.* 2016;7:65171-65184.
 11. Lannutti BJ, Shim MH, Blake N, Reems JA, Drachman JG. Identification and activation of Src family kinases in primary megakaryocytes. *Exp Hematol.* 2003;31:1268-1274.
 12. Salmond RJ, Filby A, Qureshi I, Caserta S, Zamoyska R. T-cell receptor proximal signaling via the Src-family kinases, Lck and Fyn, influences T-cell activation, differentiation, and tolerance. *Immunol Rev.* 2009;228:9-22.
 13. Tarabra E, An Lee TW, Zammit VA, et al. Differential activation of Fyn kinase distinguishes saturated and unsaturated fats in mouse macrophages. *Oncotarget.* 2017;8:86634-86645.
 14. Jain AK, Jaiswal AK. GSK-3beta acts upstream of Fyn kinase in regulation of nuclear export and degradation of NF-E2 related factor 2. *J Biol Chem.* 2007;282:16502-16510.
 15. Sun Z, Zhang S, Chan JY, Zhang DD. Keap1 controls postinduction repression of the Nrf2-mediated antioxidant response by escorting nuclear export of Nrf2. *Mol Cell Biol.* 2007;27:6334-6349.
 16. Jiang T, Harder B, Rojo de la Vega M, Wong PK, Chapman E, Zhang DD. p62 links autophagy and Nrf2 signaling. *Free Radic Biol Med.* 2015;88:199-204.
 17. Kim JE, Roh E, Lee MH, et al. Fyn is a redox sensor involved in solar ultraviolet light-induced signal transduction in skin carcinogenesis. *Oncogene.* 2016;35:4091-4101.
 18. Matte A, De Falco L, Federti E, et al. Peroxiredoxin-2: a novel regulator of iron homeostasis in ineffective erythropoiesis. *Antioxid Redox Signal.* 2018;28:1-14.
 19. Matte A, De Falco L, Iolascon A, et al. The interplay between Peroxiredoxin-2 and nuclear factor-Erythroid 2 is important in limiting oxidative mediated dysfunction in beta-Thalassemic erythropoiesis. *Antioxid Redox Signal.* 2015;23:1284-1297.
 20. Lupo F, Tibaldi E, Matte A, et al. A new molecular link between defective autophagy and erythroid abnormalities in chorea-acanthocytosis. *Blood.* 2016;128:2976-2987.
 21. Bartnikas TB, Andrews NC, Fleming MD. Transferrin is a major determinant of hepcidin expression in hypotransferrinemic mice. *Blood.* 2011;117:630-637.
 22. de Franceschi L, Turrini F, Honczarenko M, et al. In vivo reduction of erythrocyte oxidant stress in a murine model of beta-thalassemia. *Haematologica.* 2004;89:1287-1298.
 23. Matte A, Low PS, Turrini F, et al. Peroxiredoxin-2 expression is increased in beta-thalassemic mouse red cells but is displaced from the membrane as a marker of oxidative stress. *Free Radic Biol Med.* 2010;49:457-466.
 24. Dalle Carbonare L, Matte A, Valenti MT, et al. Hypoxia-reperfusion affects osteogenic lineage and promotes sickle cell bone disease. *Blood.* 2015;126:2320-2328.
 25. Franco SS, De Falco L, Ghaffari S, et al. Resveratrol accelerates erythroid maturation by activation of FoxO3 and ameliorates anemia in beta-thalassemic mice. *Haematologica.* 2014;99:267-275.
 26. Liu J, Zhang J, Ginzburg Y, et al. Quantitative analysis of murine terminal erythroid differentiation in vivo: novel method to study normal and disordered erythropoiesis. *Blood.* 2013;121:e43-e49.
 27. Konstantinidis DG, Giger KM, Risinger M, et al. Cytokinesis failure in RhoA-deficient mouse erythroblasts involves actomyosin and midbody dysregulation and triggers p53 activation. *Blood.* 2015;126:1473-1482.
 28. Flygare J, Rayon Estrada V, Shin C, Gupta S, Lodish HF. HIF1alpha synergizes with glucocorticoids to promote BFU-E progenitor self-renewal. *Blood.* 2011;117:3435-3444.
 29. Matte A, Pantaleo A, Ferru E, et al. The novel role of peroxiredoxin-2 in red cell membrane protein homeostasis and senescence. *Free Radic Biol Med.* 2014;76:80-88.
 30. Gothwal M, Wehrle J, Aumann K, Zimmermann V, Grunder A, Pahl HL. A novel role for nuclear factor-erythroid 2 in erythroid maturation by modulation of mitochondrial autophagy. *Haematologica.* 2016;101:1054-1064.
 31. Petrillo S, Chiabrando D, Genova T, et al. Heme accumulation in endothelial cells impairs angiogenesis by triggering paraptosis. *Cell Death Differ.* 2018;25:573-588.
 32. Kalish BT, Matte A, Andolfo I, et al. Dietary omega-3 fatty acids protect against vasculopathy in a transgenic mouse model of sickle cell disease. *Haematologica.* 2015;100:870-880.
 33. Fiorito V, Forni M, Silengo L, Altruda F, Tolosano E. Crucial role of FLVCR1a in the maintenance of intestinal Heme homeostasis. *Antioxid Redox Signal.* 2015;23:1410-1423.
 34. Ingoglia G, Sag CM, Rex N, et al. Hemopexin counteracts systolic dysfunction induced by heme-driven oxidative stress. *Free Radic Biol Med.* 2017;108:452-464.
 35. Marty C, Lacout C, Droin N, et al. A role for reactive oxygen species in JAK2 V617F myeloproliferative neoplasm progression. *Leukemia.* 2013;27:2187-2195.
 36. Zhu BM, McLaughlin SK, Na R, et al. Hematopoietic-specific Stat5-null mice display microcytic hypochromic anemia associated with reduced transferrin receptor gene expression. *Blood.* 2008;112:2071-2080.
 37. Zhang X, Camprecios G, Rimmele P, et al. FOXO3-mTOR metabolic cooperation in the regulation of erythroid cell maturation and homeostasis. *Am J Hematol.* 2014;89:954-963.
 38. Knight ZA, Schmidt SF, Birsoy K, Tan K, Friedman JM. A critical role for mTORC1 in erythropoiesis and anemia. *Elife.* 2014;3:e01913.
 39. Marino G, Niso-Santano M, Baehrecke EH, Kroemer G. Self-consumption: the interplay of autophagy and apoptosis. *Nat Rev Mol Cell Biol.* 2014;15:81-94.
 40. Wakabayashi N, Itoh K, Wakabayashi J, et al. Keap1-null mutation leads to postnatal lethality due to constitutive Nrf2 activation. *Nat Genet.* 2003;35:238-245.
 41. Chiabrando D, Vinchi F, Fiorito V, Tolosano E. Heme in pathophysiology: a matter of scavenging, metabolism and trafficking across cell membranes. *Front Pharmacol.* 2014;5:61.
 42. Kang YA, Sanalkumar R, O'Geen H, et al. Autophagy driven by a master regulator of hematopoiesis. *Mol Cell Biol.* 2012;32:226-239.
 43. Komatsu M, Kurokawa H, Waguri S, et al. The selective autophagy substrate p62 activates the stress responsive transcription factor Nrf2 through inactivation of Keap1. *Nat Cell Biol.* 2010;12:213-223.
 44. Zoncu R, Efeyan A, Sabatini DM. mTOR: from growth signal integration to cancer, diabetes and ageing. *Nat Rev Mol Cell Biol.* 2011;12:21-35.
 45. Howell JJ, Manning BD. mTOR couples cellular nutrient sensing to organismal metabolic homeostasis. *Trends Endocrinol Metab.* 2011;22:94-102.
 46. Liu X, Zhang Y, Ni M, et al. Regulation of mitochondrial biogenesis in erythropoiesis by mTORC1-mediated protein translation. *Nat Cell Biol.* 2017;19:626-638.
 47. Wang J, Tran J, Wang H, et al. mTOR inhibition improves anaemia and reduces organ damage in a murine model of sickle cell disease. *Br J Haematol.* 2016;174:461-469.
 48. Federti E, Matte A, Ghigo A, et al. Peroxiredoxin-2 plays a pivotal role as multimodal cytoprotector in the early phase of pulmonary hypertension. *Free Radic Biol Med.* 2017;112:376-386.
 49. Filomeni G, Desideri E, Cardaci S, Rotilio G, Ciriolo MR. Under the ROS ... thiol network is the principal suspect for autophagy commitment. *Autophagy.* 2010;6:999-1005.
 50. Ingley E. Integrating novel signaling pathways involved in erythropoiesis. *IUBMB Life.* 2012;64:402-410.
 51. Tilbrook PA, Palmer GA, Bittorf T, et al. Maturation of erythroid cells and erythroleukemia development are affected by the kinase activity of Lyn. *Cancer Res.* 2001;61:2453-2458.
 52. Zhang S, Macias-Garcia A, Velazquez J, Paltrinieri E, Kaufman RJ, Chen JJ. HRI coordinates translation by eIF2alphaP and mTORC1 to mitigate ineffective erythropoiesis in mice during iron deficiency. *Blood.* 2018;131:450-461.
 53. Lithanadom P, Wannatung T, Leecharoenkiat A, Svasti S, Fuchareon S, Smith DR. Enhanced activation of autophagy in beta-thalassemia/Hb E erythroblasts during erythropoiesis. *Ann Hematol.* 2011;90:747-758.
 54. Ravikumar B, Imarisio S, Sarkar S, O'Kane CJ, Rubinsztein DC. Rab5 modulates aggregation and toxicity of mutant huntingtin through

macroautophagy in cell and fly models of Huntington disease. *J Cell Sci.* 2008;121:1649-1660.

SUPPORTING INFORMATION

Additional supporting information may be found online in the Supporting Information section at the end of the article.

How to cite this article: Beneduce E, Matte A, De Falco L, et al. Fyn kinase is a novel modulator of erythropoietin signaling and stress erythropoiesis. *Am J Hematol.* 2018;1-11. <https://doi.org/10.1002/ajh.25295>

60th Congress of the American Society of Hematology, December 2018, San Diego

Dietary Omega-3 Fatty Acid Supplementation Improves Sickle Cell Bone Disease By Affecting Osteoblastogenesis and Adipogenesis

Maria Teresa Valenti, PhD^{1*}, Luca Dalle Carbonare, MD^{1*}, Alessandro Mattè, BSc, PhD^{1*}, Lorenzo Anez-Bustillos^{2*}, Mark Puder, MD^{2*}, Samuele Cheri^{1*}, Michela Deiana^{1*}, Enrica Federti, PhD^{1*}, **Serge Cedrick Toya Mbiandjeu**^{1*}, Angela Siciliano^{1*}, Carlo Brugnara, MD³ and Lucia De Franceschi, MD¹

¹University of Verona, Verona, Italy; ²Harvard Medical School, Boston Children's Hospital, Boston, MA;

³Department of Laboratory Medicine, Boston Children's Hospital, Boston, MA

Sickle bone disease (SBD) is a severe and invalidating complication related to recurrent bone vaso-occlusive events affecting patients with sickle cell disease (SCD). In a humanized mouse model for SCD, we previously showed that SBD is sustained by impaired osteoblast function and increased osteoclast activity associated with local up-regulation of pro-inflammatory cytokines and anti-oxidant systems (Dalle Carbonare L., Blood 2015;126:2320-2328). Growing evidence supports a role of ω -3 fatty acid supplementation in improving bone homeostasis (Fallon EM, et al J Surg Res 2014;191:148-155.). A diet enriched with ω -3 fatty acids beneficially impacts SCD inflammatory vasculopathy, and blunts the acute and chronic SCD-related organ damage in humanized SCD mice (Kalish BT et al Haematologica 2015;100:870-880). Here, we sought to compare the dietary effects of ω -6 (soybean oil-based, SD)- vs ω -3 (fish oilbased, FD)-enriched diets on SBD in SCD mice (*Hba*^{tm1(HBA)Tow} *Hbb*^{tm2(HBG1,HBB*)Tow}). Treated SCD and control healthy mice (AA, *Hba*^{tm1(HBA)Tow} *Hbb*^{tm3(HBG1,HBB)Tow}) (*n*=6 animals in each group) were exposed to recurrent hypoxia/reoxygenation (rH/R) stress, which closely mimics SBD natural history (Dalle Carbonare L., Blood 2015). In SCD mice, FD prevented rH/R-induced bone loss compared to animals exposed to SD by decreasing osteoclast and increasing osteoblast activities. Up-regulation of molecular osteogenic markers such as *Runx2* and *Sparc* and downregulation of *Rank* and *RankL*, molecular markers of osteoclast recruitment and activity were observed in FD SCD mice exposed to rH/R compared to SD SCD animals. Similar changes, but to a lesser extent, were also observed in AA control mice exposed to rH/R stress. Expression of IL-6 (*Il6*) and matrix-metalloproteinase-9 (*Mmp9*) regulators which

interact with RankL on osteoclastic activity and bone resorption were studied. In SCD mice, FD markedly reduced the up-regulation of both genes compared to SD SCD animals in conjunction with down-regulation of peroxiredoxin-2 (*Prx2*) gene expression, an important cytoprotective and antioxidant system. We also evaluated bone adipogenesis, which is believed to be an important contributor to bone impairment in SBD. Bone immunohistochemistry for Peripilin-1 which coats storage lipid droplets revealed increased adipogenesis in SD SCD mice compared to either FD SCD animals or AA controls, in association with downregulation of miR205, which decreases adipogenesis and enhances osteogenic activity. Our data thus indicate that in SCD exposed to rH/R, FD (i) improves osteoblastogenesis; (ii) decreases osteoclast activity; (iii) modulates the bone inflammatory response; iv) reduces adipogenesis. These findings provide new insights on the mechanism of action of ω -3 fatty acid supplementation on the pathogenesis of SBD and strengthen the rationale for ω -3 fatty acid dietary supplementation in SCD as a complementary therapeutic intervention targeting an amplified inflammatory response and sickle cell-related bone impairment.

60th Congress of the American Society of Hematology, December 2018, San Diego

Imatinib Protects Against Hypoxia/Reoxygenation Induced Lung and Kidney Injury in a Humanized Mouse Model for SCD

Alessandro Mattè, BSc, PhD^{1*}, Enrica Federti, PhD^{1*}, Antonio Rechiutti^{2*}, Antonella Panataleo^{3*}, Roberta Russo^{4*}, Francesco Turrini, MD, PhD^{5*}, Angela Siciliano^{1*}, Pierre Louis Tharaux, MD, PhD^{6,7*}, Wassim El Nemer, PhD^{8,9,10,11*}, **Serge Cedrick Toya**^{12*}, Anne Janin, PhD^{13*}, Christophe Leboeuf^{13*}, Wilson Babu^{14*}, Achille Iolascon, MD, PhD^{15*}, Carlo Brugnara, MD¹⁶ and Lucia De Franceschi, MD^{1,17}

¹University of Verona, Verona, Italy; ²UNiversity of Chieti, Chieti, Italy; ³University of Sassari, Sassari, Italy; ⁴UNiversity Federico II, Naples, Italy; ⁵University of Torino, Torino, Italy; ⁶UMR 970, Inserm,/University Paris Descartes, Paris, France; ⁷Laboratory of Excellence GR-Ex, Paris, France; ⁸UMR_S 1134, Université Paris Diderot/Inserm/INTS, Paris, France; ⁹Université Paris Diderot, Paris, France; ¹⁰Laboratoire d'Excellence GR-Ex, Paris, France; ¹¹Sorbonne Paris Cité University, Paris Diderot University, INSERM, Institut National de la Transfusion Sanguine, UMR_S 1134 Integrated Biology of the Red Cell, Laboratoire d'Excellence GR-Ex, Paris, France; ¹²University of Verona, Verona, Italy; ¹³University Diderot of Paris, Paris, France; ¹⁴UNiversity of Verona, Verona, Italy; ¹⁵CEINGE University Federico II of Naples, CEINGE University Federico II of Naples, Naples, Italy; ¹⁶Department of Laboratory Medicine, Boston Children's Hospital, Harvard Medical School, Boston, MA; ¹⁷Policlinico GB Rossi, Univ. of Vero, Verona, Italy

Imatinib is an oral Tyrosine (Tyr)-kinase inhibitor, developed for the treatment of chronic myeloid leukemia (CML). Few case reports on SCD patients with CML undergoing imatinib treatment highlight the beneficial impact of imatinib on severity and recurrence of acute VOCs in SCD. In red blood cells (RBCs), Imatinib has been shown to interfere with Tyr-phosphorylation state of the integral membrane protein band 3, affecting RBC microparticle formation. Here, we study the actions of Imatinib on a model of acute VOCs using humanized SCD mice (*Hba*^{tm1(HBA)Tow}*Hbb*^{tm2(HBG1,HBB*)Tow}). We treated SCD and control healthy mice (AA, *Hba*^{tm1(HBA)Tow}*Hbb*^{tm3(HBG1,HBB)Tow}) (*n*=6-7 animals in each group) with Imatinib 50 mg/Kg/d for 2 weeks before hypoxia/Reoxygenation (H/R) stress used to mimic acute VOCs. Under normoxia, we found that in SCD mice Imatinib significantly reduced (i) Tyr-phosphorylation state of sickle red cell membrane proteins; (ii) the amount of phosphatidyl-serine (PS)+ sickle RBCs; and (iii) the release of erythroid microparticles, which was associated with accumulation of hemichromes and a more efficient erythrophagocytosis compared to vehicle treated animals. In SCD mice exposed to H/R stress, imatinib significantly decreased the H/R-induced (i)

increase in peripheral neutrophil count; (ii) lung inflammatory cell infiltrate; (iii) kidney inflammatory cell infiltrate. In the lung of H/R SCD mice, Imatinib inhibited the H/R induced NF- κ B activation and prevented the up-regulation of (i) pro-inflammatory cytokines such as ET-1; (ii) vascular endothelial activation markers (VCAM-1, ICAM-1); (iii) pro-fibrotic markers such as PDGF-B and (iv) the activation of UPR system. In the kidney of H/R SCD mice, Imatinib significantly reduced H/R induced expression of ET-1, VCAM-1 and E-selectin, which were again associated with inhibition of NF- κ B. In addition, Imatinib significantly upregulated the expression of the microRNAs miR200a/b, which has been described to reduce renal fibrosis. Finally, in isolated aorta from Imatinib treated SCD exposed to H/R stress, a significant reduction in vascular activation markers was observed compared to vehicle treated animals. Collectively, our data indicate that Imatinib acts on multiple targets, modulating signal transduction and reducing inflammatory vasculopathy and extracellular matrix remodeling process related to VOC in SCD. Thus, Imatinib might represent a new therapeutic tool in clinical management of SCD patients.

59th Congress of the American Society of Hematology, December 2017, Atlanta, Georgia

REPROGRAMMING CELL-SIGNALING BY DELIVERING THE CATALYTIC DOMAIN OF PTPRG AMELIORATES ANEMIA OF β -THALASSEMIA

Matte Alessandro, Elisabetta Beneduce,* Michela Mirenda,* Roberta Russo,* Achille Iolascon, Antonella Pantaleo, Franco Turrini, Angela Siciliano, Enrica Federti, **Serge Cedrick MbiandjeuToya**, Janin Anne, Lebouef Christophe, Carlo Laudanna, Lucia De Franceschi

*These authors have equally contributed

β -thalassemia (β -thal) is one of the most common monogenetic disorders worldwide, characterized by ineffective erythropoiesis leading to a chronic, debilitating anemia associated with high morbidity and mortality. Erythroid maturation is a dynamic process tightly regulated by complex signaling mechanisms, only partially described either in normal and diseased erythropoiesis. To investigate this issue, we carried out a high throughput kinome analysis by taking advantage of Kinexus array technology (<http://www.kinexus.ca>), in sorted erythroid precursors from mouse model of ($Hbb^{3th/+}$) compared to wild-type animals. In β -thal mice, we found differential modulation of many protein kinases. Network computational analysis unveiled common as well as erythroid precursor-specific signaling mechanisms of altered erythrocyte differentiation in beta thalassemia, suggesting a selective perturbation in protein kinase/phosphatase balance in β -thal **erythropoiesis**.

We reasoned that balancing kinome anomalies, by increasing phosphatome activity, could normalize kinome signaling pathways, thus ameliorating erythropoiesis. We explore the expression and function of different protein phosphatase and we found reduced expression and function of protein Tyrosine phosphatase receptor type, gamma (PTPRG). To investigate PTPRG role in erythropoiesis, we exploited a novel Trojanfusion protein (TAT-ICD) we recently patented that delivers intracellularly the catalytic domain of PTPRG and up-modulates its signaling cascade, as both a research tool to map dysfunctional pathways and as a potential therapeutic agent. In β -thal mice, TAT-ICD acted on multiple abnormally activated targets identified by computational analysis. TAT-ICD

significantly reduced the activation of (i) Jak2-STAT5 pathway; (ii) Bruton tyrosine kinase (BTK) that has been reported to be part of the erythropoietin cascade; (iii) Akt that is involved in TGF- β -smad signaling pathway. This was associated with down-regulation of *Erfe* and *Gdf11* gene expression in sorted erythroblasts from TAT-ICD treated β -thal mice. Collectively, TAT-ICD treatment resulted in amelioration of β -thal ineffective erythropoiesis, evaluated by multiple approaches, including the profile of erythroid maturation and the amount of Annexin-V⁺ erythroid cells, reticulocyte count, circulating erythroblasts and hemolytic indices (*U.S. Patent #62/109,555*). The improvement of anemia was also associated with reduction in alpha aggregates and membrane bound hemichromes in circulating erythrocytes. We also found a reduction of liver and spleen iron accumulation in agreement with the beneficial effects on the hematologic phenotype. It is of note that TAT-ICD treatment did not affect either peripheral leukocyte counts or spleen lymphocyte pattern.

Our data unveil abnormalities in signal transduction pathways as new mechanism involved in β -thal erythropoiesis, and validate a novel, breakthrough, therapeutic approach to reset back to homeostatic equilibrium altered kinome in diseased erythropoiesis.

59th Congress of the American Society of Hematology, December 2017, Atlanta, Georgia

FYN KINASE IS INVOLVED IN EPO RECEPTOR SIGNALING AND IS REQUIRED TO HARMONIZE THE RESPONSE TO OXIDATION

Elisabetta Beneduce, Alessandro Matte, Luigia De Falco, **Serge Cedrick Mbiandjeu Toya**, Emanuela Tolosano, Deborah Chiabrando, Angela Siciliano, Achille Iolascon, Mohandas Narla, Lucia De Franceschi

CEINGE and Dept. of Biochemistry, Federico II University, Naples; Italy

New York Blood Center, NY, USA

Dept. Molecular Biotechnology and Health Sciences, University of Torino, Torino, Italy

Erythropoiesis is a complex multistep process during which committed erythroid progenitors undergo terminal differentiation to produce circulating mature red cells. Erythroid differentiation is characterized by the production of reactive oxygen species (ROS) both in response to erythropoietin (EPO) and to the large amount of iron imported into the cells for heme biosynthesis. During erythropoiesis, ROS might function as second messenger by modulating intracellular signaling pathways. Fyn, an Src kinase, has been previously reported to participate in signaling pathways in response to ROS in various cell types. Here, we explore the potential contribution of Fyn to normal and stress erythropoiesis by studying 2-4 months-old Fyn knockout mouse strain ($Fyn^{-/-}$) and C57B6/2J as wild-type controls. $Fyn^{-/-}$ mice showed a mild compensated microcytic anemia associated with signs of dyserythropoiesis. Increased ROS levels and Annexin-V⁺ cells were presented in all $Fyn^{-/-}$ erythroblast subpopulations compared to wild-type, suggesting a possible reduction in the efficiency of erythropoietin (EPO) signaling pathway in the absence of Fyn. Indeed, in $Fyn^{-/-}$ erythroblasts, we observed a reduction in Tyr-phosphorylation state of EPOR associated with a compensatory activation of Jak2 without major change in Lyn activity. A reduction in STAT5 activation resulting in down-regulation of *Cish*, a known direct STAT5 target gene, was noted in $Fyn^{-/-}$ erythroblasts. This was paralleled by a reduction in GATA1 and increased HSP70 nuclear translocation compared to wild type, supporting a higher cellular pro-oxidant environment in the absence of Fyn. Using the vitro cell forming colony unit assay, we found a lower in CFU-E and BFU-E cells production, which once again was associated with decreased activation of EPO mediated cascade in the absence of Fyn. To explore the possible role of Fyn in stress erythropoiesis, mice were treated with either phenylhydrazine (PHZ) or doxorubicin (Doxo). $Fyn^{-/-}$ mice showed prolonged anemia after either PHZ or Doxo treatment with a delayed hematologic recovery compared to wild-type animals. When we analyzed the expression of a battery of ARE-genes related to oxidative response such as catalase, Gpx, heme-oxygenase 1 and peroxiredoxin-2, we noted up-regulated

expression of these genes in sorted Fyn^{-/-} erythroblasts compared to wild-type cells. In agreement, we observed increased activation of the redox-sensitive transcriptional factor Nrf2 targeting ARE-genes, whose regulation has been previously linked to Fyn. In fact, Nrf2 is switched-off by Fyn, ubiquitinated and delivered to the autophagosome by the p62 cargo protein. In Fyn^{-/-} sorted erythroblasts, we observed (i) accumulation of p62 in large clusters; and (ii) reduction of Nrf2-p62 complex compared to wild-type cells. To address the question whether the perturbation of Nrf2-p62 system results in impairment of autophagy in the absence of Fyn, we used LysoTrack to explore late phases of autophagy. Lysosomal progression was defective in Fyn^{-/-} reticulocytes and it was associated with accumulation of p62 during in vitro reticulocyte maturation. These data indicate that the absence of Fyn blocks the Nrf2 post-induction response to oxidation, resulting in impaired autophagy. To validate our working hypothesis, we treated Fyn^{-/-} mice with Rapamycin, an inducer of autophagy. In Fyn^{-/-} mice, Rapamycin treatment resulted in decrease dyserythropoiesis, ROS levels and Annexin V+ cells, associated with reduction in accumulation of p62 in Fyn^{-/-} erythroblasts. As a proof of concept, we treated both mouse strains with PHZ with or without Rapamycin. This latter worsened PHZ induced acute anemia in wild-type mice but not in Fyn^{-/-} animals. Collectively, our data enabled us to document a novel role for Fyn in erythropoiesis, contributing to EPO-R activation and harmonizing the Nrf2-p62 adaptive cellular response against oxidation during normal and more importantly in stress erythropoiesis.

Fyn plays a novel key role in erythropoiesis as oxidative sensor

Beneduce E¹, Matte A¹, De Falco L², **Cedrick Mbiandjeu Toya S¹**, Iolascon A², Siciliano A¹, Valenti MT¹, Tolosano E³, Chiabrando D³, De Franceschi L¹

¹Dept. of Medicine, University of Verona and AOUI-Verona, Italy;²CEINGE, Advanced Biotechnologies, Naples, Italy;³Dept of Molecular Biotechnology and Health Sciences and Molecular Biotechnology Center, University of Turin, Italy.

Background

Fyn is a member of the Src family of tyrosine kinases (SFKs) and shares high homology with Lyn that has been previously involved in erythropoiesis. Previous reports have shown that Lyn targets EPO-R/Jak2/STAT5 signaling pathway. Although progresses have been done in the knowledge of molecular mechanisms involved in normal and diseased erythropoiesis, much still remains to be investigated on signal transduction pathway during erythroid differentiation and maturation.

Aims

Functional characterization of erythropoiesis in Fyn^{-/-} mice.

Methods

Female aged between 2-4 months from C57BL/6J, as wild-type (WT) controls, and Fyn^{-/-} mouse strains were used. Phenylhydrazine (PHZ) at 40 mg/kg or Doxorubicin at 0,25mg/kg by intraperitoneal injection were used to explore stress erythropoiesis. Hematologic parameters, red indices and reticulocyte count were evaluated as previously reported (Matte A, et al. ARS, 2015). Mouse erythropoiesis was studied using the CD44/Ter119 gating strategy by FACS. ROS levels and the amount of Annexin V⁺ cells were also evaluated in erythroblast subpopulations. In vitro colony-forming unit assay was performed to obtain CFU-Es and BFU-Es. Immunoblot analysis was carried out to study early and late erythropoiesis.

Results

Fyn^{-/-} mice showed signs of dyserythropoiesis associated with increased total erythroblasts (CD44⁺TER119⁺FSC^{high}), without extramedullary erythropoiesis. Fyn^{-/-} erythroblasts showed higher ROS levels and increased amount of Annexin V⁺ cells, compared to WT, indicating increase oxidative stress and cell apoptosis. High ROS levels in erythroblasts have been described in β -thalassemic mouse erythroid cells as model of stress erythropoiesis. This has been linked with instability of GATA-1, which nuclear translocation is prevented and requires the stabilization of heat shock protein (HSP70-90). In Fyn^{-/-} mice, we explored GATA-1/HSP70 distribution in subcellular fractions. Fyn^{-/-} erythroblasts showed reduction in GATA-1 nuclear translocation, compared to WT. In agreement with reduced GATA-1 nuclear translocation, a marked decrease in β -globin chain synthesis, resulting in an imbalance in α/β globin chain levels, was observed in Fyn^{-/-} mice. To further characterize the impact of the absence of Fyn on erythropoiesis, we set up a colony-forming unit assay for CFU-E and BFU-E. The lack of Fyn resulted in a significant decrease in CFU-E and BFU-E colonies, suggesting an impairment of early erythropoiesis. Erythroid commitment and differentiation is strictly dependent on EPOR/Jak2/STAT5 signaling pathway. The absence of Fyn resulted in a marked decrease in STAT5 activation, supported by a significant down-regulation of *Cish*, that is strictly regulated by STAT5 function.

Using Doxorubicin and PHZ, we found a delay in increased reticulocyte count related to either Doxorubicin or PHZ treatment, shedding new light on the role of Fyn in stress erythropoiesis.

In addition, we found chronic activation of Nrf2 related to lack of its physiologic inhibitor, Fyn. Indeed, we found increased ARE-related genes such as heme oxygenase-1 (HO-1), which expression seems to become independent from heme concentration in the absence of Fyn. In fact, biliverdin reductase (BVR) that is functionally linked to Nrf2 but it depends from another transcriptional factor was similar to that observed in WT mice.

Conclusions

Our preliminary data support a novel role of Fyn as both oxidative sensor and new modulator of the EPO/STAT5 pathway.

Nrf2 plays a key role in erythroid maturation and sensitivity to exogenous stress

Cedrick Mbiandjeu Toya S¹, Matte A¹, Russo R², Iolascon A², Siciliano A¹, Valenti MT¹, Beneduce E¹, Di Paolo ML³, De Franceschi L¹.

¹Dept of Medicine, University of Verona and AOUI-Verona, ²CEINGE, Advanced Biotechnologies, Naples, Italy, ³Department of Molecular Medicine, University of Padova, Italy

Background. Nuclear factor erythroid-derived 2 (Nrf2) is a transcription factor that participates in acute phase response to oxidative stress and controls the expression of adaptive systems to environmental stressors. Nrf2 modulates the expression of antioxidant responsive element (ARE-) related genes, drug-metabolizing systems and metabolic pathways. Mice genetically lacking Nrf2 show a chronic hemolytic anemia related to an increased phagocytosis of damaged red blood cells (*Lee M. J. et al PNAS 2004*). In mouse pathologic erythropoiesis, a functional interplay between Nrf2 and peroxiredoxin-2 (Prx2) has been recently reported (*Matte A et al ARS 2015*). Here, we carried out functional characterization of erythroid cells genetically lacking Nrf2 (in Nrf2^{-/-} mice).

Methods. We used 6 -12 months-old wild type (WT) and Nrf2 knockout mice (Nrf2^{-/-}) divided in groups of 5-6 mice each. Intracellular levels of reactive oxygen species (ROS) and exposition of phosphatidyl-serine (PS) in circulating red cells (RBCs). We separated the cytosolic fraction from membrane proteins of mouse RBCs for Western-blot analysis. We examined the in vitro effects on mouse RBCs of treated with different oxidative agent (Diamide, Hydrogen peroxide and Phenylhydrazine). We carried out cell-based assay on CFU-E and BFU-E cell forming colonies and prepared isolated cells for Western-blot analysis.

Results. In Nrf2^{-/-} mouse RBCs, we observed increased ROS levels associated with higher exposition of phosphatidyl-serine (PS), as a marker of membrane lipid peroxidation. In addition, Nrf2^{-/-} mouse RBCs showed reduced expression of key antioxidant systems such as Nqo1, Prx2 and Catalase linked to Nrf2 function. This was associated with increased membrane translocation of HSP 70 and 90, supporting higher levels of membrane protein oxidation that requires chaperone intervention. Nrf2^{-/-} RBCs also displayed a higher sensitivity to exogenous H₂O₂ mediated oxidation as compared to WT. This was further supported by increased levels of ROS levels and of Annexin V⁺ cells in Nrf2^{-/-} erythrocytes compared to either treated WT RBCs or untreated erythrocytes. In addition, we found increased Prx2 dimer formation and PrxSO₃ levels in H₂O₂ treated Nrf2^{-/-} red cells, supporting the amplified oxidation of Nrf2^{-/-} erythrocytes compared to either WT or untreated Nrf2^{-/-} red cells. In agreement, we found significant increase in band 3 Tyr-phosphorylation state related to activation of Syk pathway in response to H₂O₂ treatment in Nrf2^{-/-} erythrocytes. We then we explored the effects of the absence of Nrf2 on erythropoiesis. We first carried out cell-based assay on CFU-E and BFU-E cell forming colonies. Nrf2^{-/-} CFU-Es were significantly lower compared to WT. Reduced expression of Nrf2 related anti-oxidant systems such as Catalase, Prx2 and Nqo1 were documented in Nrf2^{-/-} CFU-Es by Western-blot analysis.

Conclusions. Our data suggest that the absence of Nrf2 promotes a high pro-oxidant environment, resulting in increase sensitivity of red cells to exogenous H₂O₂ treatment. The preliminary results on CFU-E support an important role of Nrf2 in the early phase of erythropoiesis.

